PB84-163302

Examination of One-Hour N02 Predictions from Photochemical Air Quality Models

(U.S.) Environmental Sciences Research Lab.
Research Triangle Park, NC

Mar 84

U.S. Department of Commerce
National Technical Information Service
NTIS

EPA-600/3-84-046
March 1984

PB84-163302

EXAMINATION OF ONE-HOUR NO_2 PREDICTIONS FROM PHOTOCHEMICAL AIR QUALITY MODELS

by

Kenneth L. Schere and Jack H. Shreffler
Meteorology and Assessment Division
Environmental Sciences Research Laboratory
Research Triangle Park, North Carolina 27711

ENVIRONMENTAL SCIENCES RESEARCH LABORATORY
OFFICE OF RESEARCH AND DEVELOPMENT
U.S. ENVIRONMENTAL PROTECTION AGENCY
RESEARCH TRIANGLE PARK, NORTH CAROLINA 27711

REPRODUCED BY
NATIONAL TECHNICAL
INFORMATION SERVICE
U.S. DEPARTMENT OF COMMERCE
SPRINGFIELD, VA. 22161

TECHNICAL REPORT DATA (Please read Instructions on the reverse before completing)		
1. REPORT NO. EPA-600/3-84-046	2.	3. RECIPIENT'S ACCESSION NO. PB84 163502
4. TITLE AND SUBTITLE EXAMINATION OF ONE-HOUR NO_2 PREDICTIONS FROM PHOTOCHEMICAL AIR QUALITY MODELS		5. REPORT DATE March 1984 6. PERFORMING ORGANIZATION CODE
7. AUTHOR(S) Kenneth L. Schere and Jack H. Shreffler		8. PERFORMING ORGANIZATION REPORT NO.
9. PERFORMING ORGANIZATION NAME AND ADDRESS (same as 12.)		10. PROGRAM ELEMENT NO. CDWA1A/01-2058 (FY-84) 11. CONTRACT/GRANT NO.
12. SPONSORING AGENCY NAME AND ADDRESS Environmental Sciences Research Laboratory - RTP, NC Office of Research and Development U.S. Environmental Protection Agency Research Triangle Park, NC 27711		13. TYPE OF REPORT AND PERIOD COVERED In-house 14. SPONSORING AGENCY CODE EPA/600/09
15. SUPPLEMENTARY NOTES		

16. ABSTRACT

This report discusses an evaluation of three photochemical air quality simulation models for predictions of 1-h NO_2 concentrations in urban areas using the data from the Regional Air Pollution Study in St. Louis. There is a need for models to estimate such concentrations should a short-term National Ambient Air Quality Standard (NAAQS) for NO_2 be promulgated by the U.S. Environmental Protection Agency. This work is an extension of the urban-scale model evaluation study conducted by EPA for estimating 1-h O_3 concentrations. The models discussed here include the Photochemical Box Model (PBM), the Lagrangian Photochemical Model (LPM), and the Urban Airshed Model (UAM). Simple statistical methods and graphical techniques are used to test model performance for NO_2 over a sample of 20 days selected from nearly two years of data. An analysis of the NO_2 record of the Regional Air Pollution Study (RAPS) revealed that there was an insufficient number of high 1-h NO_2 concentrations in the data base to conduct a conclusive model evaluation. Simulations conducted with the models, however, showed that the PBM and UAM generally underpredicted maximum NO_2 values and that the LPM demonstrated a tendency to overpredict. The variance in the residuals for all models was quite high and prevented an endorsement of any of the tested models for use in air quality analysis for NO_2 at this time.

17. KEY WORDS AND DOCUMENT ANALYSIS		
a. DESCRIPTORS	b. IDENTIFIERS/OPEN ENDED TERMS	c. COSATI Field/Group
18. DISTRIBUTION STATEMENT RELEASE TO PUBLIC	19. SECURITY CLASS (This Report) UNCLASSIFIED 20. SECURITY CLASS (This page) UNCLASSIFIED	21. NO. OF PAGES 115 22. PRICE

EPA Form 2220-1 (9-73)

NOTICE

This document has been reviewed in accordance with U.S. Environmental Protection Agency policy and approved for publication. Mention of trade names or commercial products does not constitute endorsement or recommendation for use.

AFFILIATION

Mr. Schere and Dr. Shreffler are on assignment to the Meteorology and Assessment Division, Environmental Sciences Research Laboratory, from the National Oceanic and Atmospheric Administration, U.S. Department of Commerce.

ABSTRACT

This report discusses an evaluation of three photochemical air quality simulation models for predictions of 1-h NO_2 concentrations in urban areas using the data from the Regional Air Pollution Study in St. Louis. There is a need for models to estimate such concentrations should a short-term National Ambient Air Quality Standard (NAAQS) for NO_2 be promulgated by the U.S. Environmental Protection Agency. This work is an extension of the urban-scale model evaluation study conducted by EPA for estimating 1-h O_3 concentrations, and the same model simulations used in that study were reanalyzed for use in the current work.

The models discussed here include the Photochemical Box Model (PBM) developed in-house by EPA, the Lagrangian Photochemical Model (LPM) developed by Environmental Research and Technology, Inc., and the Urban Airshed Model (UAM) developed by Systems Applications, Inc. Simple statistical methods and graphical techniques are used to test model performance for NO_2 over a sample of 20 days selected from nearly two years of data.

An analysis of the NO_2 record of the Regional Air Pollution Study (RAPS) revealed that there was an insufficient number of high 1-h NO_2 concentrations in the data base to conduct a conclusive model evaluation. Simulations conducted with the models, however, showed that the PBM and UAM generally underpredicted maximum NO_2 values and that the LPM demonstrated a tendency to overpredict. The variance in the residuals for all models was quite high and prevented an endorsement of any of the tested models for use in air quality analysis for NO_2 at this time.

This report covers a period from October 1981 to September 1982.

CONTENTS

Abstract iii
Figures vi
Tables viii

1. Introduction 1
2. Conclusions and Recommendations 3
3. Observations of NO_x in St. Louis 6
   - Introduction 6
   - Results from one-hour average data 8
   - A stagnation episode 10
   - Concluding remarks 11
4. Photochemical Box Model 17
   - Overview 17
   - Results 20
   - Conclusions 28
5. Lagrangian Photochemical Model 39
   - Overview 39
   - Results 41
   - Conclusions 48
6. Urban Airshed Model 58
   - Overview 58
   - Results 60
   - Conclusions 71

References 87
Appendices

A. UAM - Time series for remaining test days 89
B. UAM - Contour plots for remaining test days 98

FIGURES

Number		Page
1	The St. Louis region with locations of RAPS stations	12
2	Distributions of daily maximum 1-h concentrations of NO and NO_2	13
3	Occurrence of daily maximum 1-h concentrations of NO and NO_2 by station	13
4	Occurrence of daily maximum 1-h concentrations of NO and NO_2 by time of day	14
5	Occurrence of high daily maximum 1-h concentrations of NO and NO_2 during the year	14
6	Daily maximum 1-h concentration of NO_2 versus wind speed	15
7	Distribution of 24-h NO_2 concentrations in central city	15
8	Time series of pollutant concentration data for 1 October 1976	16
9	Schematic drawing of the PBM domain	30
10	Map of the PBM domain	31
11	PBM simulation results for Day 184-75	32
12	PBM simulation results for Day 251-75	33
13	PBM simulation results for Day 159-76	34
14	PBM simulation results for Day 160-76	35
15	PBM simulation results for Day 237-76	36
16	PBM simulation results for Day 275-76	37
17	PBM simulation results summary for all NO_2 data	38
18	Schematic of the Lagrangian parcel in LPM	50
19	LPM simulation results for Day 182-75	51
20	LPM simulation results for Day 184-75	52
21	LPM simulation results for Day 231-75	53
22	LPM simulation results for Day 251-75	54
23	LPM simulation results for Day 226-76	55
24	LPM simulation results for Day 275-76	56
25	Average residuals of NO_2 concentrations for the sample	57
26	NO_x source emissions map for the UAM domain	74
27	Schematic drawing of the UAM domain	75
28	UAM simulation results for Day 184-75	76
29	UAM time series of NO_2 results for site 104 on Day 184-75	77
30	UAM contours of maximum NO_2 field on Day 184-75	77
31	UAM simulation results for Day 251-75	78
32	UAM time series of NO_2 results for site 112 on Day 251-75	79
33	UAM contours of maximum NO_2 field on Day 251-75	79
34	UAM simulation results for Day 159-76	80
35	UAM time series of NO_2 results for site 104 on Day 159-76	81
36	UAM contours of maximum NO_2 field on Day 159-76	81
37	UAM simulation results for Day 237-76	82
38	UAM time series of NO_2 results for site 106 on Day 237-76	83
39	UAM contours of maximum NO_2 field on Day 237-76	83
40	UAM simulation results for Day 275-76	84

41 UAM time series of NO_2 results for site 101 on Day 275-76 85
42 UAM contours of maximum NO_2 field on Day 275-76 85
43 UAM locations of maximum pred. and obs. NO_2 on all days 86
A-1 UAM time series of NO_2 results for site 102 on Day 142-75 90
A-2 UAM time series of NO_2 results for site 103 on Day 178-75 90
A-3 UAM time series of NO_2 results for site 106 on Day 182-75 91
A-4 UAM time series of NO_2 results for site 106 on Day 183-75 91
A-5 UAM time series of NO_2 results for site 106 on Day 207-75 92
A-6 UAM time series of NO_2 results for site 110 on Day 209-75 92
A-7 UAM time series of NO_2 results for site 102 on Day 221-75 93
A-8 UAM time series of NO_2 results for site 112 on Day 230-75 93
A-9 UAM time series of NO_2 results for site 102 on Day 231-75 94
A-10 UAM time series of NO_2 results for site 104 on Day 160-76 94
A-11 UAM time series of NO_2 results for site 102 on Day 195-76 95
A-12 UAM time series of NO_2 results for site 112 on Day 211-76 95
A-13 UAM time series of NO_2 results for site 113 on Day 212-76 96
A-14 UAM time series of NO_2 results for site 106 on Day 225-76 96
A-15 UAM time series of NO_2 results for site 101 on Day 226-76 97
B-1 UAM contours of maximum NO_2 field on Day 142-75 99
B-2 UAM contours of maximum NO_2 field on Day 178-75 99
B-3 UAM contours of maximum NO_2 field on Day 182-75 100
B-4 UAM contours of maximum NO_2 field on Day 183-75 100
B-5 UAM contours of maximum NO_2 field on Day 207-75 101
B-6 UAM contours of maximum NO_2 field on Day 209-75 101
B-7 UAM contours of maximum NO_2 field on Day 221-75 102
B-8 UAM contours of maximum NO_2 field on Day 230-75 102
B-9 UAM contours of maximum NO_2 field on Day 231-75 103
B-10 UAM contours of maximum NO_2 field on Day 160-76 103
B-11 UAM contours of maximum NO_2 field on Day 195-76 104
B-12 UAM contours of maximum NO_2 field on Day 211-76 104
B-13 UAM contours of maximum NO_2 field on Day 212-76 105
B-14 UAM contours of maximum NO_2 field on Day 225-76 105
B-15 UAM contours of maximum NO_2 field on Day 226-76 106

TABLES

Number		Page
1	Summary of Meteorological Conditions on 20 Test Days	19
2	Summary of Predicted and Observed NO_2 Maxima for the PBM	25
3	Summary of NO_2 Model Performance Statistics from the PBM	27
4	Initial Pollutant Concentrations Assigned in the LPM	42
5	Summary of Predicted and Observed NO_2 Maxima for the LPM	45
6	Temporal Correlation Coefficients for the LPM	47
7	Summary of NO_2 Mean Concentration Data from the UAM	66
8	Summary of NO_2 Analysis of Trends Data from the UAM	67
9	Summary of Predicted and Observed NO_2 Maxima for the UAM	69

SECTION 1

INTRODUCTION

Evaluation of several photochemical air quality simulation models has recently been carried out using data from the Regional Air Pollution Study (RAPS) in St. Louis (Shreffler and Schere, 1982, subsequently referred to as Report I; and Schere and Shreffler, 1982, subsequently referred to as Report II). The models were built specifically to predict short-term O_3 concentrations in urban areas but they also predict nitrogen oxides and a variety of other chemical species involved in the photochemical processes. Reports I and II focused on the models' ability to predict short-term O_3. The importance of 1-h O_3 predictions lies in the possibility of using them to attain compliance with the National Ambient Air Quality Standard (NAAQS). Currently, the NAAQS for O_3 states that 1-h average concentrations should not exceed .120 ppm more than once a year on the average. On the other hand, the NAAQS for NO_2, another pollutant implicated in deleterious health effects, states that the annual average concentration should not exceed .053 ppm.

Use of the short-term models to predict annual averages would be highly inefficient, but recently there has been some discussion of setting a 1-h or 24-h standard for NO_2. Therefore, the Office of Air Quality Planning and Standards (OAQPS) requested that the Environmental Sciences Research Laboratory (ESRL) provide a report analyzing the models' performance in predicting 1-h NO_2 concentrations. This report utilizes the results of the previous model evaluation simulations and presents in more detail the results involving NO_2.

Prior to presentation of model results, the complete records of NO and NO_2 measurements from RAPS are surveyed and summarized. The summary places model results, which are for 20 selected high O_3 days, in the context of the entire two-year record. Furthermore, concentration distributions will allow comparison of the St. Louis experience with that of other cities and, therefore, provide insight into the usefulness of model results in alternate locations.

Presently, there is no impending move to establish a national short-term NO_2 standard. California has established a 1-h standard of .250 ppm, and this level is exceeded regularly in the Los Angeles air basin. Health data fail to clearly indicate adverse effects at concentrations below 1.0 ppm. From extensive statistical studies of major urban areas in the United States, OAQPS currently believes that, if the .053 ppm annual standard for NO_2 is met, the short-term peaks should present no health risk (Rhoads, 1982).

SECTION 2

CONCLUSIONS AND RECOMMENDATIONS

The primary objective of this study has been the evaluation of urban-scale photochemical dispersion models for estimating 1-h NO_2 concentrations. Progress toward this goal was hampered by a number of factors, although limited success was achieved in clarifying the models' performance for NO_2 predictions. The models tested here include those from the box (PBM), trajectory (LPM) and grid (UAM) categories and are all based on numerical solutions to mass-conservative equations. This volume is the third in a series concerning the evaluation of urban-scale photochemical dispersion models and the first specifically emphasizing NO_2.

Prior to evaluating model performance the NO and NO_2 measurements from the RAPS data base were characterized to assess the adequacy of evaluation data. The most striking aspect of this characterization relating to model evaluation is the absence of sufficient numbers of high NO_2 concentration data values. Isolating only the daily maximum 1-h NO_2 values observed at each monitoring station over the two-year period, it was seen that only about 5% were greater than 0.10 ppm and only 4 of the 25 monitoring stations reported maximum values exceeding 0.06 ppm on at least 10% of the days. These values may be contrasted with the present NAAQS for annual average NO_2 concentrations of 0.053 ppm and California's 1-h standard of 0.25 ppm, which was rarely exceeded during the entire RAPS data record. Another significant aspect of the NO_2 characterization was that the strength and frequency of peak RAPS NO_2 measurements occurring in the evening period (after 1800h) were significantly greater than those of peaks occurring at any other time of the day. This aspect of the data base affects model evaluation since the model simulations were conducted only through 1700 or 1800h.

It should be noted that these model simulations were conducted chiefly for the purpose of evaluating predictions of O_3 concentrations which commonly reach a peak before 1800h; the model simulations are re-evaluated here for NO_2 predictions. No new simulations were conducted for this study.

These conclusions from the data base analysis preclude a definitive evaluation of the models for NO_2 predictions. Nonetheless, within the limits of the available data some statements may be made concerning model performance for NO_2 on the RAPS data base. The PBM generally underpredicted the domain-average peak NO_2 concentrations. Over the sample of 20 days modeled the PBM's average underprediction was 17% and on the 6 days with the highest NO_2 values in the sample the average underprediction was 31%. The simplistic treatment of point source emissions, which includes a substantial fraction of the total NO_x emissions, in the PBM and its large volume size prevent this model from giving strict NO_2 point estimates. It may be most useful as a screening model for a more complex photochemical model. Simulations with the LPM were conducted along the air parcel trajectories leading to the monitoring station recording the highest 1-h O_3 value. The trajectory did not necessarily coincide with that for the highest NO_2 values for that day and this posed some additional problems in evaluating the LPM for NO_2. The level-3 average residual concentration over the sample of days modeled for NO_2 with the LPM was nearly zero with a large variance among the residuals; those for level-1 showed substantial overpredictions. The UAM showed serious underpredictions of maximum 1-h NO_2 values over the 20 test days. The average value was a 37% underprediction but individual cases were as high as 78%. Results with this model for the less restrictive unpaired data set show an average model overprediction of 8% with a large variance. This may imply that the UAM has the potential to perform better once the deficiencies are identified and corrected.

The three models tested here cannot yet be endorsed as effective tools for assessing short-term NO_2 concentrations in urban areas. While the PBM may be applicable as a screening model, the LPM and the UAM would need further testing and refinement to qualify as useful models in assessing short-term NO_2, especially if more serious consideration is given to promulgating a NAAQS short-term standard. At the very least, a data base should be used for model evaluation that includes a substantial number of values above the proposed standard.

SECTION 3

OBSERVATIONS OF NO_x IN ST. LOUIS

INTRODUCTION

The Regional Air Pollution Study (RAPS), a major air quality assessment program of the U.S. Environmental Protection Agency (EPA), was conducted in St. Louis, Missouri, from late 1974 through early 1977 (Pooler, 1974; Schiermeier, 1978). St. Louis is a continental city of negligible topographic relief; about 2.3 million people reside in the metropolitan area. The principal objective of RAPS was to collect a comprehensive data base for use in evaluating air quality models designed to assess emissions-control strategies. Indeed, using RAPS data, extensive tests have been completed on models simulating the formation of photochemical O_3 (Report II).

The central purpose of this section is to characterize the measurements of NO and NO_2 taken over a two-year period during RAPS. This effort complements previous work conducted to characterize the O_3 record (Shreffler, 1982), and results possibly can be extrapolated to many other U.S. cities with similar meteorological regimes, emissions composition, and lack of significant topographic features.

Figure 1 shows the St. Louis region with monitoring sites numbered 101-125. Each site had a tower of either 10 m or 30 m height, indicated by open or solid circles respectively. Measurements included basic meteorological parameters as well as concentrations of pollutant gases, and data were recorded continuously as 1-min averages over the entire RAPS period. The 1-min data were later screened and used to form 1-h averages suitable for many research and modeling applications.

A chemiluminescent analyzer measured both NO and NO_x continuously with an intake manifold at about 4 m height above ground. The minimum detection limit was 5 ppb, and NO_2 was determined by differencing. Gas analyzers were automatically calibrated each day between the hours of 2000 and 2400 CST (local time).

The primary emphasis of this analysis is on hourly NO and NO_2 concentrations recorded during all of 1975-1976. Notwithstanding the routine data screening done when the hourly archives were developed, there remained some obvious outliers. Computer scans of the data were used to print, for subsequent visual inspection, the highest and second-highest hourly concentrations recorded each day. The second-highest was determined for a station other than the station of the highest, since single stations tended to fail for several consecutive hours before being adjusted or removed. Experience with visual inspection led to maximum allowable differences between the highest and second-highest as a function of absolute concentration. For example, with NO_2 > .120 ppm it was unreasonable to allow the highest to be more than 50% larger than the second-highest, and, when this happened, the second-highest replaced the highest as the valid data point. Over the whole data base, valid daily maxima of NO and NO_2 were not found above .600 ppm and .300 ppm, respectively.

The locations of the RAPS stations were chosen to avoid the influence of local sources, and this was generally not a problem. However, site 102 showed substantial influence from a point source to the WNW, and maxima recorded with wind from that direction were discarded since they were not representative of areal averages.

Subject to the above editing, the hourly data base was scanned and basic information about the maxima of NO and NO_2 for each day was recorded on computer files for further analysis.

RESULTS FROM ONE-HOUR AVERAGE DATA

Figure 2 shows the distributions of daily maximum 1-h average concentrations of NO and NO_2 over the two-year period. As in all subsequent histograms and scatter plots, the number of data points (days) are printed in the upper right portion of the figure. While the peaks of both distributions are at less than .100 ppm, the distribution of NO has a substantial tail into higher concentrations. The difference probably reflects the role of NO as a primary emission which impinged directly on monitoring sites; NO_2, being secondary, was more diffuse.

Figure 3 shows the distributions of maxima by RAP station (abbreviated 1-25). To emphasize the more significant values, only maxima above .060 ppm were used in forming this and subsequent figures. Generally the station distributions of NO and NO_2 are similar, probably reflecting the importance of automotive exhaust in the central city. The far-rural stations (122-125) almost always had values below the detection limit of the instruments. Site 101 was located near the center of the St. Louis business district. Notably, NO_2 maxima tended to occur more frequently than NO maxima at some outlying stations (e.g. 106, 112, 113, 114, and 121). This difference again was a consequence of the secondary nature of NO_2, and reflected transport away from the center of strongest NO emissions.

The distributions of the daily 1-h maxima with time of day indicate morning and evening peaks as seen in Figure 4. Accumulation of NO during 0600-0700 CST resulted from rush-hour automotive exhaust trapped under a low morning mixing height. NO_2 reached a peak most frequently during the next hour as increasing solar radiation induced photochemical reactions, and, quite possibly, O_3 aloft was entrained by a rising mixing height. The decreasing mixing height in the evening again tended to trap pollutants near the surface. Ozone produced during the day rapidly oxidized NO emissions, with the net effect that NO_2 peaks were proportionately more frequent than NO peaks in the early evening. O_3 was depleted rapidly in

the lower atmosphere as the evening progressed, and the frequency of NO_2 maxima decreased accordingly. Although these distributions represent the frequency of occurrences of the daily maxima, they can quite reasonably be thought of as displaying relative concentrations. That is, the more frequent occurrences of the daily maximum NO_2 during 2000-2100 CST would strongly suggest that concentrations tended to be higher, on the average, than for the morning peak. The well-defined diurnal cycles displayed in Figure 4 (showing the behavior of NO and NO_2 concentrations relative to each other) are a consequence of both the length of the available record and the number of measurement stations in the network. For each day, the maximum was chosen from among all stations in the network, thus negating to some degree the confounding influence of advection. Even under the most extreme stagnations, it is difficult to identify the expected diurnal changes at a single site in such an unequivocal manner.

Figure 5 shows the seasonal distributions of concentration maxima. As indicated on the figure, the lower limits for maxima entering the distributions were increased to emphasize high daily maxima. (Obviously, if all days were considered, the distributions would be uniform.) The seasonal changes in frequency of NO maxima can probably be explained by associated climatological conditions. The rise in frequency in the autumn was due to clear and dry conditions prevalent at that time. Those conditions are conducive to formation of strong nocturnal inversions that are very effective in trapping pollutants near the surface. Also, the shorter hours of daylight brought the stronger inversions closer to the rush-hour emissions peaks. The summer low resulted from greater atmospheric instability and the presence of higher O_3 levels, which diminished the possibility of strong NO maxima. On the other hand, the NO_2 distribution shows direct correlation of maxima with photochemistry active during the summer; the summertime enhancement of NO_2 maxima is complementary to the suppression of NO by O_3 oxidation.

Scatter diagrams were used to try to establish relationships between high concentrations of NO_2 and various meteorological parameters. Only wind speed seemed to have a clearly defined influence as seen in Figure 6. Wind speed was defined from the network resultant over a 3-h period before the maximum. Only under very calm conditons were high NO_2 values recorded.

Finally, because of possible health effects, interest in NO_2 concentrations extends to averaging times beyond one hour. Therefore, 24-h average concentrations were computed, and a distribution is displayed in Figure 7. The 24-h value was formed from all hourly data of stations 101, 102, 104, 105, 106, 112, and 113 (see Figure 3b) and represents the spatial average of the central city over each day. The median concentration was about .025 ppm, and, given the shape of the distribution, the annual average would have a similar value.

A STAGNATION EPISODE

The two highest hourly NO_2 values recorded during RAPS (see Figure 6) occurred on 1 and 2 October 1976. In this section 1-min data are presented for the day of 1 October. Network winds remained at or below 1 m/s for the entire day, making this a unique stagnation during RAPS. Figure 8 shows plots of 1-min average data from station 101 in the center of the city.

Solar radiation data indicate the day was very clear. The early morning surge in concentrations associated with automotive sources began about 0600 CST (360 min in Figure 8) as seen from the NO and CO traces. The NO_2 build-up followed at about 0730 CST (450 min), and O_3 production was evident by 0900 CST (540 min). The disappearance of NO at 1130 CST (690 min) coincided with a relative decrease in NO_2 and a rapid jump in O_3. With the approach of sunset and the set-up of the nocturnal inversion, NO_2 increased rapidly, presumably from oxidation of NO by residual O_3. NO levels rose only after depletion of O_3 by this reaction and surface deposition.

Routine instrument calibration resulted in some data gaps in the late evening. However, before midnight there was a sudden decrease in surface concentrations of NO and CO. This event was probably the result of transient vertical mixing, evident from an accompanying decrease in the stable vertical temperature gradient (not shown). Notably, NO_2 did not decrease at this time, indicating a more uniform vertical profile over the city. Evans (1979) has found that O_3 concentrations at a height of several hundred meters remain in the .060-.100 ppm range during the night, while being negligible at the surface. Therefore, a large reservoir of O_3 is available to oxidize NO diffusing away from the surface and produce a deeper layer of NO_2.

CONCLUDING REMARKS

The present NAAQS in the United States calls for limiting annual average NO_2 concentrations to .053 ppm. This standard was based largely on results of a study on lung performance of children exposed to NO_2 over long periods (Shy et al., 1970). The RAPS data (see Figure 7) indicate that no action would be necessary to meet the annual standard in St. Louis and, by inference, other similar cities. Currently, there is some discussion on setting a standard for shorter averaging times. The State of California has set a 1-h standard for NO_2 of .250 ppm, and this level is exceeded regularly in the Los Angeles air basin (44 days in 1980) according to the California Air Resources Board (1982). However, even the rather contained air basin around San Francisco showed only one violation of the standard in 1980, a rate that might be projected for St. Louis based on the RAPS data.

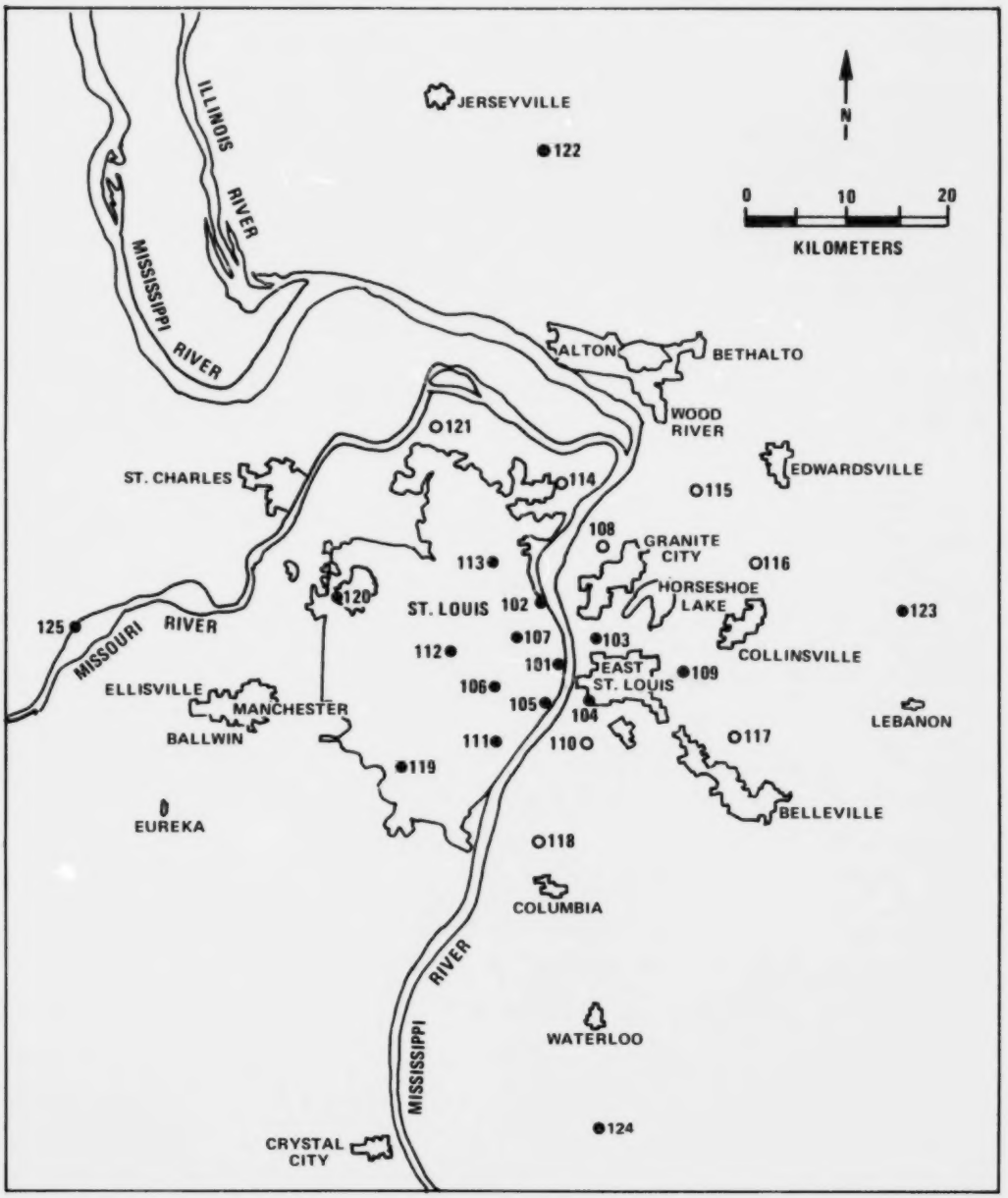

Figure 1. The St. Louis region with locations of RAPS stations.

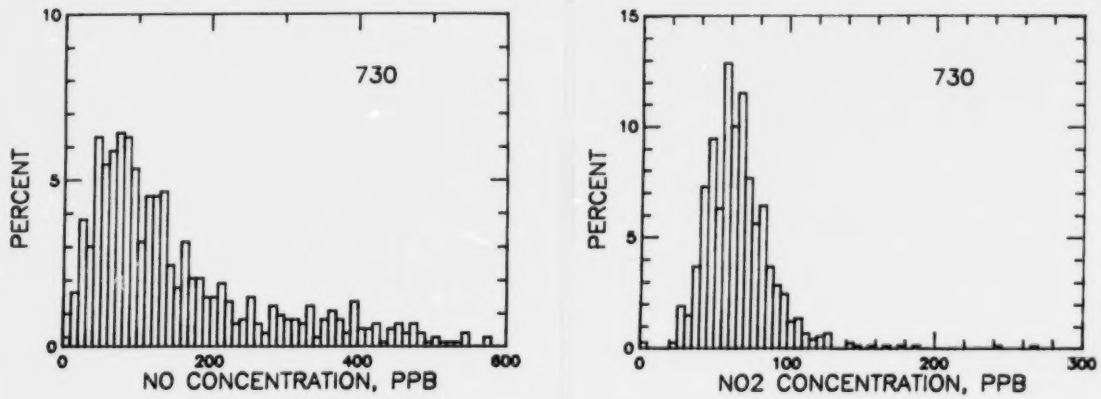

Figure 2. Distribution of daily maximum 1-h concentrations from RAPS: (a) NO, (b) NO_2.

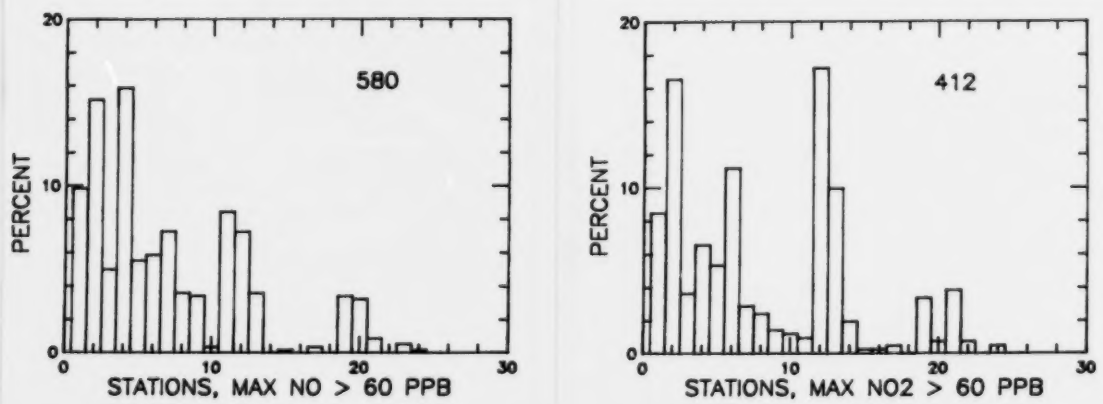

Figure 3. Occurrence of daily maximum 1-h concentrations by RAPS station: (a) NO, (b) NO_2.

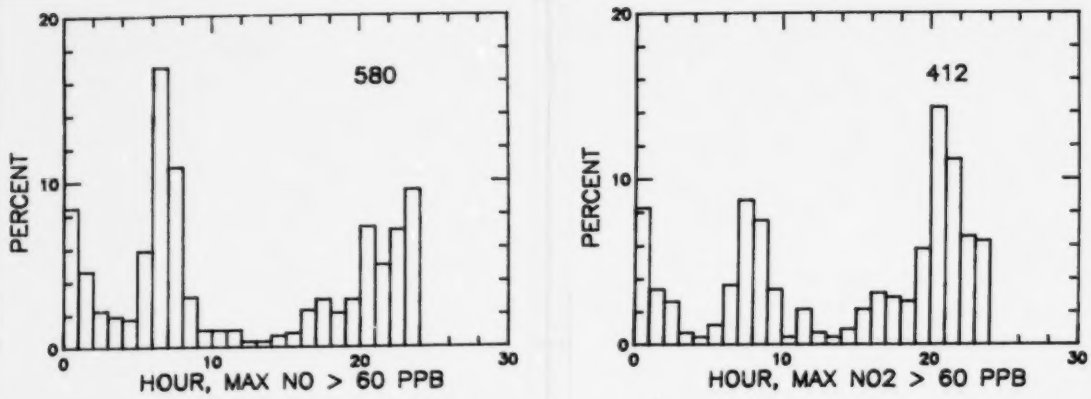

Figure 4. Occurrence of daily maximum 1-h concentrations by hour of the day: (a) NO, (b) NO_2.

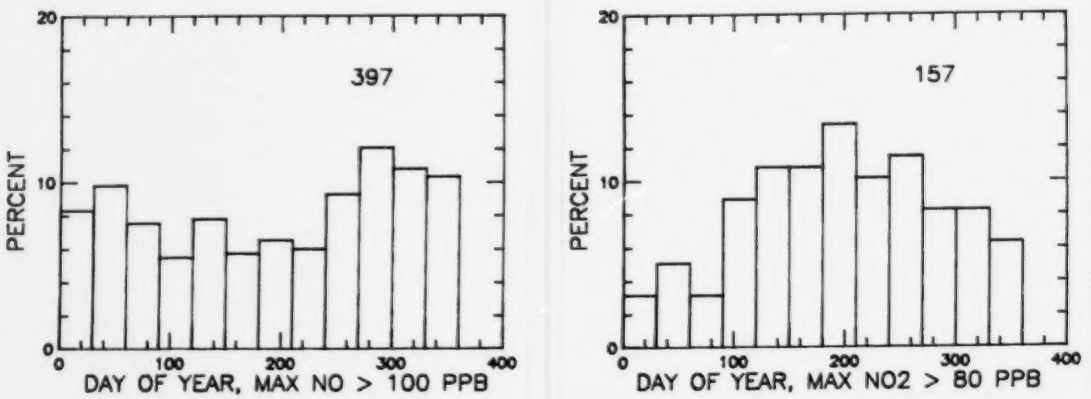

Figure 5. Occurrence of high daily maximum 1-h concentrations by 30-day segments of the year: (a) NO, (b) NO_2.

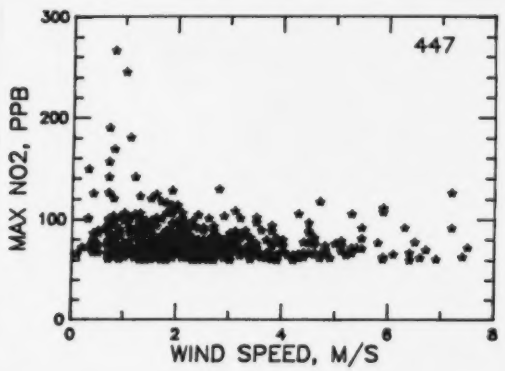

Figure 6. Scatter diagram of daily maximum 1-h concentration of NO_2 versus network resultant speed.

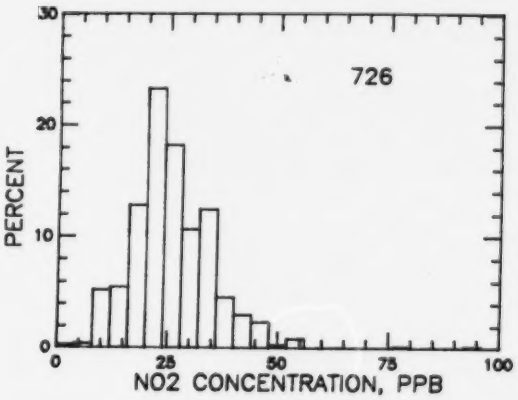

Figure 7. Distribution of 24-h NO_2 concentrations averaged from hourly data of central stations (101, 102, 104, 105, 106, 112, and 113).

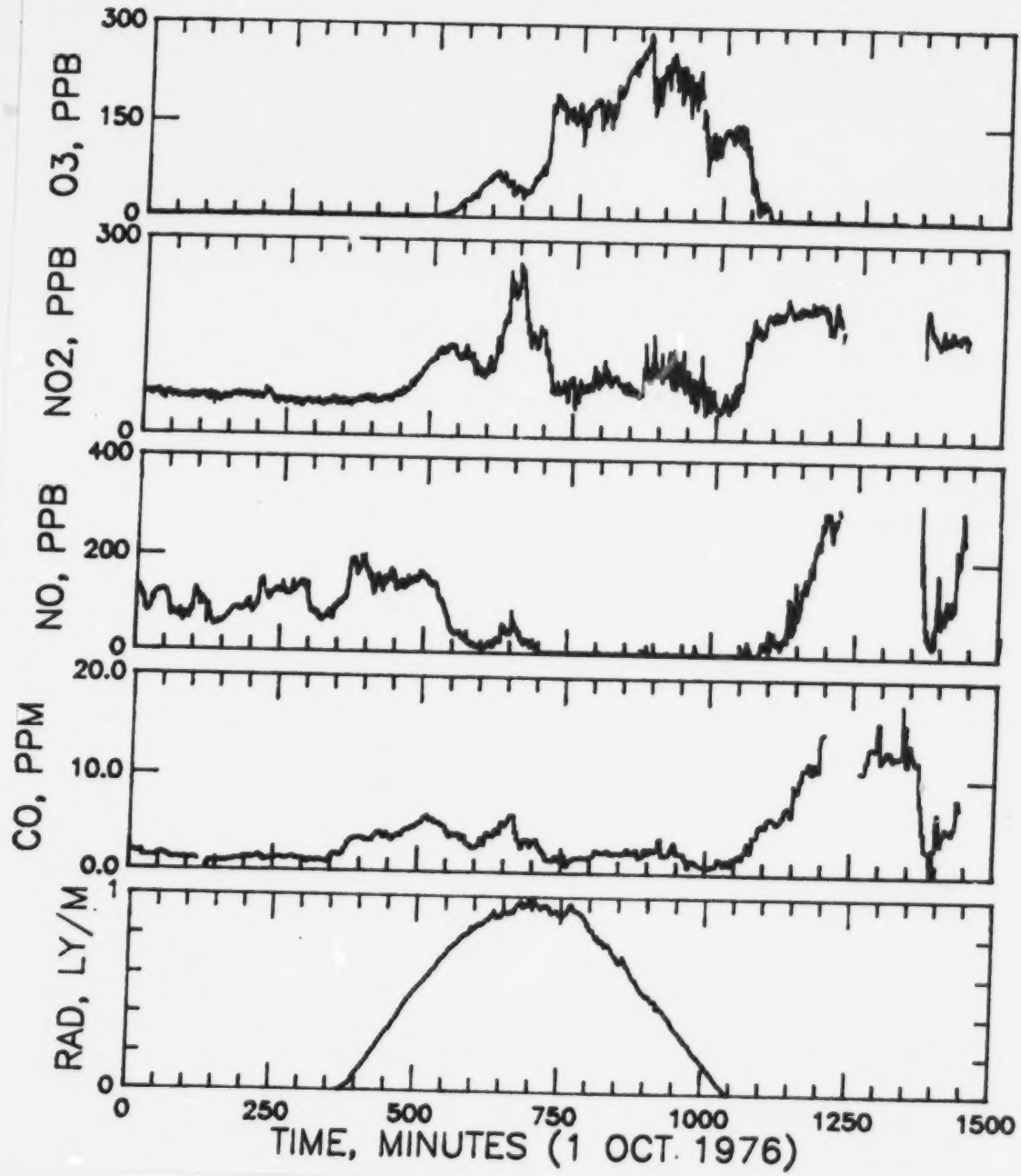

Figure 8. Time series of 1-min data of 1 October 1976. Gas data are from station 101; solar radiation data are from stations 103 and 104. Time is measured in minutes from midnight.

SECTION 4

PHOTOCHEMICAL BOX MODEL

OVERVIEW

The Photochemical Box Model (PBM), a single-cell Eulerian air quality simulation model, accounts for the transport and chemical transformation of air pollutants in smog-prone urban atmospheres. The model domain is a well-mixed, variable volume reacting cell where the physical and chemical processes responsible for photochemical smog are mathematically created. These processes include the transport and dispersion of pollutant species through the cell, the injection of primary precursor species by emission sources, and the chemical transformation of the reactive species into intermediate and secondary products. They are schematically illustrated in Figure 9.

The horizontal length scale of the cell was 20 km in the model configuration for the St. Louis RAPS data base, and the vertical scale was time-dependent, proportional to the depth of the mixed layer. The model domain is centered on downtown St. Louis and includes most of the major line and area emissions sources in the central business district and suburban areas. However, it does not include several major NO_x point sources located in the outlying areas. These are the electric power plant plumes of Labadie to the west, Sioux to the north and Merramac to the south of the domain. Effects from these sources on the PBM simulation are accounted for in the NO_x boundary concentrations for the model. Source emissions within the model domain were assumed to be distributed uniformly across the surface face of the cell. Point sources within the domain are simply added to the area and line source emissions fluxes; they are not treated separately and plume rise is not considered. Twelve of the surface monitoring stations as well as one upper air sounding

location were situated within the cell boundaries. The remaining surface stations were available for determining the hourly boundary concentrations for the model. The St. Louis PBM domain is illustrated in Figure 10.

There are three data preprocessors that must be executed before the model simulation itself. They access the RAPS data base and retrieve the appropriate parameters required by the PBM. The method for performing a PBM simulation is described in Report I. Both Reports I and II emphasize the model simulation results for O_3, although there are no differences in the method for preparing a model simulation where we focus upon the NO_2 results. Both NO_2 and O_3 are components of urban photochemical smog and the model simulation of one can never exclude the other. It is assumed that there is no significant effect of long-distance transport of NO_2. Therefore, although a boundary concentration at the top surface of the model domain is specified for O_3 because of its ability to be transported long distances, none is required for NO_2. Local effects, however, require the horizontal inflow boundaries of the model to have the concentrations of both NO_2 and O_3 specified.

PBM simulations were conducted for each of the 20 test days listed in Table 1. The table also presents selected meteorological attributes of the test days. These days were chosen primarily for their high O_3 levels in St. Louis as discussed in Reports I and II. Levels of NO_2 associated with these same photochemical smog days were also generally high and thus may also be used for the evaluation of the PBM for NO_2 predictions in St. Louis. Although results for NO_2 on all days are summarized, detailed descriptions are presented for only 6 days. These are the six highest cases of domain-average observed NO_2 concentrations at any hour of the model simulation period. This excludes from consideration those few occurrences of maximum NO_2 after 1800 or before 0500 h. We are more interested in studying the PBM's ability to simulate daytime NO_2 patterns. The 6 days focused on are 184 and 251 of 1975 and 159, 160, 237 and 275 of 1976. Time-series of observed and predicted NO and NO_2 concentrations are shown for these days.

TABLE 1. A SUMMARY OF WIND SPEED (WS), WIND DIRECTION (WD), TEMPERATURE, SOLAR RADIATION (ALL WAVELENGTHS), AND MAXIMUM AFTERNOON MIXING HEIGHT (MH) FOR THE 20 DAYS EXAMINED.*

Date	Day (Julian)	WS (m/s)	WD (deg)	Temp (°C)	Solar (ly/min)	Max MH (m)
5/22/75	142	1.1	224	29	1.12	1504
6/27/75	178	0.4	245	29	0.96	1822
7/01/75	182	1.4	70	29	0.99	2606
7/02/75	183	1.4	15	30	0.92	2488
7/03/75	184	1.8	324	30	0.85	1875
7/26/75	207	1.0	139	26	0.98	1477
7/28/75	209	2.0	18	30	0.98	1909
8/09/75	221	0.4	88	26	0.98	1195
8/18/75	230	1.6	167	27	0.96	1488
8/19/75	231	1.3	168	28	0.95	1052
9/08/75	251	1.8	181	25	0.89	1797
6/07/76	159	1.0	129	25	1.06	1972
6/08/76	160	1.3	284	27	1.01	1772
7/13/76	195	2.3	145	28	1.02	1853
7/29/76	211	0.3	251	26	0.53	1706
7/30/76	212	1.7	205	30	0.82	1304
8/12/76	225	2.3	253	29	0.70	730
8/13/76	226	1.1	273	30	0.86	1427
8/24/76	237	1.3	110	28	0.82	2124
10/01/76	275	0.6	222	22	0.78	527

*Meteorological variables (except MH) are network averages over the period 0700-1359 CST.

RESULTS

Of the 20 modeled days only 4 had single station NO_2 observed maxima located outside of the area bounded by the PBM domain. These cases consisted of late afternoon or evening maxima. More commonly the maximum NO_2 values observed in the St. Louis area are found within the 20 km square area centered on the downtown district. Unlike O_3 maxima which typically occur in this area only under stagnation conditions the NO_2 maxima are more source-oriented and tend to occur closer to the major emissions areas.

The PBM-simulated concentrations represent spatial averages over the volume of the box. The proper observed concentration with which to compare predictions is the average over all 12 monitoring sites within the box. These observed average concentrations are represented by the open circles in the concentration time series described below for Figures 11-16. The observed range of concentrations among the 12 sites within the PBM domain is described by the dashed lines in the time series. A coarse measure of model performance is made by observing whether the PBM-predicted concentrations (shown as solid lines) fall within the range of observed concentrations (between the dashed lines) and preferably as close as possible to the average observed concentrations.

The first of the six test days described in the PBM evaluation study is Day 184-75. The synoptic meteorological features on this day showed a large high-pressure system prevailing over the central U.S. and extending upwards to at least the 500-mb level. Winds at the surface in the St. Louis vicinity were from the north and northeast at approximately 2.0 m sec^{-1}. There was a partial high cloud cover during most of the day. The maximum single station hour-average NO_2 measurement occurred at monitoring site 104 at 0700 h in East St. Louis. According to the time referencing style employed here, the 0700 hour-average refers to average concentration from 0700 to 0800 h.

The concentration time series for NO and NO_2 on Day 184 are shown in Figures 11a and b, respectively. Concentrations of NO tend to be underpredicted in the early hours of the simulation. This is fairly typical for the PBM and for many simulation models defining a starting cell size of a finite depth. In reality the primary pollutant NO is emitted into a stable atmospheric situation at night and during the early morning hours forming shallow pockets of high concentrations of mass. The range of observed NO values in the monitoring network is usually large and the highest values bias the PBM domain average. The predicted NO concentrations during this same time period result from emissions being spread through a layer of "artificial" finite vertical extent and are thus usually less than those showing the average observed concentrations. The time series in Figure 11a is a good example of this phenomenon.

The mass of NO in the atmosphere is converted fairly rapidly to NO_2 after sunrise by photochemical reaction processes. The peak NO_2 concentration is often reached several hours into the model simulation period when atmospheric mixing is vigorous and the impediments to model simulation discussed for NO are not as severe. The model predictions of NO_2 on Day 184 fall within the concentration envelope throughout the simulations. The predicted peak of 0.075 ppm occurs 1 hour before the observed peak of 0.079 ppm, a 5% model underprediction. It is significant that in the vicinity of the observed NO_2 peak shown in the Figure 11b time series the maximum within the concentration range is considerably larger than the average and has undoubtedly inflated the domain-average value.

Following chronologically, the next test day focused on is Day 251-75. A relatively weak cold front lying to the northwest of St. Louis through central Illinois separated two areas of high pressure on this day. The front approached St. Louis during the day, and wind speeds were 2.0-3.0 m sec^{-1} from the south and southwest. Skies were clear through most of the model simulation period. The front passed through and became stationary just south of St. Louis during the evening hours and the winds shifted to the northeast.

The concentration time series for NO and NO_2 on Day 251 are displayed in Figures 12a and b, respectively. The model predictions for NO again are lower than observations in the area of the observed peak concentration. Concentrations of NO typically fall to very low levels shortly after the morning heavy traffic period as seen in Figure 12a. The time series for NO_2 in Figure 12b is particularly interesting. Model predictions and observations track quite well through most of the simulation period except in the vicinity of the peak observation. The sharp increase seen in the plot at the top of the range of observed concentrations within the model domain suggests that at least one of the monitoring stations was affected by a strong NO_2 plume during this period. Since the wind flow was from the southwest at this time the plume from the large Labadie power plant may have been responsible. If this was the case, the PBM is insensitive to effects from individual plumes and could not handle this case properly. High observed NO_2 concentrations at the upwind boundary monitoring stations would be one way that the PBM might account for a situation like this, although on Day 251 at this time period these stations did not indicate high NO_2. The peak observed NO_2 occurred at 0900 h at 0.067 ppm, and the highest model estimate was 0.046 ppm at 0700 h, a 31% underprediction.

Days 159 and 160-76 occurred in the middle of an atmospheric stagnation episode over the central U.S. The center of the large stalled high-pressure zone was directly over the Missouri-Illinois area on these two days. Wind flow was light and variable on both days. Speeds were from 1.0-2.0 m sec^{-1} generally from a southeast through southwest direction. Skies were completely clear on both days.

The concentration time series for NO and NO_2 on Days 159 and 160 are shown in Figures 13 and 14, respectively. Maximum observed concentrations of both species are greater on the first day of this episode than on the second. Model predictions of NO are generally less than observations during the first hours of simulation. Nitrogen dioxide predictions fall within the concentration envelope during the simulation

period on both days. On Day 159 the trend in the predictions is nearly identical to the observations, although the observed concentrations are consistently larger as clearly seen in Figure 13b. Figure 14b shows the NO_2 predictions to be larger than the observations at all but two hours near the peak observed concentration on Day 160. On Day 159 the maximum observed NO_2 level was 0.094 ppm at 0700 h and the peak prediction was 0.082 ppm at 0600 h, a 13% underprediction. Day 160 showed a maximum PBM-domain NO_2 concentration of 0.065 ppm at 0700 h and a model estimated peak of 0.069 ppm at 0600 h, a 6% overprediction.

The synoptic meteorological conditions on Day 237-76 showed St. Louis to be on the western side of a large high-pressure system over the east coast of the U.S. Wind flow over the area was from the southeast and speeds were 1.0 to 2.0 m sec^{-1}. Skies were mostly clear although a high-level partial overcast persisted during the early afternoon.

PBM results and observations for Day 237 are shown for NO and NO_2 in Figures 15a and b, respectively. The time series of concentrations here show fairly severe underpredictions of both NO and NO_2 by the model. The model predictions fall below the envelope of the range of observed concentrations just after the point of the maximum observation for both pollutant species. The PBM shows a 37% underprediction of peak observed NO_2 on this day, the worst performance for NO_2 by the PBM of all 20 days modeled. The maximum observed concentration was 0.083 ppm at 0700 h and the peak model prediction was 0.052 ppm at the same hour.

The last of the six days discussed here is Day 275-76, probably the most extreme case of stagnation occurring during the 1975-76 period of the RAPS in St. Louis. The synoptic meteorological conditions showed a high-pressure region over the Texas-Arkansas area with northwest flow aloft over St. Louis. Near the surface however, winds were very light and variable in direction with little transport through the area. Skies were clear all day, and a strong subsidence inversion over the city held the mixed depth to a maximum of approximately 500 m above ground during the afternoon.

Concentration time series for NO and NO_2 for Day 275 are presented in Figures 16a and b, respectively. Ambient levels of NO_x were higher on this day than on most of the others in the evaluation study. During the model simulation period the predictions and observations generally agree quite well. The NO time series in Figure 16a shows remarkably good agreement considering the primary emitted nature and volatility of the species. The slow ascent of the mixed layer depth and consequent low dilution rate probably afford the PBM a better chance at modeling NO here. Typically the model dilutes a primary emitted pollutant at too high a rate during the morning hours after sunrise because of the assumption of complete mixing within the box volume.

The NO_2 predictions show somewhat smoother temporal gradients in Figure 16b than the observations do, but the overall trend is very good between the two data sets. The maximum domain-average NO_2 ambient value on Day 275 was 0.108 ppm and occurred at 1700 h, the last hour of the model simulation period. Atmospheric stability increased greatly on this day as the sun began to set and caused near-ground concentrations of primary pollutants to rise quickly. Because of the simplistic nature of the well-mixed box assumption in the PBM this type of atmospheric behavior cannot be simulated well. The peak hour-average model prediction for NO_2 was 0.087 ppm at 1000 h, a 19% underprediction. If we compare this peak predicted value with the mid-morning ambient NO_2 peak of 0.102 ppm at 0900 h the underprediction is reduced to 15%. Concentration time series of NO_2 on the remaining 14 days in this evaluation study are contained in an appendix to Report II.

Table 2 presents a summary of maximum NO_2 concentration data from the PBM for all 20 days modeled. Model predictions are listed as paired and unpaired. Paired predictions correspond to the same hour as the observed maximum and the unpaired predictions represent the peak at any hour of the simulation. The paired and unpaired predictions may not coincide, indicating a lag between observed and predicted NO_2 peaks. Statistics on the residual concentration, ΔC, have been computed for both

TABLE 2. A SUMMARY OF PREDICTED AND OBSERVED NO_2 MAXIMA FOR THE PBM

Julian date	Observed Peak Concentration[a]		Paired[b]		Unpaired		
	Value (ppm)	Time (CST)	Value (ppm)	ΔC/OPC[c] (%)	Value (ppm)	Time (CST)	ΔC/OPC (%)
142 (1975)	0.037	0600	0.040	- 8.1	0.042	0700	-13.5
178	0.053	0700	0.043	18.9	0.046	0600	13.2
182	0.041	0600	0.053	-29.3	0.053	0600	-29.3
183	0.053	0800	0.032	39.6	0.059	0600	-11.3
184	0.079	0700	0.062	21.5	0.075	0600	5.1
207	0.042	0600	0.051	-21.4	0.051	0600	-21.4
209	0.030	0800	0.029	3.3	0.041	0700	-36.7
221	0.045	0700	0.047	- 4.4	0.047	0700	- 4.4
230	0.054	0700	0.050	7.4	0.050	0700	7.4
231	0.030	0800	0.033	15.4	0.036	0700	7.7
251	0.067	0900	0.036	46.3	0.046	0700	31.3
159 (1976)	0.094	0700	0.076	19.1	0.082	0600	12.8
160	0.065	0700	0.059	9.2	0.069	0600	- 6.2
195	0.029	1700	0.018	37.9	0.026	0600	10.3
211	0.041	1200	0.027	34.1	0.034	0700	17.1
212	0.061	0700	0.050	18.0	0.053	0600	13.1
225	0.042	1600	0.026	38.1	0.049	0700	-16.7
226	0.058	0700	0.049	15.5	0.049	0700	15.5
237	0.083	0700	0.052	37.3	0.049	0700	37.3
275	0.108	1700	0.054	50.0	0.087	1000	19.4
			$\overline{\Delta C}$ = 0.012		$\overline{\Delta C}$ = 0.004		
			s.d. (ΔC) = 0.015		s.d. (ΔC) = 0.011		
			$\overline{\lvert\Delta C\rvert}$ = 0.014		$\overline{\lvert\Delta C\rvert}$ = 0.009		

[a]During simulation time period:
0500 h - 1800 h.
[b]PBM predictions: Paired in time.
[c]ΔC = Obs.-Pred. = Residual conc.;
OPC = Obs. Peak Concentration.

the paired and unpaired predictions. The average signed residual (bias) and absolute residual (gross error), and standard deviation (s.d.) are presented for the analyses. The average bias is positive for both the paired and unpaired cases, indicating an underprediction of the maximum, although the extent of the bias is substantially less in the unpaired data set, 0.012 ppm compared to .004 ppm. There were more overpredictions in the unpaired data than in the paired data as demonstrated by the smaller difference between the gross error and the bias in the paired data. The s.d., a measure of model precision, is larger than the average bias for both cases, implying a relatively large spread in the magnitude of the residuals. Although the s.d. values here are not large in an absolute sense they appear so because the average bias values are not far from zero. The average value of the model's underprediction for NO_2 over all 20 days is 17% for the paired data and 3% for the unpaired. The average underprediction for the 6 highest ambient NO_2 days discussed in this section is 31% for the paired case and 17% for the unpaired.

The analysis presented in Table 2 only indicates model performance for estimating maximum NO_2 concentrations. To more fully understand PBM performance the model can be viewed from a broader statistical perspective. Figure 17 presents a frequency histogram (RS) of all NO_2 residual pairs for all 20 test days as well as a plot of the residuals versus observed concentrations (RO). An ideal RS would be narrow with a peak at the 0.0 residual. The distribution for NO_2 shown in Figure 17a is symmetric about a peak close to the 0.0 residual. There are several outliers on the underpredictive side. The plot in Figure 17b demonstrates no clear trend in the residuals for ambient NO_2 concentrations less than 0.05 ppm. These constitute the majority of all data pairs. Above ambient levels of 0.05 ppm there is a clear tendency toward increasing model underprediction with higher ambient concentrations.

Overall model performance statistics for NO_2 from the PBM are tabulated in Table 3. These statistics were developed from all paired data residuals over the 20 test days. The mean residual and average underprediction are very small, certainly lower than those statistics developed

TABLE 3. SUMMARY OF NO_2 MODEL PERFORMANCE STATISTICS FROM THE PBM[a]

Mean Concentration Data	Value
Mean Observed Concentration (ppm)	0.029
Mean Predicted Concentration (ppm)	0.028
Mean Residual (ppm)	0.001
RMS Error (ppm)	0.009
Mean Residual/Mean Obs. Conc. (%)	3.4
Error Band[b] (%)	60.0
Analysis of Trends Data	
Correlation Coefficient	0.876
Slope	0.753
Intercept (ppm)	0.007
Sum of Squared Error (ppm^2)	0.028

[a]Statistics are developed for all 20 test days.
[b]Percent of predictions within 25% of observations.

for the maximum NO_2 concentration data. This is not particularly surprising since it is more difficult for the model to correctly simulate the higher ambient concentration levels. The analysis of trends statistics for all paired NO_2 data show a high correlation coefficient and a linear least squares line with a slope of 0.75 and an intercept close to zero. This again helps confirm that the PBM tends to slightly underpredict NO_2 ambient domain-average values over the 20 test days modeled.

CONCLUSIONS

The performance of the PBM in predicting the average area-wide urban NO_2 levels in St. Louis has been assessed using a sample of 20 test-case days from the RAPS data base. The overall performance is quite good with only a small value of underprediction in the average. When assessing the domain-average maximum ambient NO_2 levels the model's underpredictive tendency increases but remains less than 20% for both paired and unpaired data sets. While this is a creditable result for the PBM there are serious difficulties for the use of this model in a strict regulatory sense for the prediction of maximum urban NO_2 levels.

The assumption of a homogeneous emissions distribution across the model domain is clearly flawed. While this assumption may not have as great an effect on the predictions of a purely secondary species such as O_3, it certainly does for NO or NO_2 concentrations, for which where the maximum values frequently occur downwind of a major point source or roadway. The simplistic treatment of these source emissions types precludes the determination of a relationship between domain-average NO_2 predictions and the maximum point NO_2 levels expected within the model domain. An examination of the time series of the large range of NO_2 levels observed at monitoring sites within the PBM domain seems to confirm this aspect of the model. The greatest potential use for the PBM in the prediction of urban NO_2 levels is in the capacity of a simple screening model for a more complex photochemical model.

Further developmental work for the PBM may include the continued testing and refinement of the chemical kinetic mechanism and a test of model sensitivity to variations in selected parameters.

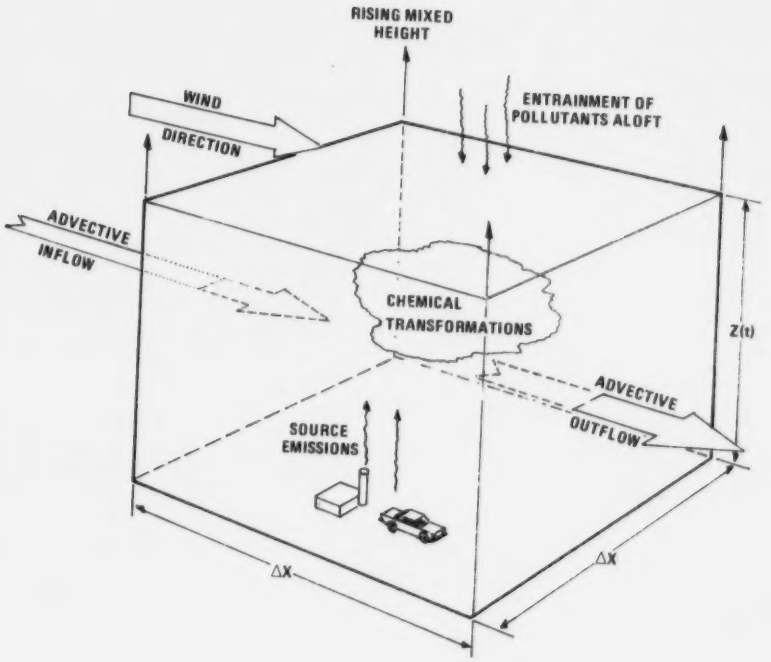

Figure 9. Schematic drawing of the PBM domain.

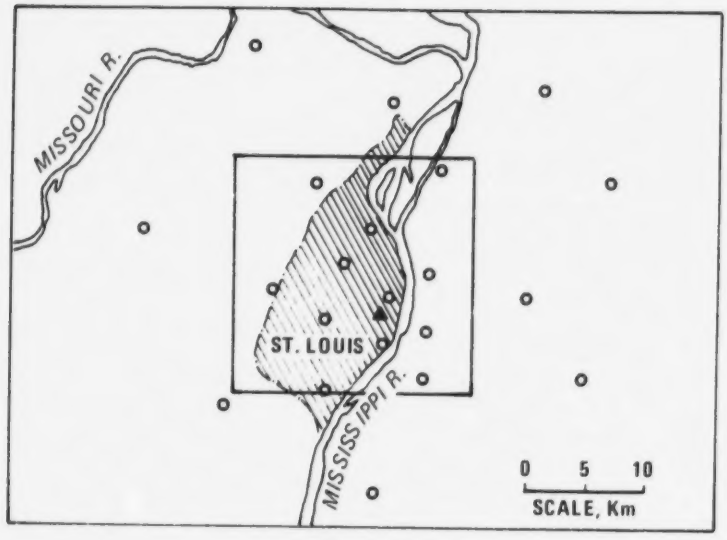

Figure 10. Map of St. Louis area depicting extent of PBM modeling domain (boxed area), city of St. Louis (shaded area), RAPS monitoring stations (circles), and radiosonde ascent site (triangle).

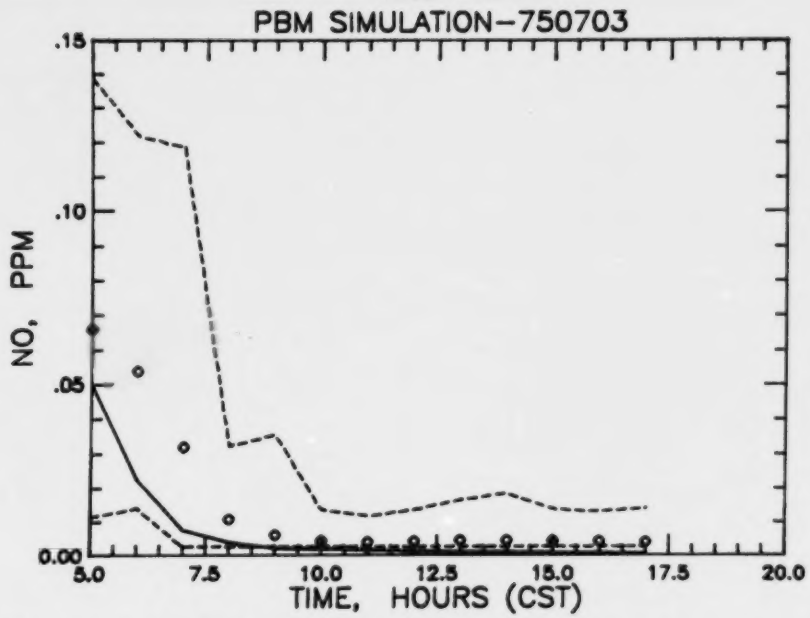

Figure 11a. PBM simulation results for Day 184 of 1975. Time series of average observed (circles), range of observed (dashed lines), and model-simulated (solid line) hour-average concentrations of NO.

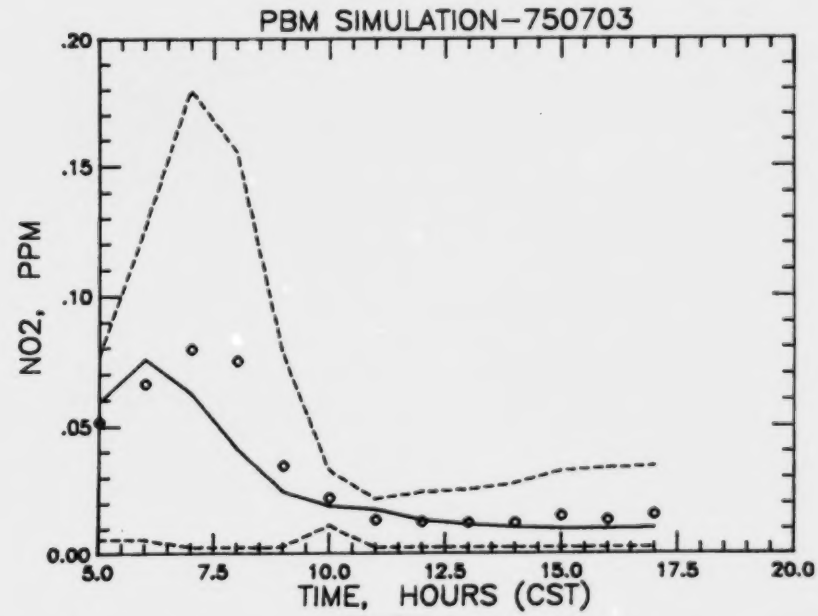

Figure 11b. PBM simulation results for NO_2 - Day 184 of 1975. Keys to figure described in 11a.

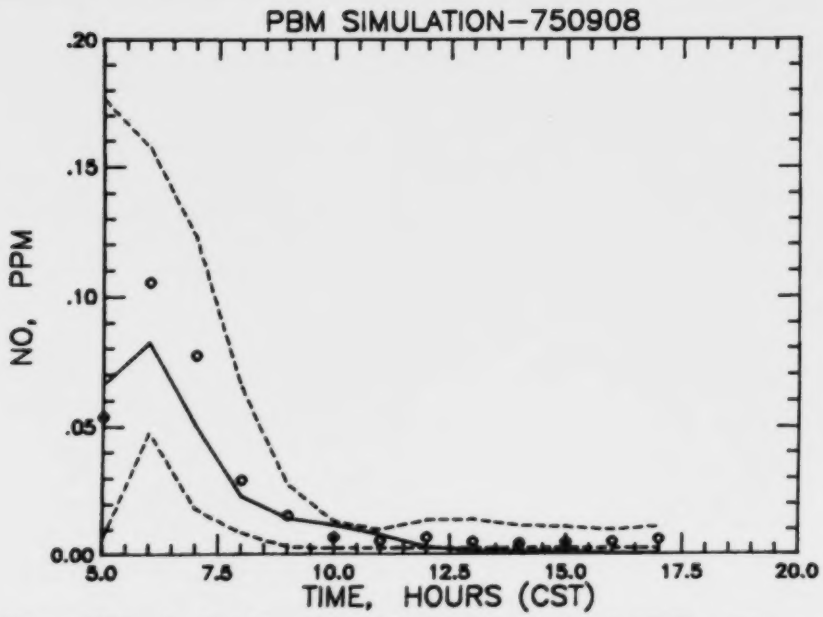

Figure 12a. PBM simulation results for Day 251 of 1975. Time series of average observed (circles), range of observed (dashed lines), and model-simulated (solid line) hour-average concentrations of NO.

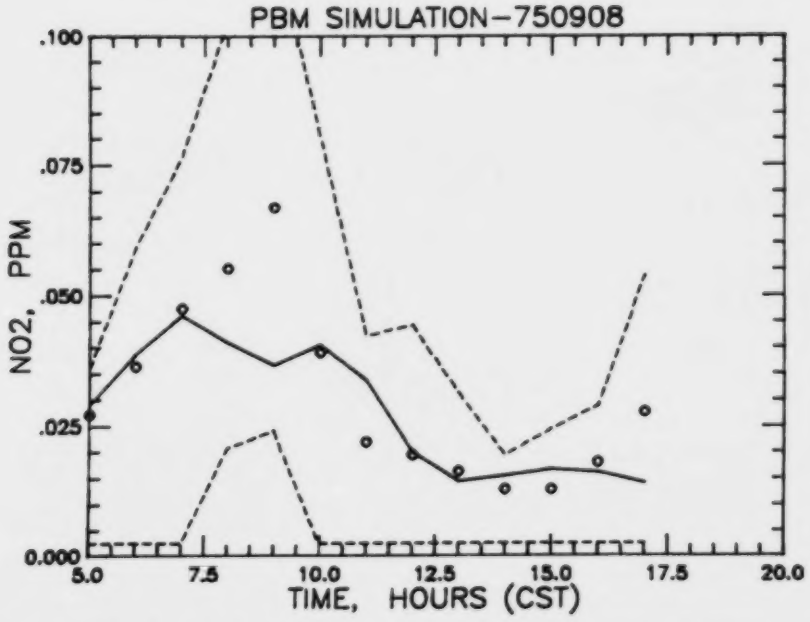

Figure 12b. PBM simulation results for NO_2 - Day 251 of 1975. Keys to figure described in 12a.

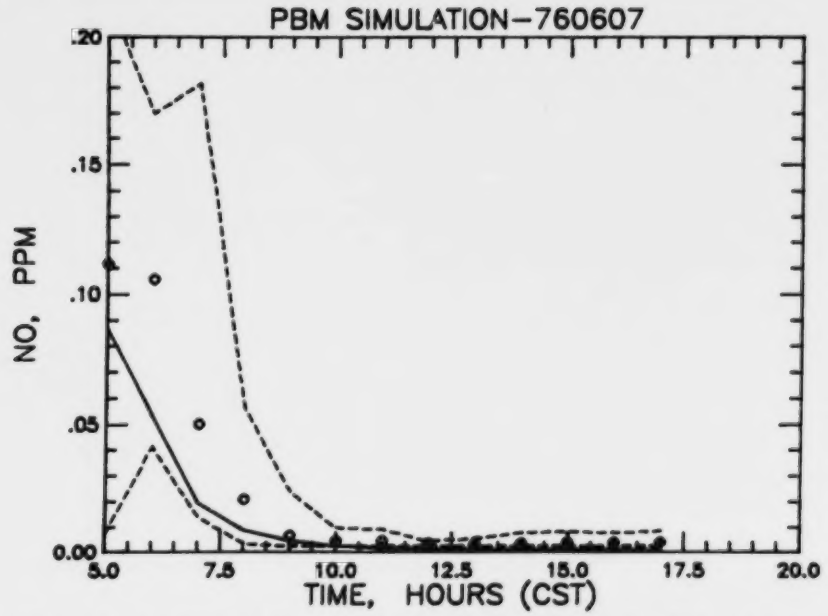

Figure 13a. PBM simulation results for Day 159 of 1976. Time series of average observed (circles), range of observed (dashed lines), and model-simulated (solid line) hour-average concentrations of NO.

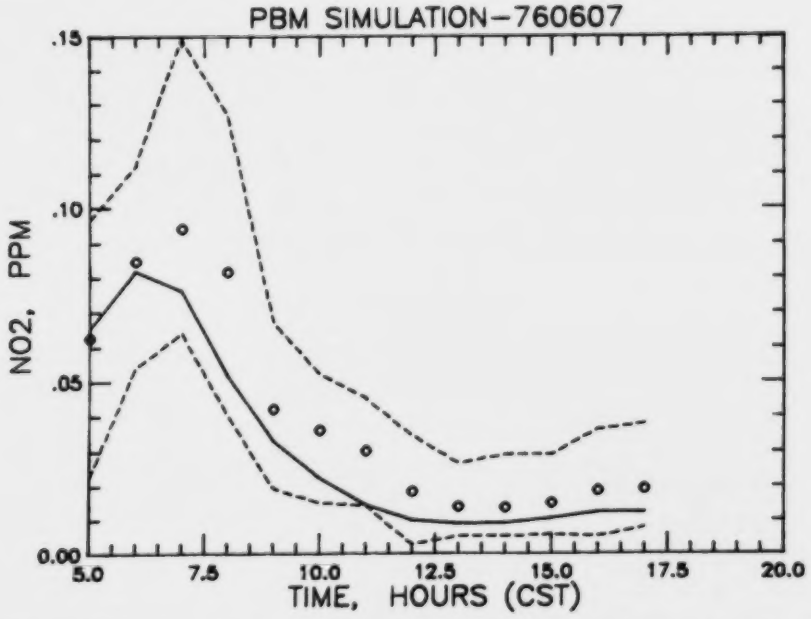

Figure 13b. PBM simulation results for NO_2 - Day 159 of 1976. Keys to figure described in 13a.

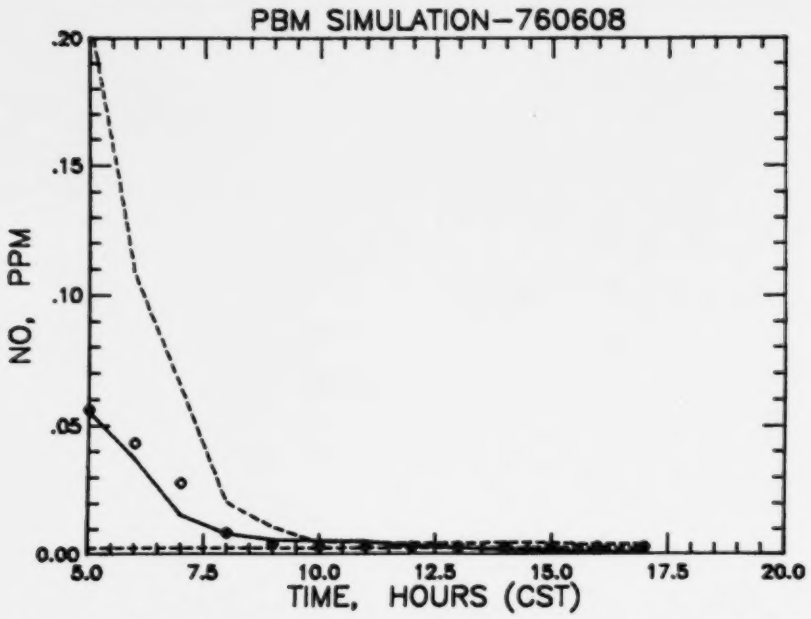

Figure 14a. PBM simulation results for Day 160 of 1976. Time series of average observed (circles), range of observed (dashed lines), and model-simulated (solid line) hour-average concentrations of NO.

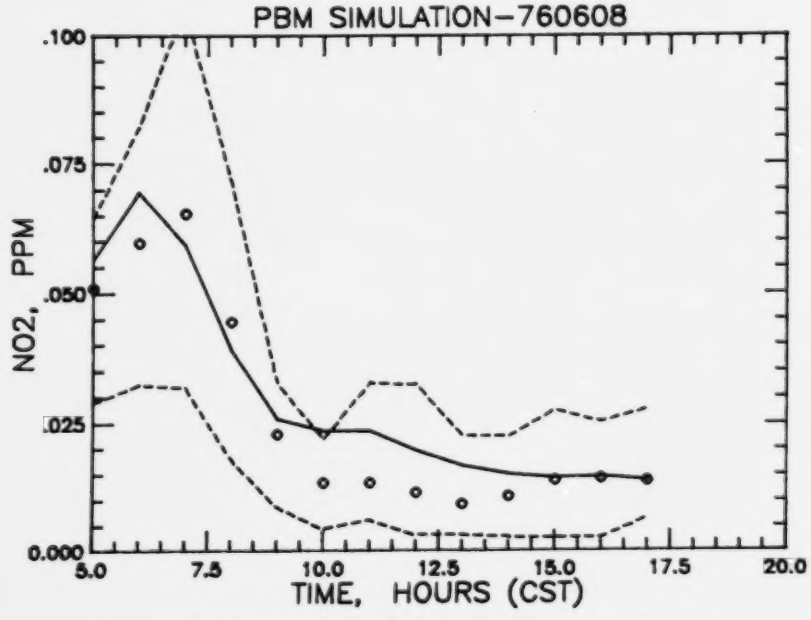

Figure 14b. PBM simulation results for NO_2 - Day 160 of 1976. Keys to figure described in 14a.

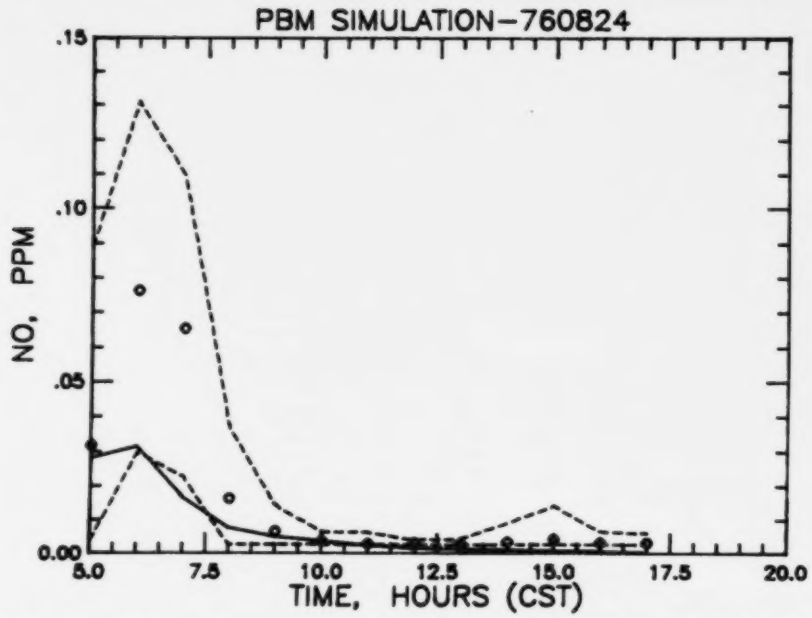

Figure 15a. PBM simulation results for Day 237 of 1976. Time series of average observed (circles), range of observed (dashed lines), and model-simulated (solid line) hour-average concentrations of NO.

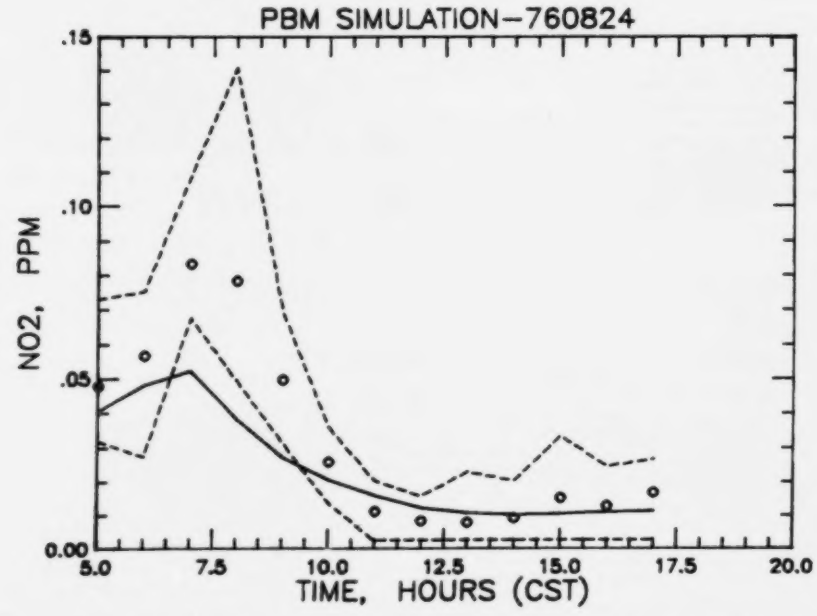

Figure 15b. PBM simulation results for NO_2 - Day 237 of 1976. Keys to figure described in 15a.

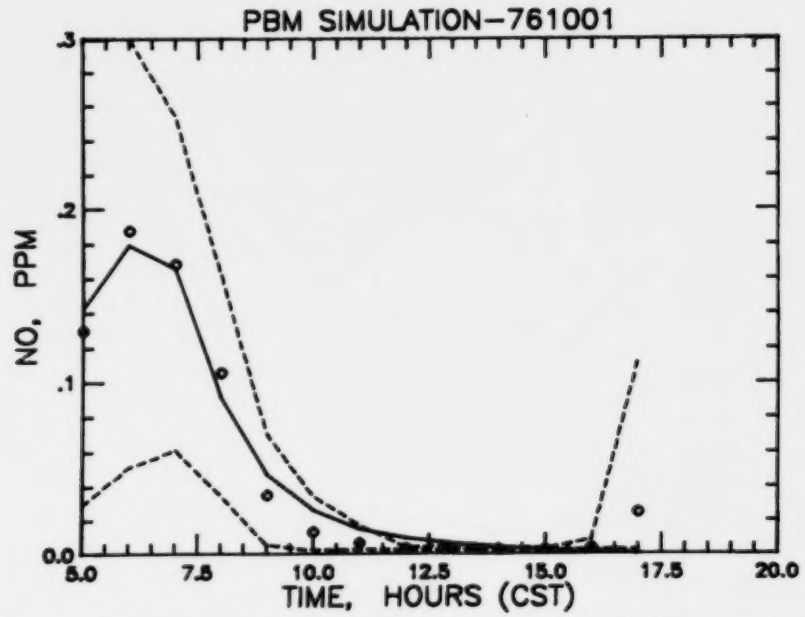

Figure 16a. PBM simulation results for Day 275 of 1976. Time series of average observed (circles), range of observed (dashed lines), and model-simulated (solid line) hour-average concentrations of NO.

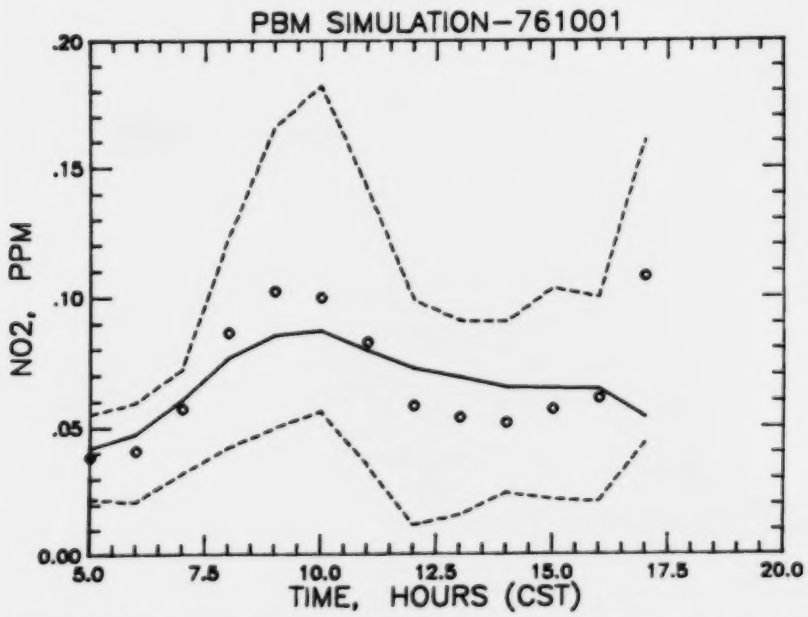

Figure 16b. PBM simulation results for NO_2 - Day 275 of 1976. Keys to figure described in 16a.

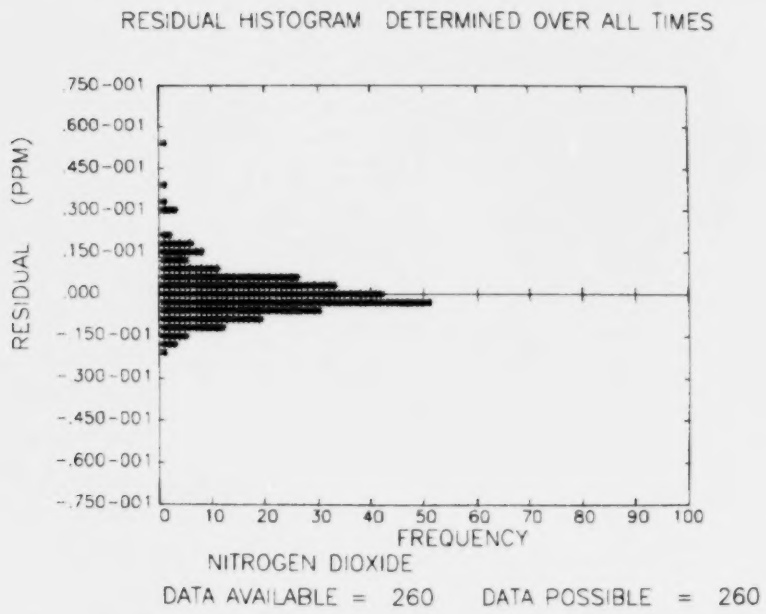

Figure 17a. Residual histogram from the PBM simulation results for all 20 test days for NO_2.

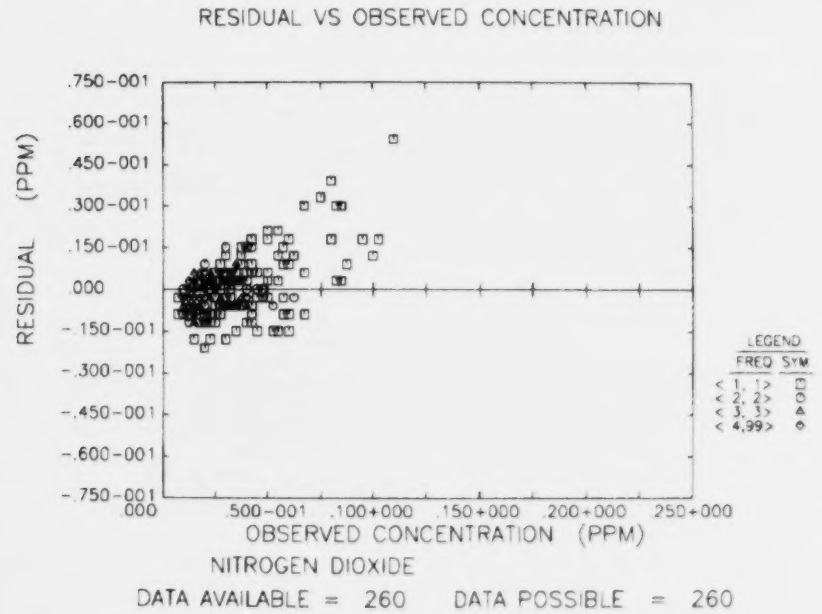

Figure 17b. Residual vs. observed plot from the PBM simulation results for all 20 test days for NO_2.

SECTION 5

LAGRANGIAN PHOTOCHEMICAL MODEL

OVERVIEW

The Lagrangian Photochemical Model (LPM) was developed by Environmental Research and Technology, Inc. and adapted under contract with EPA for use with the RAPS data base. (The LPM is essentially identical to the general-use model named ELSTAR). The LPM envisions a portion of the atmosphere as an identifiable parcel which can be tracked from early morning to the late afternoon (Figure 18). The parcel has five vertical levels extending through the depth of the mixing layer. The vertical resolution of the layers is greatest near the surface and decreases with height. As the parcel moves over the various emissions sources, pollutants are assimilated, vertically mixed, and subjected to photochemical reactions in the presence of solar radiation.

The initial horizontal dimensions of the simulated parcel were chosen as 5 km x 5 km. This rather large parcel size reflected a judgement that wind fields could not be specified with sufficient accuracy to meaningfully use a finer resolution. During the simulation the parcel is allowed to expand according to a Gaussian formulation based on an internally computed stability class. The parcel width generally reaches 7-10 km by late afternoon. However, since NO_2 peaks usually occur in the morning, the parcel expansion has little effect on the results.

Initial pollutant concentrations for reactive hydrocarbon (RHC), NO, NO_2, and O_3 are set in the lower three levels of the parcel based on observed surface values shortly after sunrise. The upper levels retain background concentrations (Schere and Shreffler, 1982). These pollutants interact in a non-linear fashion as photochemistry progresses.

The LPM represents an intermediate approach between the box model (PBM) discussed in the last section and the grid model (UAM) to be discussed in the next section. Unlike the PBM, the LPM allows spatial resolution, and, therefore, a user may better relate a specific source to a high concentration. However, that advantage is obtainable only with a spatially resolved emission inventory, which is expensive to develop. Resource requirements for the LPM are substantially less than those for the UAM. On the other hand, the LPM predicts concentrations along a specific trajectory and not over a complete field like the UAM.

A series of simulations over 20 days has been executed, and results are summarized in this section of the report. Meteorological characteristics of the test days are listed in Table 1.

The LPM is executed using a series of program modules. They are METMOD, EMMOD, and KEMOD, sequentially performing calculations on meteorology and air quality, emissions, and photochemistry. The input and running procedures described by Lurmann et al. (1979a,b) have generally been followed, with modifications as previously documented (Lurmann, 1980; 1981). The modeling methods are more fully described in Report I and Report II.

Since the 20 simulations discussed here were designed specifically to judge model performance in predicting O_3 maxima, the observed NO_2 maxima along the trajectory are not necessarily the highest recorded anywhere in the region throughout the day. The start-point of the trajectory was set so that the parcel arrives at the station observing the daily 1-h O_3 maximum at the time of that observation. Since the O_3 maxima typically occur in the afternoon, it is unlikely that the NO_2 will have a significant concentration at that time. However, the occurrence of the O_3 maximum implies initial conditions or accumulated emissions rich in RHC and NO_x and conducive to an active photochemical cycle likely to produce significant NO_2 concentrations. Because the NO_2 maximum does not coincide with the O_3 maximum, the parcel will rarely be located at a RAPS station. The

observed NO_2 concentrations along the trajectory are based on the values observed at the closest three stations and weighted by $1/R^2$ (where R is the distance to the parcel center).

RESULTS

Parcel trajectories and time series of NO_2 concentrations within the parcel are given in this section for 6 of the 20 days for which simulations have been performed. These Julian days are 182, 184, 231, and 251 of 1975 and 226 and 275 of 1976. In addition, temporal correlation coefficients between predicted and observed concentrations have been computed, and the residual (observed minus predicted) concentrations are summarized in tabular and graphical form. Report II should be consulted for the NO_2 results of other days and the results for the associated pollutants, NO and O_3.

Figure 19a presents a trajectory map for Day 182. The map covers a 100 km square area, and only 9 of the stations are located to avoid cluttering the figure. These stations are (compare Figure 1) 101 in downtown, 122 and 114 to the north, 109 and 123 to the east, 118 and 124 to the south, and 120 and 125 to the west. The start position is indicated by "S" and the start time is given above the figure. Each hour of travel is indicated by a cross. On Day 182 the parcel started at 0500 CST about 8 km north of station 120. Initial conditions of RHC and NO_x were moderately high on this day (Table 4), and the O_3 maximum occurred at 1200 CST as the parcel reached station 125. Figure 19b shows the NO_2 concentrations for Day 182. The RAPS observed values are given by a solid line. The model-predicted values at Level-1 (L-1, understood to be the surface) are given by a dotted line, and the Level-3 (L-3, about 300 m in most cases) predictions are given by a dashed line. (The reader is reminded that the time series represent the concentrations within a moving parcel and not at a single point in space). The observed NO_2 reaches a maximum at Hour 7 (computed from data during 0700-0759), whereas the predicted NO_2 peaks about one hour earlier. The results of this

TABLE 4. INITIAL SURFACE CONCENTRATIONS ASSIGNED TO THE PARCEL FOR REACTIVE HYDROCARBON (RHC), NO, NO_2, and O_3.

Day	RHC (ppm)	NO (ppm)	NO_2 (ppm)	O_3 (ppm)
142	0.26	0.03	0.02	0.00[a]
178	0.19	0.01	0.02	0.00
182	0.52	0.04	0.04	0.01
183	0.15	0.01	0.01	0.01
184	0.39	0.03	0.04	0.01
207	0.11	0.01	0.01	0.01
209	0.32	0.02	0.01	0.01
221	0.14	0.01	0.02	0.02
230	0.12	0.02	0.01	0.00[a]
231	0.15	0.01	0.01	0.01
251	1.28	0.08	0.05	0.00[a]
159	0.22	0.01	0.03	0.01
160	0.05[a]	0.01	0.02	0.02
195	0.05[a]	0.00[a]	0.00[a]	0.02
211	0.07	0.01	0.00[a]	0.03
212	0.10	0.01	0.01	0.01
225	0.05[a]	0.01	0.01	0.01
226	0.41	0.01	0.02	0.04
237	1.57	0.06	1.60	0.01
275	0.70	0.10	0.04	0.01

[a]Defaults: RHC=0.05, NO_x=0.0025, O_3=0.0025

simulation seem reasonably good, showing the early morning peak and the rapid drop-off as the mixing layer deepens and the photochemical cycle progresses.

The initial concentrations are set equal to observed concentrations at the start time. Clearly there may be significant correlation between the series in the first hours due to this artifact. Some effort has been made in the analysis of model performance to evaluate this problem and remove its effects, and this will be discussed when the results are summarized.

Figure 20a presents a parcel trajectory from Day 184. The parcel starts at 0500 CST in the northwest area of the city and moves to the southeast, arriving at station 118 at 1300 CST. Initial concentrations of RHC and NO_x were again moderately high. Figure 20b shows the predicted and observed time series of NO_2. The observed maximum again occurs at 0700 CST and both the L-1 and L-3 predictions show nearby peaks. The substantial overprediction at L-1 reflects a fundamental problem in the LPM, which was identified and discussed in Reports I and II. L-1, which represents the surface, apparently tends to unduly retain surface emissions when moving over strong source areas. Perhaps the vertical diffusivity in the model is insufficient to mix the emissions rapidly enough for reasonable dilution. In fact, the reason for presenting the results for L-3 was to avoid the high sensitivity of the model to surface sources. As pointed out in Report II, the CO concentrations show similar characteristics at L-1 and L-3, so the problem is not due to the photochemical mechanism.

Figure 21a shows the parcel trajectory for Day 231. The parcel starts south of the city, moves just east of station 101, and out to the northwest. The overprediction at both L-1 and L-3 is apparent at midday in Figure 21b. A partial cause for the deviation of the predictions from observations may be that the observations are only close to the parcel and not at the same position. Only at 1400 CST, when the parcel is at

station 121, and the O_3 maximum is recorded, are the parcel predictions and the observation strictly comparable. In this simulation, they are identical at that time. When the distance to a station is less than 1 km, only that single station is used to compute the observation.

The trajectory for Day 251 is given in Figure 22a. The start point is near downtown St. Louis, and initial loading of the parcel with HC and NO is high. Furthermore, winds are very low during the first four hours so that the parcel accumulates large quantities of pollutants from emissions. After 1000 CST the parcel moves more rapidly and arrives at station 122 at 1400 CST. The overprediction, especially at L-1, is evident in Figure 22b for the early morning when the central-city emissions are accumulating. Incidently, the highest 1-h O_3 observation of the RAPS program was recorded on this day at station 122.

The trajectory on Day 226 is found in Figure 23a. Day 226 represented a definite stagnation of the larger scale flow. The trajectory started some 10 km south of station 120, looped out to the east, and returned to the city in the evening. The L-1 predictions show the strong overprediction when the parcel is over the city's emissions, both in the morning and evening. The L-3 prediction, however, tracks the observations quite well.

The most extreme stagnation of the RAPS program occurred on Day 275. Although a parcel trajectory is given in Figure 24a, no actual meaning can be attached to such a path. As in the previous case, the L-1 prediction displays high values corresponding to the morning and evening peaks of automotive traffic, while the L-3 predictions appear quite good.

Table 5 presents model prediction of the NO_2 maxima observed on each test day. At the bottom of the table are statistics to summarize the performance over the test days. From examination of the data of Day 237, it was not possible to determine if the extraordinarily high measurements at station 113 were erroneous or influenced by a nearby source. The LPM

TABLE 5. A SUMMARY OF PREDICTED AND OBSERVED NO_2 MAXIMA FROM THE LPM FOR 20 DAYS SELECTED FROM 1975-1976.

Julian date[a]	Hour[b]	Station[c]	Observed 4-meters (ppm)	LPM Predicted Maximum Level-1 (ppm)	Level-3 (ppm)
142 (1975)	6	119	0.032	0.039	0.039
178	9	112	0.039	0.109	0.042
182	7	120	0.060	0.073	0.058
183	7	117	0.028	0.044	0.015
184	7	120	0.053	0.108	0.060
207	12	107	0.027	0.063	0.036
209	9	104	0.039	0.081	0.049
221	8	115	0.044	0.034	0.039
230	8	106	0.037	0.042	0.024
231	11	102	0.037	0.074	0.066
251	10	113	0.077	0.110	0.099
159 (1976)	7	115	0.038	0.030	0.031
160	7	120	0.029	0.039	0.023
195	13	102	0.064	0.023	0.014
211	11	112	0.088	0.058	0.040
212	10	107	0.028	0.055	0.025
225	15	117	0.023	0.020	0.019
226	8	112	0.034	0.083	0.044
237	7	113	1.849	1.400	1.530
275	10	107	0.112	0.213	0.144

ΔC = Obs minus L-1 Pred	ΔC = Obs minus L-3 Pred
$\overline{\Delta C}$ = -0.022	$\overline{\Delta C}$ = 0.001
s.d.(ΔC) = 0.034	s.d.(ΔC) = 0.021
$\lvert\overline{\Delta C}\rvert$ = 0.031	$\lvert\overline{\Delta C}\rvert$ = 0.015

[a]Day 237 values are excluded from all statistics.

[b]Hour of the maximum observed NO_2 concentration, excluding the initial hour where the observed and model values are identical.

[c]The closest of three stations which contribute to the observed value by $1/R^2$ weighting.

was executed including these data, but inclusion of the single maximum for Day 237 would unduly influence the statistics of model perforance over the set of test days. Therefore, the results of Day 237 were excluded. (Note that data of station 113 were deleted before execution of the PBM and UAM). The average observed NO_2 maximum for the remaining 19 days is 0.047 ppm with a standard deviation of 0.023 ppm. The average residual (observed minus predicted) is negligible for the L-3 results, although the s.d.(ΔC) is substantial considering the typical observed value. Results for L-1 indicate overprediction as has been discussed above.

Figure 25 displays the average hourly values of observed NO_2 concentrations and the residuals from model predictions averaged over 19 days of simulations (not including Day 237). The vertical bars indicate standard deviations of the sample mean. The observed values tend to be highest in the morning and decrease through the day. The peak average of about 35 ppb is well below the 53 ppb annual level specified by the NAAQS. The model tends to strongly overpredict at L-1 during midday. The overprediction is less at L-3, but still about 1/3 of the typical observed value. These graphs tend to show a more serious discrepancy between the model and observations than is indicated solely by the statistics of Table 5.

Temporal correlation coefficients were computed between observed and predicted series from the start time to the lesser of 1700 CST or the end of the run. Coefficients give some sense of how the two series compare in shape but not necessarily in magnitude. Results for L-1 and L-3 are found in Table 6, as are the average and standard deviation of the coefficients over the 20 days. As can be seen from Table 6, the six series selected for display in this section show above average correlation. In the average, the correlation is not particularly high and the variance is considerable.

TABLE 6. TEMPORAL CORRELATION COEFFICIENT (r) BETWEEN OBSERVED AND LPM-PREDICTED POLLUTANT CONCENTRATIONS FOR THE PERIOD FROM THE START OF THE SIMULATION TO 1700 CST OR EARLIER TERMINATION.

Day	NO_2	
	L-1	L-3
142 (1975)	-0.26	-0.03
178	-0.39	-0.71
182	0.94	0.94
183	0.65	0.65
184	0.77	0.81
207	0.32	0.53
209	0.93	0.93
221	0.77	0.85
230	0.43	0.42
231	0.62	0.57
251	0.84	0.92
159 (1976)	0.89	0.92
160	-0.09	0.23
195	0.61	0.44
211	0.70	0.78
212	0.30	0.30
225	-0.36	0.07
226	0.28	0.88
237	0.83	0.87
275	0.66	0.87
	$\bar{r}$ = 0.47	0.56
	σ_r = 0.42	0.42

CONCLUSIONS

The LPM results for 20 days of active photochemistry have been analyzed to indicate the ability of the model to predict the observed NO_2 concentrations along a particular trajectory.

In terms of predicting the maximum observed concentrations along the trajectory, the L-3 results show an average residual of nearly zero. However, the standard deviation of the residuals is about 45% of the mean observed value. The L-1 residuals show substantial overprediction.

Correlation coefficients between observed and predicted time series, relatively high on some days and low or even negative on others, are rather disappointing. The average coefficient of 0.5 ± 0.4 is not significant.

There are perhaps two major problems in the analysis.

(1) NO_2 values in St. Louis are relatively low, with the average 1-h observed maximum only .047 ppm for the 19 cases entering the analysis (Day 237 recorded .185 ppm). This is slightly below the NAAQS annual standard. This analysis does not deal with situations relevant to a possible short-term standard.

(2) The running strategy for the model, developed for O_3, does not contribute to an independent judgement of performance for NO_2. The computed observed value is usually from three close stations rather than at the parcel location. Furthermore, early morning NO_2 peak predictions must be rather highly correlated to initial conditions. At present, the LPM cannot be run through sunrise, so it is not possible to start earlier in the morning to alleviate the problem.

In summary, the predictions of NO_2 concentrations are perhaps consistent with the general levels expected from a photochemical model simulating the St. Louis situations. However, the low observed concentrations and difficulties in interpreting model results do not allow further definitive statements about how the model may perform in situations where a reasonable short-term standard would be violated.

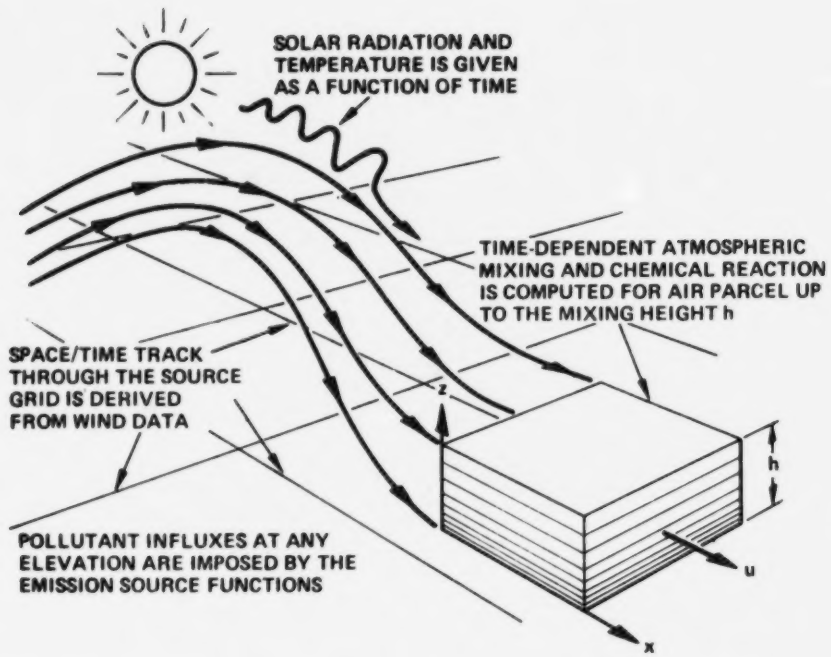

Figure 18. Schematic of the moving Lagrangian parcel as described in the LPM.

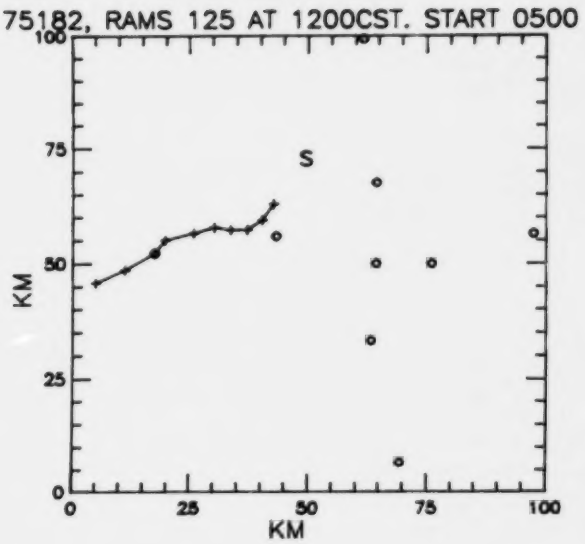

Figure 19a. LPM parcel trajectory for Day 182 of 1975.

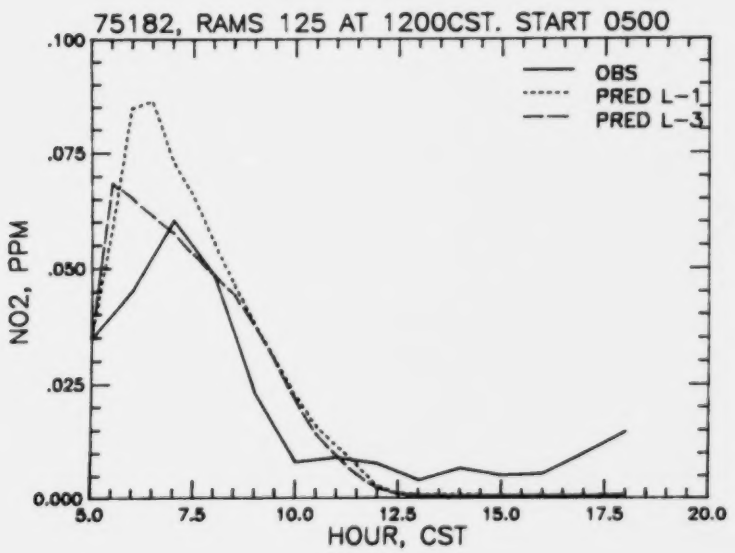

Figure 19b. LPM time series of observed and predicted NO_2 hourly concentrations on Day 182 of 1975.

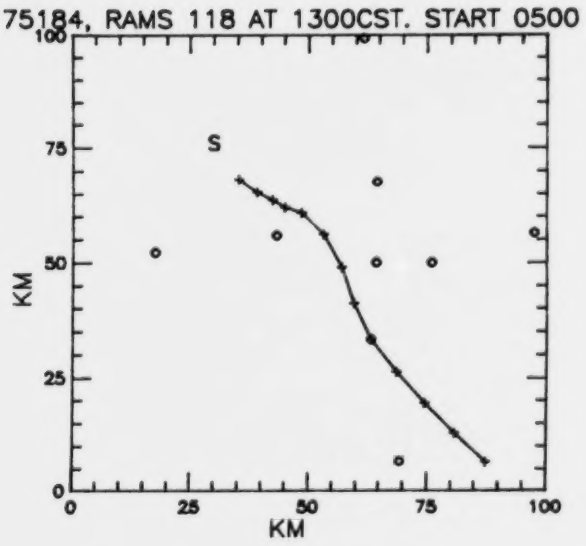

Figure 20a. LPM parcel trajectory for Day 184 of 1975.

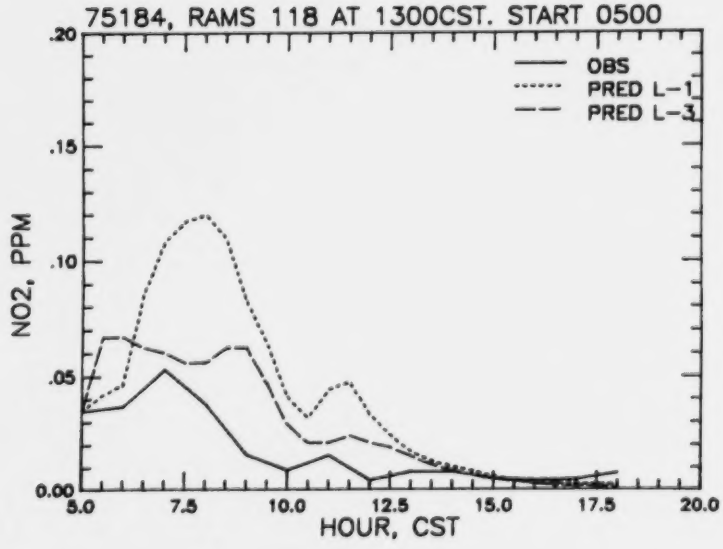

Figure 20b. LPM time series of observed and predicted NO_2 hourly concentrations on Day 184 of 1975.

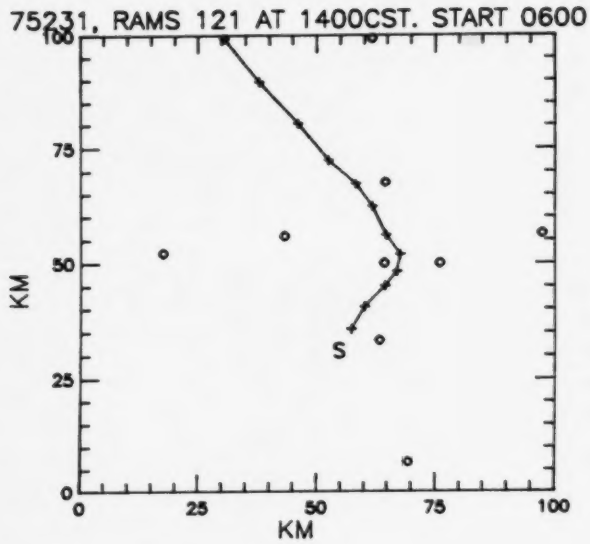

Figure 21a. LPM parcel trajectory for Day 231 of 1975.

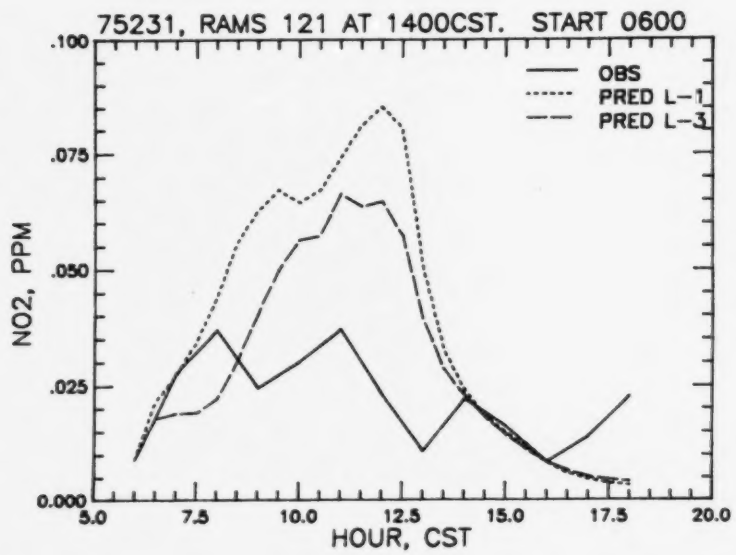

Figure 21b. LPM time series of observed and predicted NO_2 hourly concentrations on Day 231 of 1975.

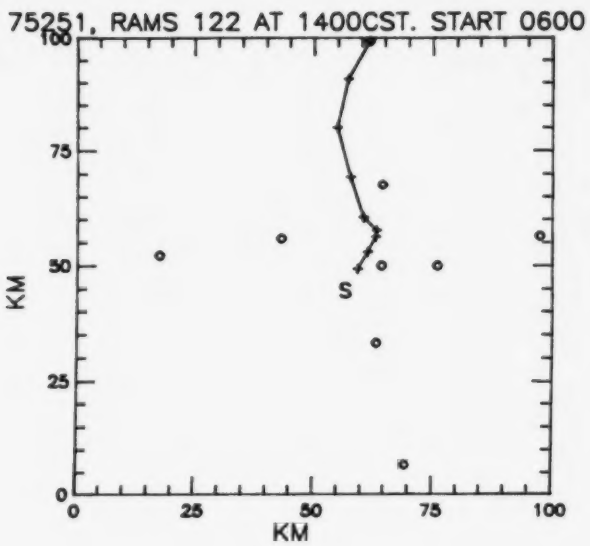

Figure 22a. LPM parcel trajectory for Day 251 of 1975.

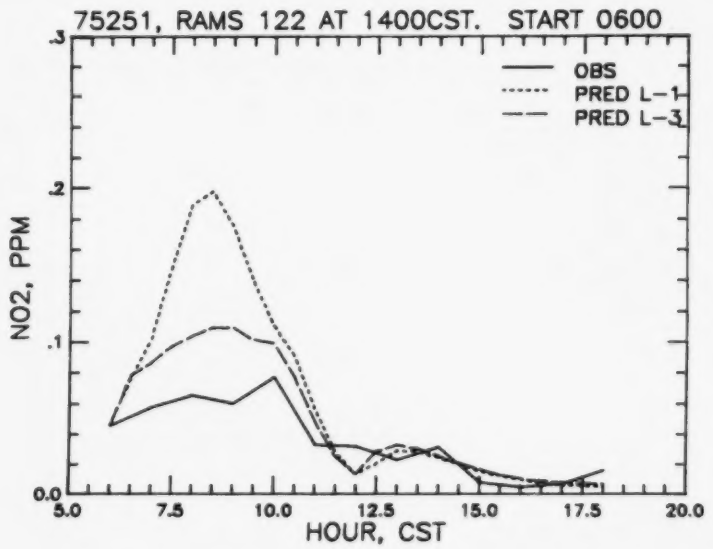

Figure 22b. LPM time series of observed and predicted NO_2 hourly concentrations on Day 251 of 1975.

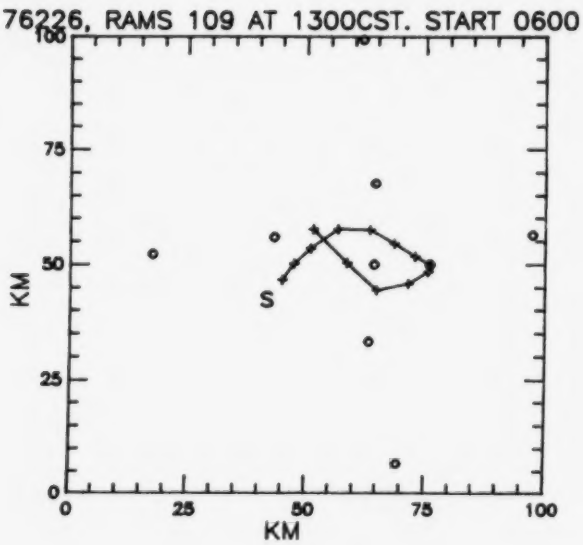

Figure 23a. LPM parcel trajectory for Day 226 of 1976.

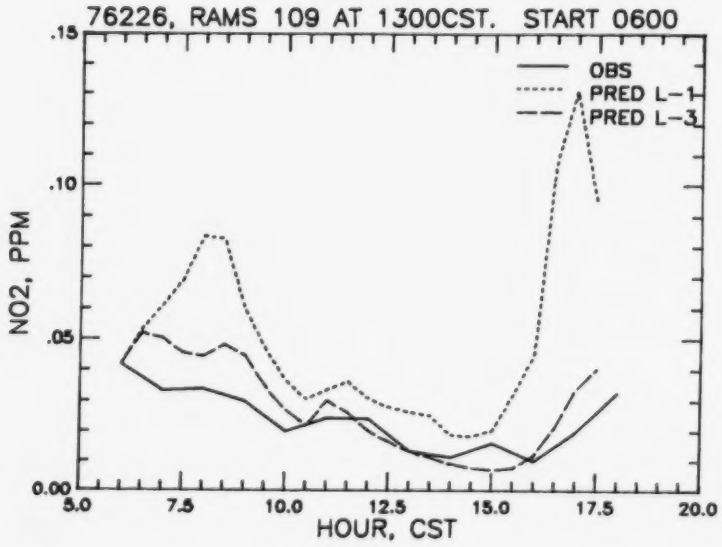

Figure 23b. LPM time series of observed and predicted NO_2 hourly concentrations on Day 226 of 1976.

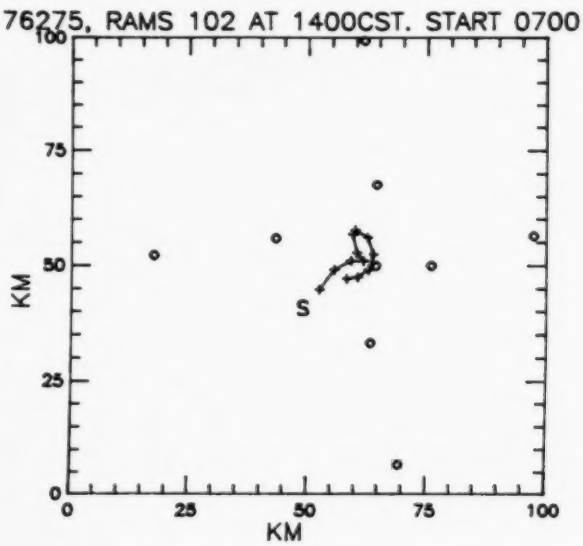

Figure 24a. LPM parcel trajectory for Day 275 of 1976.

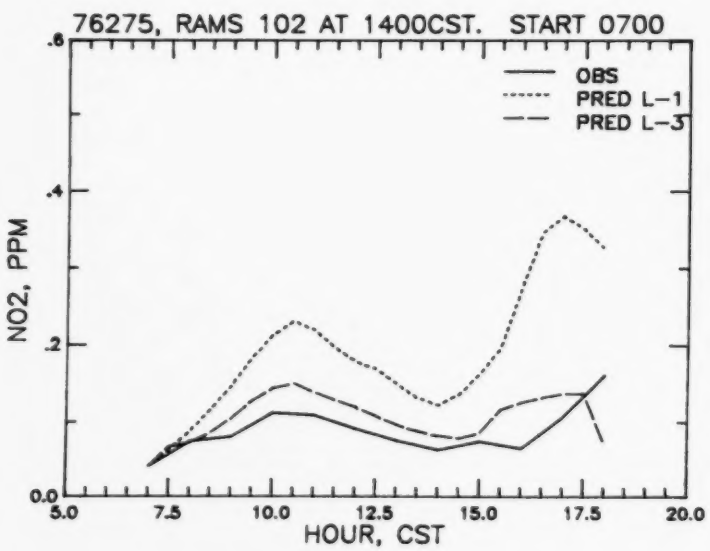

Figure 24b. LPM time series of observed and predicted NO_2 hourly concentrations on Day 275 of 1976.

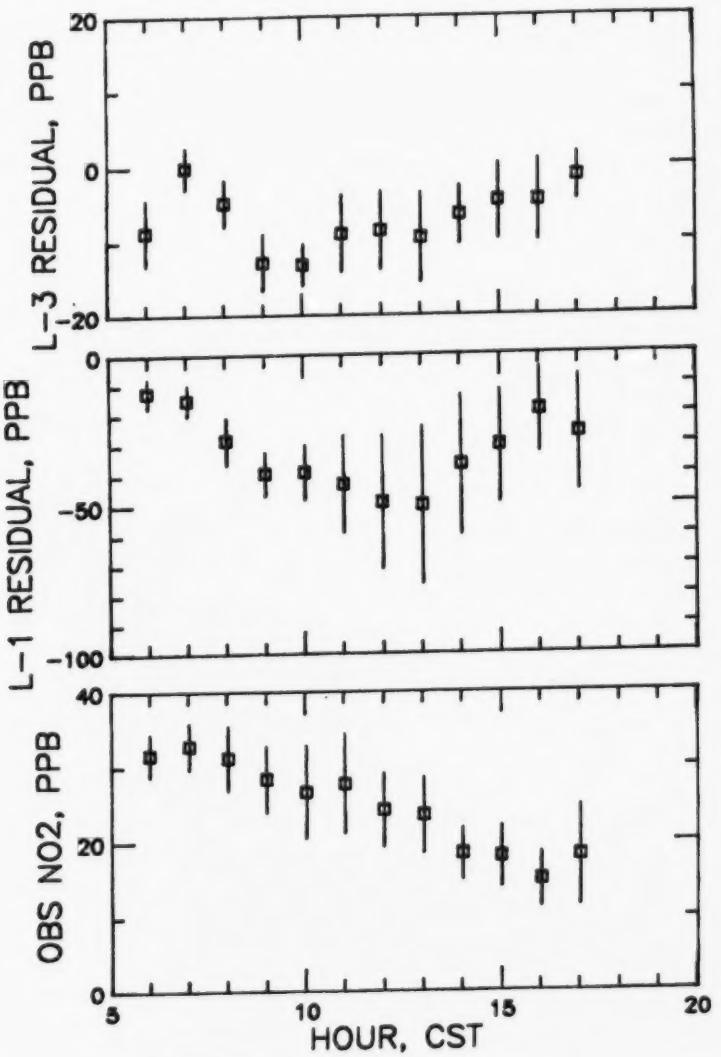

Figure 25. Plots of average observed and residual (observed minus predicted) NO_2 concentrations from each hour of 19 simulations using the LPM. Standard deviations of the means are given by vertical bars.

SECTION 6

URBAN AIRSHED MODEL

OVERVIEW

The Urban Airshed Model (UAM) is a 3-D grid-type photochemical air quality simulation model (PAQSM) developed by Systems Applications, Inc. (SAI) of San Rafael, California. The model structure consists of a latticework array of cells, whose total volume represents an urban-scale domain and in which the physical and chemical processes responsible for photochemical smog are mathematically simulated. These include the advection of pollutant species through the modeling domain, the species' entrainment from aloft by a growing mixed layer, diffusion of material from cell to cell, the injection of primary source emissions into the modeled volume, and the chemical transformation of reactive species into intermediate and secondary products. The horizontal dimensions of each cell are constant but cell heights vary throughout a model simulation as mixed layer depth in the UAM changes accordingly.

The area modeled in the St. Louis application was 60 km wide and 80 km long. Individual cells were 4 km square in the horizontal. Vertically, cells totaled 4 layers; the bottom two cells included the extent of the well-mixed layer and the top two represented the region immediately above the mixed layer. The domain of the UAM was centered just west of downtown St. Louis and included the entire metropolitan area. Nearly all of the major emissions sources of NO_x are located within the boundaries of this modeling domain with the exception of the Labadie electric power station to the west. The emissions distribution of NO_x fluxes for the SAI grid shown in Figure 26 illustrates the major sources in the area. The downtown area of St. Louis and the industrial sections of Illinois directly across the Mississippi R. include major area and line sources of NO_x

and may be clearly identified in the center of the grid. Two of the largest point sources of NO_x are also within the grid area; the Sioux electric power plant, at cell (8,19), and the Merramac power plant, at cell (7,5). Within the UAM the plume rise from point source stacks is calculated, and the total emissions flux from that source is attributed to the grid cell above the stack corresponding to the stack height plus the plume rise. These calculations are updated at each hour of model simulation. Should the height of the plume exceed that of the modeling region the emissions are lost for the simulation at that particular hour. However, except for very tall stacks in stable conditions this phenomenon rarely occurred during the simulations performed in this study.

Figure 27 shows a horizontal cross-section of the domain as applied to the RAPS monitoring network. All 25 monitoring station locations are given in relation to the grid pattern. The outer ring contains the boundary cells for the model. Although model simulation does not occur in the boundary cells they are an important part of the advective transport portion of the UAM. Four monitoring stations, 122-125, lie outside of the computational domain and are available for determining boundary concentrations. The remaining sites lie within the domain, no two residing in the same cell. The UAM attempts to estimate the hour-average observed concentration of a modeled pollutant species at each monitoring site within the model domain.

Details of the method for performing a St. Louis simulation with the UAM are described in Reports I and II. Model simulations begin at 0500 CST and continue through 1700 CST. The earlier reports emphasized model performance for O_3 for the 20 test-case days listed in Table 1. This study makes use of the model results from these 20 UAM simulations and describes the model performance for NO_2 in greater detail than the earlier reports did. No model simulations were repeated for this study except for Day 237-76 which was found to contain an erroneous NO_2 inflow boundary concentration. This was corrected and the simulation was performed again.

Model results for NO_2 are described in detail here for the 5 days with the highest ambient NO_2 concentrations observed within the model domain among all 20 test days. These days include 184-75, 251-75, 159-76, 237-76, and 275-76 from the RAPS data base. Model results from the remainder of the days are summarized.

On 8 of the 20 test days the maximum observed NO_2 concentration occurred during a time period outside of the range of model simulation, and on 1 of the 20 days the maximum occurred at a station outside of the UAM domain. For these days the ambient NO_2 maximum is considered to be the highest hour-average concentration observed at any station within the model domain during the simulation period.

RESULTS

The UAM simulates air quality within each grid cell. Species concentration predictions at particular RAPS monitoring site locations are interpolated from predictions in the surrounding cells by a distance-weighted (1/r) formula. A grid model provides a wealth of information from a simulation including the spatial and temporal concentration variations of all modeled species throughout the grid. In order to summarize model performance for NO_2 on each of the days examined here the analysis techniques of Bencala and Seinfeld (1979) will be used, including residual histograms (RS) and the residual vs. observed concentration plot (RO). On any one simulation day there were 21 sites for each of 13 hours of simulation to account for, or 273 possible data points.

Aside from the global view of NO_2 performance, the model's ability to predict the maximum ambient NO_2 concentrations was examined. For this purpose the time series of observed and predicted NO_2 concentrations are presented for the station where the peak hour-average measurement occurred. Also shown are contour plots of observed and predicted NO_2 concentrations over the model domain at the hour the peak ambient NO_2 occurred. This type of analysis will help to evaluate the accuracy of the spatial orientation of the concentration fields. It would not be

possible to determine this from the time series or residual concentration data alone.

Synoptic meteorological conditions on the 5 test days discussed here were presented in the discussions of PBM results in Section 4. Background NO_2 concentrations for the top boundary of the modeling domain were assumed to be low, 0.002 ppm. Implicit in this assumption is that NO_2 is not transported in significant concentrations over regional distances as O_3 often is. Concentrations of NO_2 on the lateral boundaries were determined from air quality monitoring data.

The RS and RO plots for NO_2 on Day 184-75 are shown in Figures 28a and b, respectively. The histogram of NO_2 residuals has a peak at 0.0 but is skewed toward the positive, or underpredictive side. The RO plot in Figure 28b again confirms that most of the model results are underpredicted and there appears to be a gradual trend of larger errors with increasing NO_2 concentration.

The maximum ambient NO_2 level on Day 184 occurred at RAMS site 104 at 0700 h at 0.180 ppm. The time series of observed and predicted concentrations at site 104 are given in Figure 29. It is obvious that the UAM has grossly underpredicted the peak concentration. The maximum predicted concentration is 0.080 ppm occurring at 0600 h, a 56% underprediction. The time series after 1000 h shows better agreement although the concentration levels are rather low. Figure 30 presents the contours of predicted and observed concentrations of NO_2 on Day 184 at 0700 h, the hour of ambient peak NO_2. Both patterns show the area of highest concentrations as located in the same section of the model domain, just southeast of the downtown area. The difference in the magnitudes and gradients of concentration between the predicted and observed cases is considerable. The observed contour pattern appears more structured than the predicted pattern. In part, this is an artifact of the interpolation scheme on which the contouring algorithm is based. In the model-predicted case the contours have been objectively drawn based on the 300 regularly spaced grid

values for the lowest layer of cells in the UAM. For the observed case the contours are based on the 25 irregularly spaced monitoring locations, four of which lie outside of the model domain. Here the objective algorithm responsible for generating the contours works best toward the center of the domain where the density of sites, represented in the figure by small crosses, is greatest. The credibility of the contours near the edges is not as high, especially in terms of the extent of the area circumscribed by a given contour.

The RS and RO plots for NO_2 on Day 251-75 are shown in Figures 31a and b, respectively. The histogram of residuals has a normal shaped distribution with a peak at the 0.0 residual. The RS plot reveals no particular trends with concentration, although the five highest ambient NO_2 levels are all underpredicted. At concentrations less than 0.05 ppm the model has more overpredictions than underpredictions.

The highest hour-average NO_2 observation on Day 251 occurred at site 112 at 0900 h at 0.120 ppm. The NO_2 concentration time series for this site is presented in Figure 32. The predictions are again much lower than the observations during the peak morning period. The maximum predicted NO_2 level at site 112 is 0.058 ppm at 1000 h, 52% less than the observed maximum. The contour patterns in Figure 33 also appear dissimilar. However, the maximum contour level magnitudes are not very different. The area of predicted maximum concentrations lies just to the east of the maximum observed area. The open contours in the southwest section of the observed grid are probably a result of the interpolation assumptions and do not reflect monitored data in that area. The disparity in the locations of peak concentration areas could well be due to the inaccurate specification of the wind field here.

The RS and RO plots for NO_2 on Day 159-76 are presented in Figures 34a and b, respectively. The residual histogram shown in Figure 34a is broader than the ones previously discussed but also has a normal shape with a peak at the 0.0 residual. There is some skewness toward the

underpredictive side. The RO plot shows substantial scatter in the residuals on this day, with the majority of data points corresponding to observed concentrations less than 0.05 ppm. Most residuals above this level are on the underpredicted side.

The peak hour-average observed NO_2 on Day 159 of 0.149 ppm occurred at site 104, in East St. Louis, at 0700 h. The time series of NO_2 concentrations for this site are shown in Figure 35. The trends in predicted and observed concentrations here are nearly the same. The UAM peak occurs at 0700 h, the same hour as the ambient peak, at 0.098 ppm, a 34% underprediction. The contours of predicted and observed NO_2 for 0700 h are shown in Figures 36a and b, respectively. The location, shape, and magnitude of the contours in the two panels display good agreement. The difference in the observed and predicted maxima at site 104 appears to be more a result of a slight difference in alignment in the contour pattern than of a major difference in their location or magnitudes. It is interesting to note the bulges in the predicted concentration patterns at the north and south of the central grid area. These do not appear in the observed contour pattern. The locations of these secondary high NO_2 concentration areas are roughly equivalent to the locations of two large power plants. Their effect on the NO_2 predictions from the UAM in the area immediately downwind of the plants can be considerable. This effect will be discussed further later in the report.

The RS and RO plots for NO_2 on Day 237-76 are shown in Figures 37a and b, respectively. The residual histogram in Figure 37a appears normally shaped with a peak at the 0.0 residual. There are, however, numerous outliers in the tail on the underpredictive side. The RO plot in Figure 37b conveys a strong trend of greater model underprediction with increasing ambient NO_2 concentration. Most of the data points corresponding to lower ambient concentrations are clustered near the 0.0 residual.

The peak hour-average NO_2 level on Day 237 was measured at site 106, just south of downtown St. Louis and near the Mississippi R., at 0800 h at

0.141 ppm. Figure 38 displays the concentration time series of NO_2 for this site. It is again apparent that the UAM has severely underpredicted the peak NO_2 concentration and is quite far from correctly estimating the observed temporal NO_2 gradients at this site. The maximum predicted NO_2 concentration in this time series is 0.068 ppm at 0700 h, a 52% model underprediction. The contours of predicted and observed NO_2 over the model domain at the hour of peak observed concentration are shown in Figures 39a and b, respectively. The two panels correspond only in the sense that both display a peak near the center of the domain although the magnitudes of the peaks are very different. The contours of predicted NO_2 in Figure 39a also show three distinct high concentration areas, roughly pointing to the high emissions areas of downtown St. Louis and the two large power plants mentioned previously. The contours of observed NO_2 in Figure 39b again do not show similar effects from the power plant emissions.

The last of the 5 days discussed here is Day 275-76, a case of extreme atmospheric stability and stagnation. The RS and RO plots for NO_2 are given in Figures 40a and b, respectively. The residual histogram has a roughly normal distribution about the 0.0 residual. There are groups of outliers in each of the tails of the distribution. The RO plot in Figure 40b shows no clear model trends below ambient NO_2 concentrations of 0.100 ppm, although numerous model overpredictions are shown throughout this range of concentrations; the first time this has been seen in the UAM predictions for NO_2 thus far. Above ambient NO_2 levels of 0.100 ppm there is a more discernible tendency for greater model underpredictions with increasing observed concentration levels.

The greatest hour-average NO_2 concentration observed in the RAPS surface network on Day 275 actually occurred at night at 2200 h at 0.244 ppm. The maximum value observed during the model simulation period was 0.182 ppm at 1000 h at site 101 in downtown St. Louis. The NO_2 time series of observed and predicted concentrations at site 101 are shown in Figure 41. The trends in the observations and predictions do not match.

The model profile continues to increase beyond the observed peak, reaching a maximum of 0.150 ppm at 1400 h, an 18% underprediction. This is considerably better than the other model results in the group of 5 test days, but the time lag between observed and predicted peaks is greater. Figure 42 presents the contours of predicted and observed NO_2 at 1000 h for Day 275. The highest concentrations for both cases are located near the center of the model domain. The maximum contour level is 0.100 ppm in the predicted case and 0.180 ppm in the observed. Also, the major axis through the concentration field seems to be oriented north-south in the observed field and east-west in the predicted, although this effect may be an artifact of the interpolation algorithm of the contouring scheme.

The RS and RO plots for NO_2 on the remaining 15 days of the model evaluation study are contained in Report II. Also, the NO_2 time series for the site of peak ambient concentration and the contour plots for the hour of peak ambient concentration are presented in appendices to this report.

Table 7 displays summary statistics on the mean NO_2 concentration data from each of the 20 test days in the evaluation study. All observed and predicted concentration pairs on each test day were included in the analysis. Generally the mean residuals, or bias, appear small, although as percentages of the mean observed concentrations they show a broad range of behavior from an overprediction of 38% to an underprediction of 23%. Another indication of the degree of accuracy at overall NO_2 predictions is the error band or the percent of the predictions falling within 25% of the observations. Table 7 shows that these figures are relatively low; the highest is just over 40%. A review of the RO plots though reveals that the majority of NO_2 observations occur at low concentrations, making the 25% error band a restrictive measure of model performance.

Table 8 summarizes an analysis of trends in all NO_2 observed and predicted data pairs from the UAM on each test day. Correlation coefficients were calculated for spatial, temporal, and overall distributions.

TABLE 7. SUMMARY OF NO_2 MEAN CONCENTRATION DATA FROM THE UAM.

Julian date	Mean observed concentration (ppm)	Mean predicted concentration (ppm)	Mean residual (ppm)	RMS error (ppm)	Mean residual / Mean obs. conc. (%)	Error band[a] (%)
142-75	0.013	0.018	-0.005	0.011	-38.5	30.8
178-75	0.021	0.026	-0.005	0.017	-23.8	28.6
182-75	0.017	0.013	0.004	0.011	23.8	28.6
183-75	0.023	0.022	0.001	0.016	4.3	32.1
184-75	0.025	0.021	0.004	0.022	16.0	28.9
207-75	0.013	0.018	-0.005	0.008	-38.5	29.9
209-75	0.015	0.019	-0.004	0.010	-26.7	31.6
221-75	0.019	0.018	0.001	0.013	5.3	30.6
230-75	0.019	0.022	-0.003	0.010	-15.8	38.5
231-75	0.016	0.019	-0.003	0.009	-18.8	37.1
251-75	0.025	0.028	-0.003	0.019	-12.0	39.1
159-76	0.028	0.023	0.005	0.013	17.9	35.8
160-76	0.020	0.021	-0.001	0.013	- 5.0	28.7
195-76	0.016	0.015	0.001	0.010	6.3	41.1
211-76	0.021	0.017	0.004	0.011	19.0	38.1
212-76	0.018	0.019	-0.001	0.011	- 5.6	31.2
225-76	0.021	0.022	-0.001	0.012	- 4.8	35.2
226-76	0.024	0.023	0.001	0.015	4.2	27.9
237-76	0.019	0.016	0.003	0.014	15.8	30.2
275-76	0.051	0.052	-0.001	0.032	- 2.0	35.1

[a]Percent of predictions within 25% of observations.

TABLE 8. SUMMARY OF NO_2 ANALYSIS OF TRENDS DATA FROM THE UAM.

Julian date	Correlation coefficient	Mean spatial correlation	Mean temporal correlation	Slope	Intercept (ppm)	Sum of squared error (ppm^2)
142-75	0.621	0.689	0.489	0.665	0.001	0.018
178-75	0.478	0.598	0.388	0.447	0.010	0.050
182-75	0.771	0.518	0.779	0.523	0.010	0.038
183-75	0.685	0.466	0.559	0.574	0.010	0.060
184-75	0.683	0.549	0.521	0.397	0.017	0.157
207-75	0.791	0.734	0.682	0.751	0.000	0.014
209-75	0.741	0.536	0.682	1.01	-0.004	0.021
221-75	0.675	0.612	0.615	0.493	0.010	0.042
230-75	0.824	0.804	0.606	0.774	0.002	0.019
231-75	0.772	0.706	0.552	0.790	0.001	0.016
251-75	0.600	0.410	0.576	0.585	0.009	0.063
159-76	0.887	0.676	0.732	0.740	0.010	0.055
160-76	0.796	0.747	0.637	0.535	0.009	0.056
159-76	0.660	0.654	0.321	0.457	0.009	0.033
211-76	0.621	0.685	0.373	0.415	0.014	0.032
212-76	0.798	0.642	0.538	0.503	0.009	0.042
225-76	0.704	0.657	0.578	0.657	0.006	0.033
226-76	0.561	0.688	0.368	0.331	0.016	0.067
237-76	0.823	0.827	0.639	0.509	0.011	0.066
275-76	0.597	0.761	0.329	0.604	0.019	0.183

The slope and intercept of the calculated linear least squares line are given as well as the sum of squared error, a measure of dispersion about the line of regression. Averaged over all 20 days taken separately, the overall correlation coefficient, spatial correlation and temporal correlation for NO_2 in the model results are 0.704, 0.648 and 0.548, respectively. The smaller value for the temporal correlation than for the spatial is at first surprising because the trends in the time series between observed and predicted concentrations are generally not very different. However, the repeated occurrence of high observed NO_2 concentrations toward the center of the model grid affords the UAM a chance to produce a higher degree of spatial concurrence than would be possible with a more distributed range of concentrations. The slopes of the regression lines are generally much less than 1, indicating an overall tendency for the model to underpredict NO_2. The intercepts are also fairly small and the scatter, as measured by the sum of squared error, is significant.

The most intense interest in a grid model such as the UAM is in its ability to predict the maximum values of a pollutant of interest. Table 9 presents a summary of the model results in this regard for NO_2. For each of the 20 model test days, the peak observed concentration during the simulation time period and within the model domain is listed, along with the monitoring site location and the hour of occurrence. Three sets of model predictions are also shown. The first consists of the predictions paired in space and time. These correspond to the model results at the same time and location (interpolated) as the observed peak concentration and are the most restrictive set of pairings. The next set consists of the model predictions paired in space but not in time. For the location of observed maximum, the peak model estimate at any time during the simulation period is found and paired with the peak observed concentration. The value and time of occurrence of the prediction are listed. The converse case, model predictions paired in time but not in space, is not analyzed here. Finally, the last set of model predictions shown is the unpaired or least restrictive set. Here the peak observed concentration is matched with the largest model prediction at any time or place of

TABLE 9. A SUMMARY OF PREDICTED AND OBSERVED NO_2 MAXIMA FOR THE UAM.

Julian date	Observed Peak Concentration[a]			PST[b]		PSC[c]			UPD[d]			
	Value (ppm)	Location (RAPS site)	Time (CST)	Value (ppm)	ΔC/OPC[e] (%)	Value (ppm)	Time (CST)	ΔC/OPC (%)	Value (ppm)	Location[f]	Time (CST)	ΔC/POC (%)
142 (1975)	0.046	102	1300	0.065	-41.3	0.065	1300	-41.3	0.080	(10,11)	1000	-73.9
178	0.070	103	0700	0.046	34.3	0.052	0900	25.7	0.088	(9,11)	1200	-25.7
182	0.087	106	0800	0.035	59.8	0.066	0600	24.1	0.071	(8,19)	1000	18.4
183	0.106	106	0700	0.093	12.3	0.096	0800	9.4	0.100	(9,11)	0800	5.7
184	0.180	104	0700	0.071	60.6	0.080	0600	55.6	0.091	(10,11)	0600	49.4
207	0.062	106	0600	0.053	14.5	0.053	0600	14.5	0.098	(8,19)	1100	-58.1
209	0.050	110	0800	0.055	-10.0	0.059	0900	-18.0	0.090	(7,5)	1200	-80.0
221	0.073	102	0800	0.034	53.4	0.048	0500	34.2	0.083	(8,19)	1100	-13.7
230	0.080	112	0800	0.043	46.3	0.047	0700	41.3	0.107	(8,20)	1600	-33.8
231	0.057	102	1000	0.062	- 8.8	0.062	1000	- 8.8	0.090	(8,19)	1100	-57.9
251	0.120	112	0900	0.050	58.3	0.058	1000	51.7	0.121	(10,11)	0900	- 0.8
159 (1976)	0.149	104	0700	0.098	34.2	0.098	0700	34.2	0 125	(10,11)	0700	16.1
160	0.106	104	0700	0.057	46.2	0.070	0600	34.0	0.094	(8,19)	1600	11.3
195	0.066	102	0600	0.021	68.2	0.037	1000	43.9	0.088	(8,20)	1100	-33.3
211	0.092	112	1100	0.020	78.3	0.029	1400	68.5	0.057	(9,11)	1200	38.0
212	0.093	113	0700	0.048	48.4	0.049	0500	47.3	0.059	(9,13)	0600	36.6
225	0.080	106	1500	0.055	31.3	0.066	1600	17.5	0.078	(10,10)	1500	2.5
226	0.099	101	0700	0.042	57.6	0.042	0600	57.6	0.090	(8,19)	1600	9.1
237	0.141	106	0800	0.066	53.2	0.068	0700	51.8	0.093	(8,19)	0900	34.0
275	0.182	101	1000	0.096	47.3	0.150	1400	17.6	0.177	(8, 9)	1700	2.7
				$\overline{\Delta C}$ = 0.041		$\overline{\Delta C}$ = 0.032			$\overline{\Delta C}$ = 0.003			
				s.d.(ΔC) = 0.032		s.d.(ΔC) = 0.029			s.d.(ΔC) = 0.032			
				$\overline{\lvert\Delta C\rvert}$ = 0.044		$\overline{\lvert\Delta C\rvert}$ = 0.036			$\overline{\lvert\Delta C\rvert}$ = 0.025			

[a]Within UAM domain and during simulation time period: 0500 h - 1800 h.
[b]UAM predictions: Paired in space and time.
[c]UAM predictions: Paired in space only.
[d]UAM predictions: Unpaired.
[e]ΔC = Obs. - Pred. = Residual Concentration; OPC = Obs. Peak Concentration
[f]Cell coordinate of grid shown in Figure 27; (1,1) is at bottom left.

the simulation. The value, grid location and time of occurrence of the predictions are listed. In all cases the residual concentration, ΔC, observed minus predicted, is calculated and tabulated as a percentage of the observed peak concentration. This is a measure of the model's overprediction (negative) or underprediction (positive) of peak NO_2. In addition, for each set of paired data the average residual over the 20 days, the model bias, and the standard deviation are presented. The average absolute residual value, or gross error, is also given.

As expected, the average model bias is greatest in the most restrictive set of residuals and smallest in the least restrictive set. The range is from 0.041 ppm to 0.003 ppm. The standard deviation of the bias is fairly constant at about 0.03 ppm, indicating that the model precision remains about the same while the accuracy may vary for the different sets of residuals. The closer the gross error is to the model bias the more consistent the model is at over- or underpredictions. The average bias and gross error in the set of predictions paired in space and time are very similar, 0.041 and 0.044 ppm, respectively. This implies mostly underpredictions among the model estimates. In contrast the unpaired set shows nearly no model bias on the average, yet the gross error is significant at 0.025 ppm. This indicates a mix of underpredictions and overpredictions among the model estimates. The group of residuals paired in space only, behaves on the average more like the group paired in space and time. The average model estimate for peak NO_2 for the data set paired in space and time is a 37% underprediction. It is 28% underpredicted for the set paired in space but not in time and 8% overpredicted for the unpaired set. Thus the particular model result for prediction of peak NO_2 depends upon how restrictive the pairing of the observation to the prediction is to be. In a strict sense the UAM has consistently and significantly underpredicted maximum NO_2. However, the results from the unpaired data set imply that the model may have the potential to perform better once the deficiencies are identified and corrected.

An indication of one of the UAM's deficiencies lies in the grid locations of the unpaired maximum NO_2 model predictions listed in Table 9. Several specific grid cells appear repeatedly as the locations of these maxima. The location of model observed and predicted NO_2 peaks are plotted on the UAM grid in Figure 43 from all 20 test days. Nearly all of the observed peaks occur near the center of the grid in the downtown St. Louis or industrial riverfront area. This area also claims many of the predicted maxima, although 9 predicted peaks appear far to the north clustered near two adjacent grid cells and 1 peak lies to the southwest of site 118; both locations are out of the area of observed NO_2 peaks. However, these locations are both very close to large point source NO_x emitters, electric power generating stations. While these sources have not shown themselves by producing NO_2 peaks at nearby monitoring stations, the model predictions have been affected greatly by them. Half of the 20-day sample in this study showed predicted maxima in the immediate vicinity of these plants. It is entirely possible that these are, in fact, valid NO_2 peaks that are not observed simply because there were no monitoring sites at the spots. In that event it is likely that the effects from these sources would have appeared at nearby sites. They rarely do, however, and it seems more likely that these predicted peaks result from the simplistic treatment of point sources by the UAM described earlier in this section.

CONCLUSIONS

The performance of the UAM for predicting NO_2 concentrations in the St. Louis area has been investigated. Twenty test-case days from the RAPS data base have been modeled and the results for NO_2 analyzed here. When all observations and model predictions are considered, the UAM fairly consistently underpredicted NO_2 levels. Overall correlations between the observed and predicted data sets ranged from 0.48 to 0.89 and spatial correlations from 0.41 to 0.83. However, the majority of observed NO_2 concentrations are at low levels and thus may not provide a representative picture of model performance at concentration levels of

interest. The analysis of the model performance for NO_2 maxima, summarized in Table 9, goes farther toward this end.

Contours of observed and predicted NO_2 concentrations at the hour of observed maximum, presented in this section and Appendix B, show that most of the peaks occur in the downtown and industrial areas of the model domain. The predictions also display maximum concentration areas in the vicinity of two electric power generation stations, a phenomenon not seen in the ambient data. This effect may well result from the simplistic treatment of large point sources by the UAM. Moreover, the model performance for estimating maximum NO_2 levels in any specific manner shows serious underpredictions of 28% and 37% as averages over the test sample. It is only in the least restrictive sense that the average model performance is acceptable for NO_2 with the unpaired set of observations and predictions. Yet even in this data set the range of model results spans a 49% underprediction to an 80% overprediction. It can only be concluded that this version of the UAM is not reliable as an accurate estimator of urban NO_2 levels in any sense except for the least restrictive framework. Potential problem areas are the point source treatment, wind field algorithm, and chemical kinetic mechanism. Some of these model components have already been tested independently and in conjunction with the UAM evaluation for O_3 (Reports I and II). While model results for O_3 do fall within an acceptable range, those for NO_2 do not.

Recently the group that developed the UAM at Systems Applications, Inc. has reported on a new version of the model that includes a reactive plume model nested within the airshed model for a more realistic treatment of large point source plumes (Seigneur et al., 1983). Model testing was conducted with a one-day episode from the St. Louis RAPS data base (13 July 1975) and a two-day episode from the South Coast Air Basin around Los Angeles (26-27 June 1974). Results for NO_2 with the grid-plume model differed only slightly from the grid model results and were within the uncertainty range of the measured data. The added detail made available by nesting the plume model within the urban grid model did little to

improve model results for O_3 or NO_2, yet added greatly to computational costs. The authors could not generally recommend the grid-plume model although they gave an example of assessing the effect of an upwind isolated single source (offshore oil platform) on the South Coast Air Basin and found the model very useful for that situation.

NO_x EMISSIONS (kg/hr) DAY 195–76 0800 h

0	0	0	0	0	0	0	0	0	0	0	0	0	0	0	0	0
0	0	0	0	0	0	0	2	7	13	7	5	5	5	6	5	5
0	0	4	5	6	10	7	8	10	26	7	5	7	5	7	9	9
0	0	5	7	7	9	7	8267	11	56	41	30	26	11	9	11	11
1	1	5	7	6	4	6	8	16	67	1567	302	21	8	11	11	12
3	6	6	7	7	3	9	14	15	23	22	325	115	20	25	14	16
44	28	25	142	166	35	75	79	42	10	5	31	14	8	22	17	5
30	21	98	157	173	216	175	154	147	61	49	48	36	22	21	28	14
8	11	14	131	127	200	169	192	384	66	35	34	37	24	36	25	15
5	82	37	104	135	93	151	177	351	259	475	34	28	40	32	15	11
13	322	104	88	176	91	143	237	337	1016	123	89	55	45	17	7	5
3	57	168	228	160	125	233	485	911	718	269	86	50	16	18	7	8
20	32	97	119	127	131	148	139	298	417	230	51	56	29	33	23	16
18	23	41	145	148	83	107	174	436	36	26	37	44	83	37	16	29
40	25	23	33	72	114	304	82	29	31	10	8	15	44	61	21	16
36	17	13	15	19	61	63	81	24	18	6	9	9	12	16	18	6
3	5	6	12	20	61	29	26	12	21	13	9	9	8	9	10	10
3	5	6	10	3	64	4386	10	5	4	7	4	6	7	8	10	10
4	3	7	6	3	61	19	6	4	3	9	3	4	6	8	9	13
4	1	3	4	3	184	9	3	4	4	11	3	3	5	6	7	13
1	1	4	3	10	34	3	4	4	4	3	3	2	2	3	3	5
1	4	2	2	12	37	7	6	4	2	3	3	4	3	3	3	5

Figure 26. Total source emissions of NO_x for the RAPS area on Day 195 of 1976 at 0800 CST. Grid cells are 4 km squares; the SW corner corresponds to UTM (x,y) coordinates of Zone 15: (706, 4236).

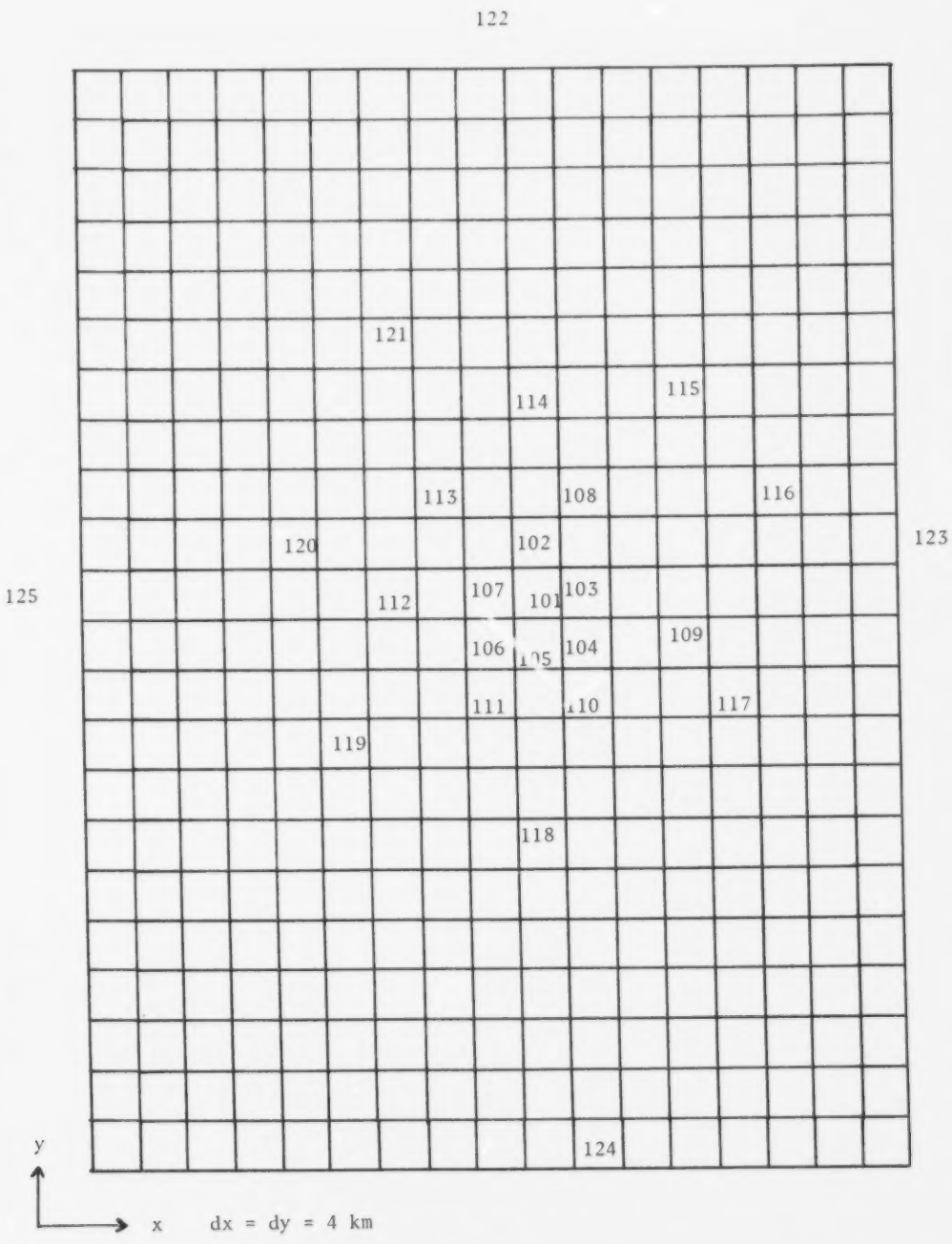

Figure 27. Schematic drawing of horizontal section of UAM domain showing locations of RAPS monitoring sites.

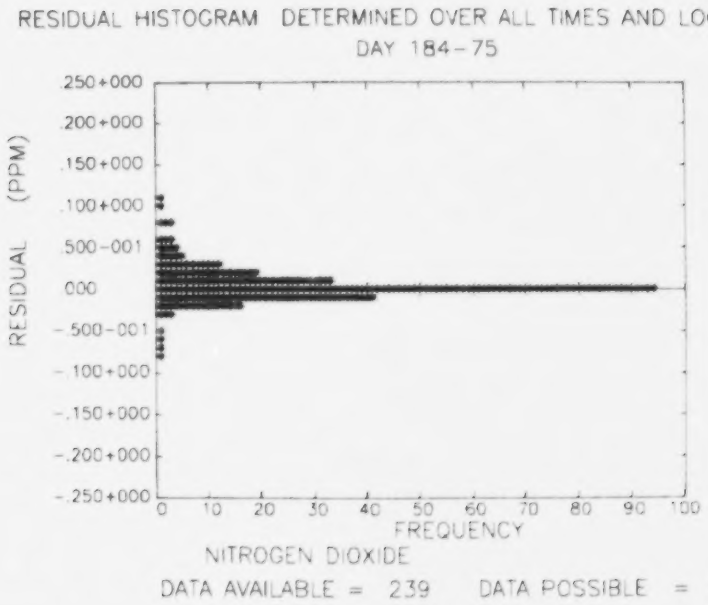

Figure 28a. Residual histogram for NO_2 from the UAM simulation results for Day 184-75.

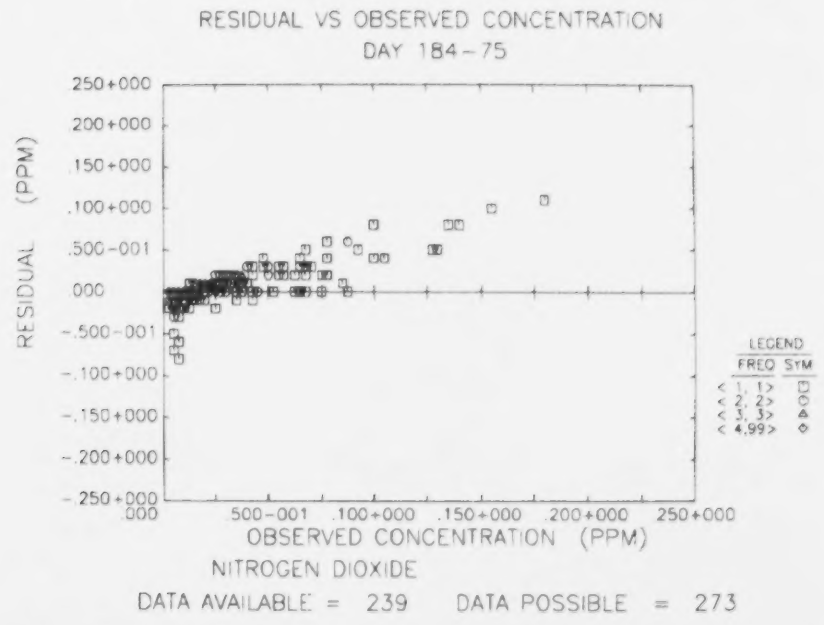

Figure 28b. Residual vs. observed plot for NO_2 from the UAM simulation results for Day 184-75.

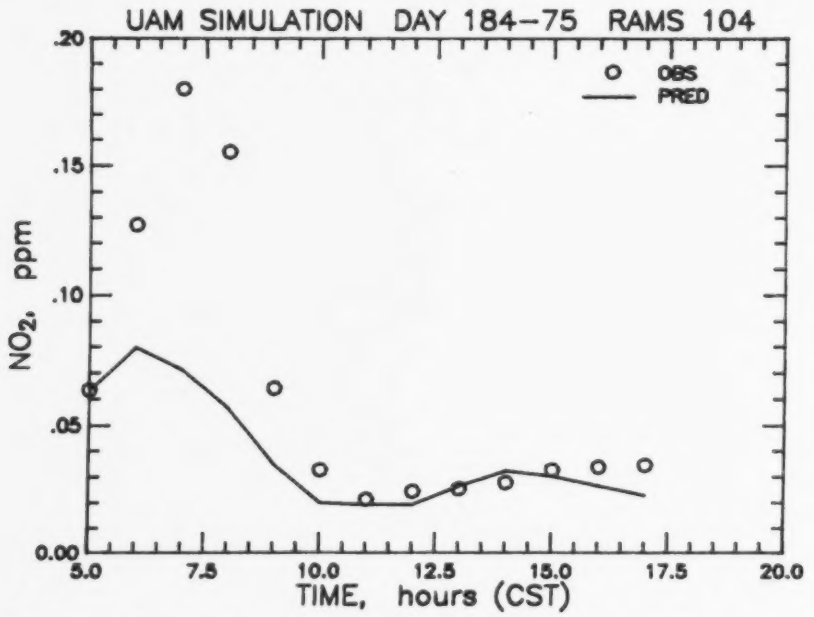

Figure 29. UAM time series of observed and predicted NO_2 concentrations at site 104 on Day 184-75.

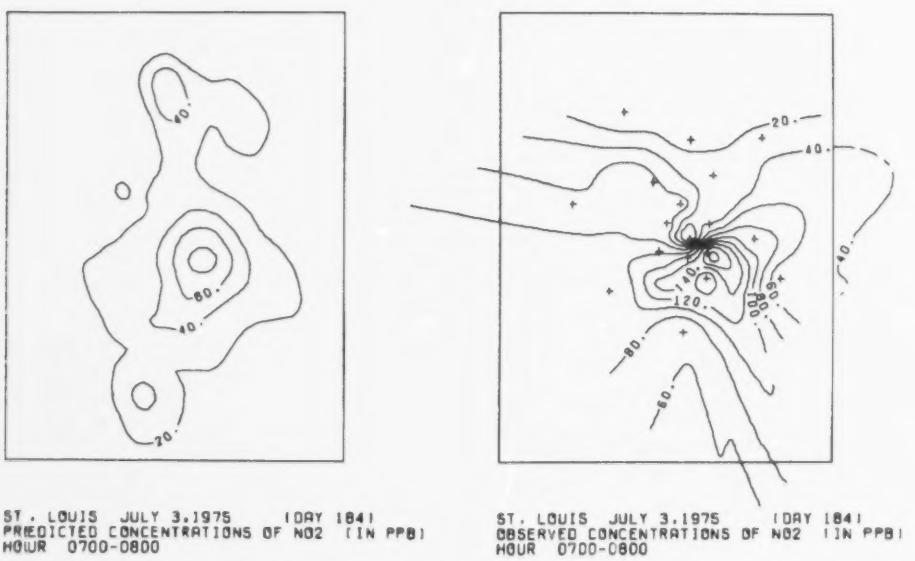
ST. LOUIS JULY 3,1975 (DAY 184)
PREDICTED CONCENTRATIONS OF NO2 (IN PPB)
HOUR 0700-0800
ST. LOUIS JULY 3,1975 (DAY 184)
OBSERVED CONCENTRATIONS OF NO2 (IN PPB)
HOUR 0700-0800

(a) (b)

Figure 30. Contours of (a) predicted and (b) observed fields of NO_2 at hour of observed maximum on Day 184-75.

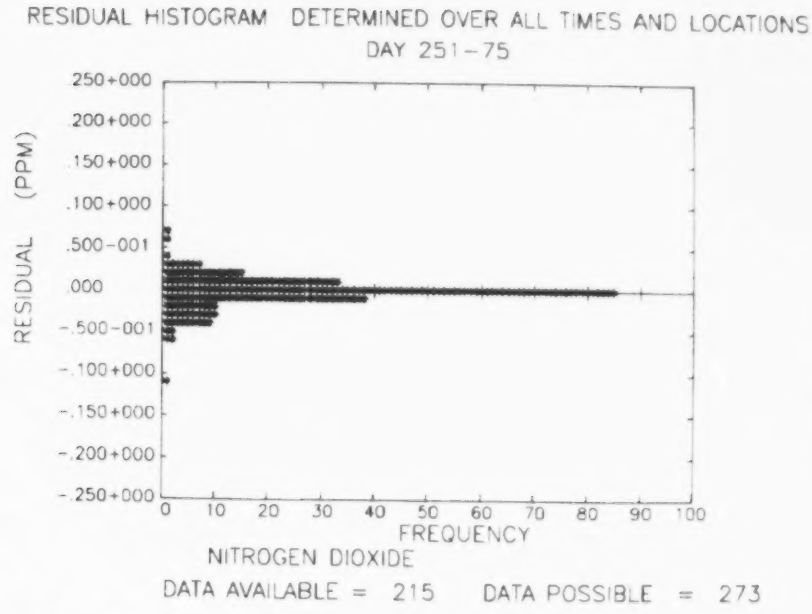

Figure 31a. Residual histogram for NO_2 from the UAM simulation results for Day 251-75.

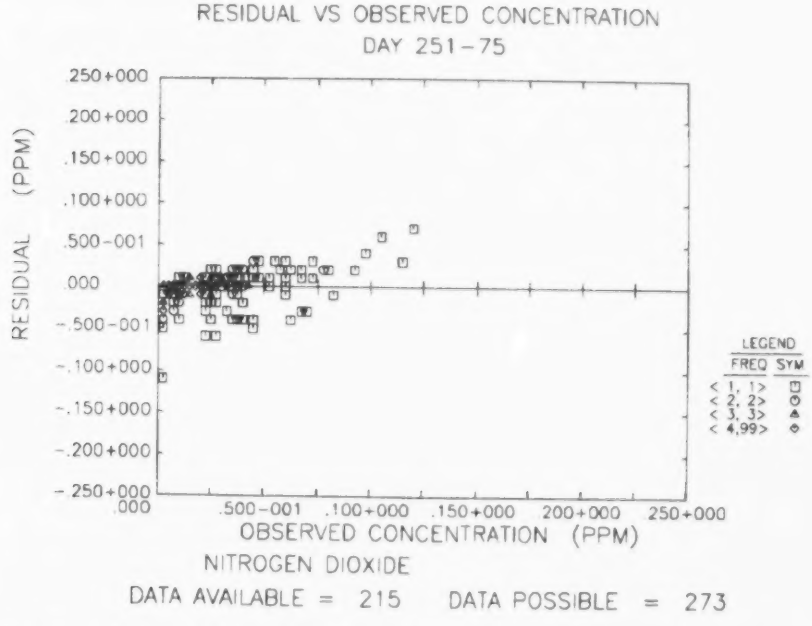

Figure 31b. Residual vs. observed plot for NO_2 from the UAM simulation results for Day 251-75.

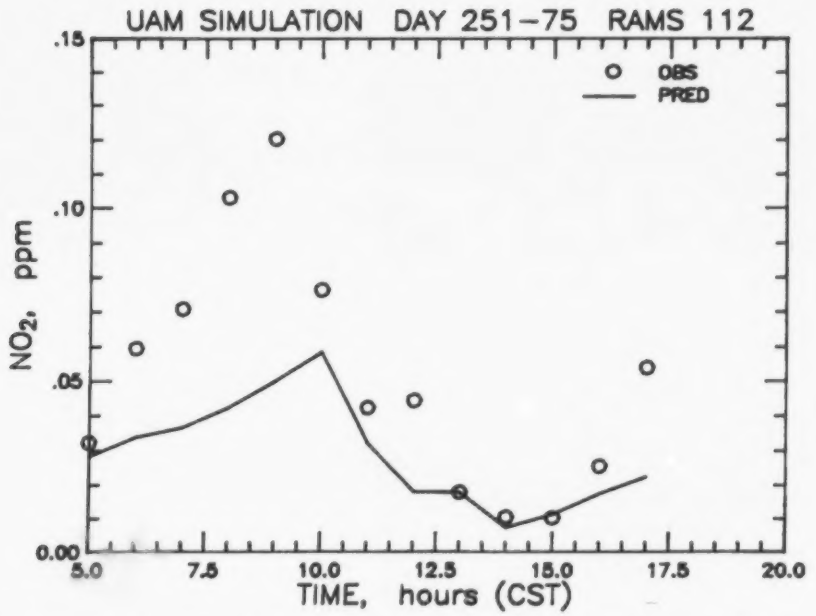

Figure 32. UAM time series of observed and predicted NO_2 concentrations at site 112 on Day 251-75.

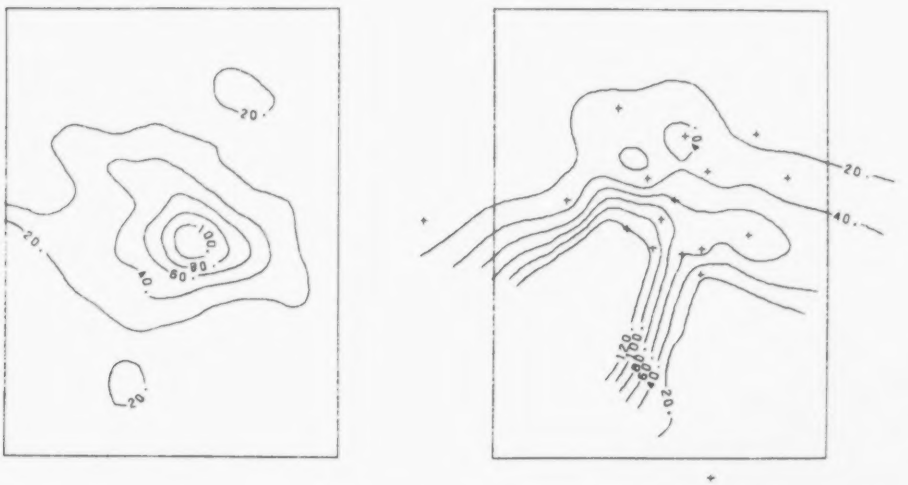
ST. LOUIS SEPT. 8,1975 (DAY 251)
PREDICTED CONCENTRATIONS OF NO2 (IN PPB)
HOUR 0900-1000
ST. LOUIS SEPT. 8,1975 (DAY 251)
OBSERVED CONCENTRATIONS OF NO2 (IN PPB)
HOUR 0900-1000

(a) (b)

Figure 33. Contours of (a) predicted and (b) observed fields of NO_2 at hour of observed maximum on Day 251-75.

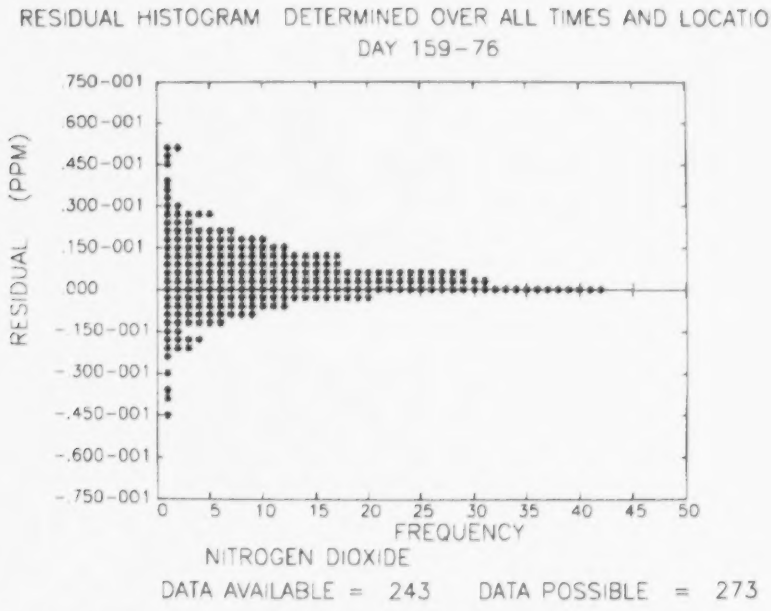

Figure 34a. Residual histogram for NO_2 from the UAM simulation results for Day 159-76.

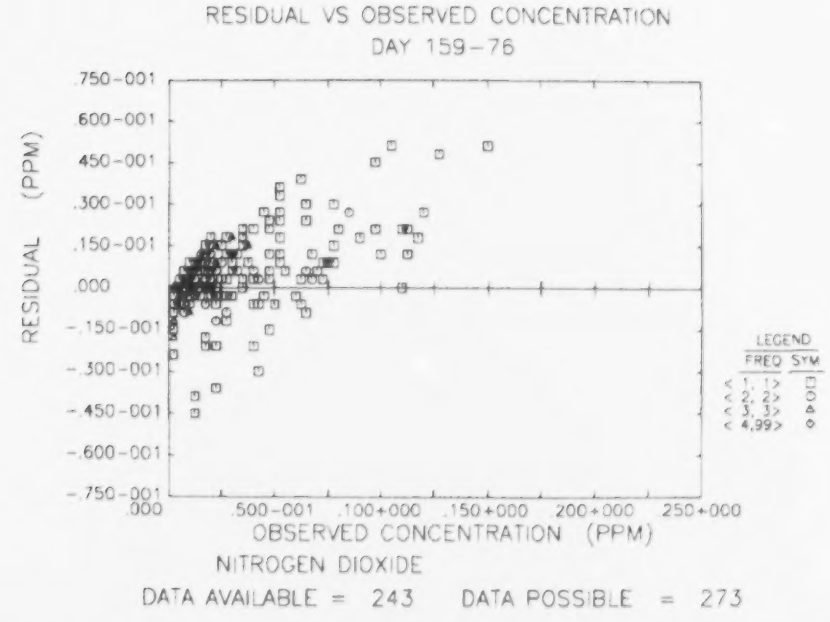

Figure 34b. Residual vs. observed plot for NO_2 from the UAM simulation results for Day 159-76.

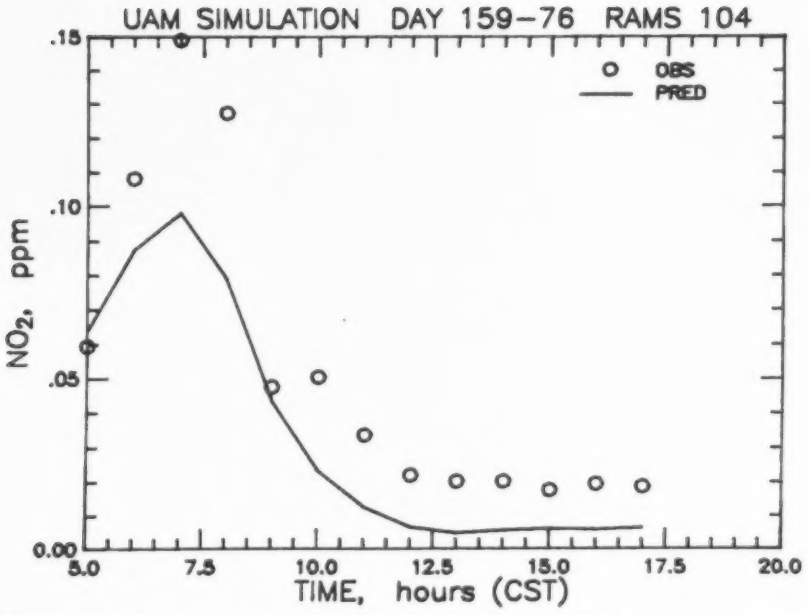

Figure 35. UAM time series of observed and predicted NO_2 concentrations at site 104 on Day 159-76.

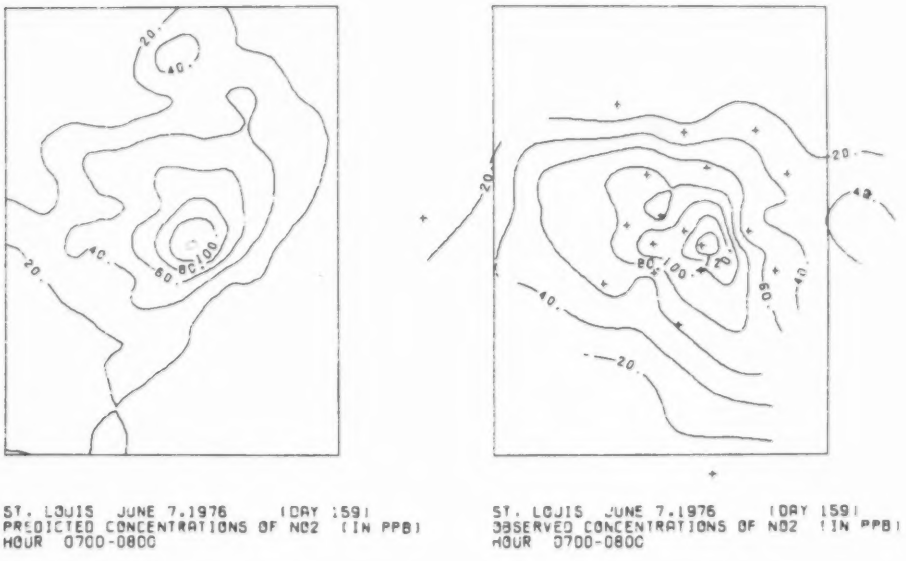
ST. LOUIS JUNE 7,1976 (DAY 159)
PREDICTED CONCENTRATIONS OF NO2 (IN PPB)
HOUR 0700-0800
ST. LOUIS JUNE 7,1976 (DAY 159)
OBSERVED CONCENTRATIONS OF NO2 (IN PPB)
HOUR 0700-0800

(a) (b)

Figure 36. Contours of (a) predicted and (b) observed fields of NO_2 at hour of observed maximum on Day 159-76.

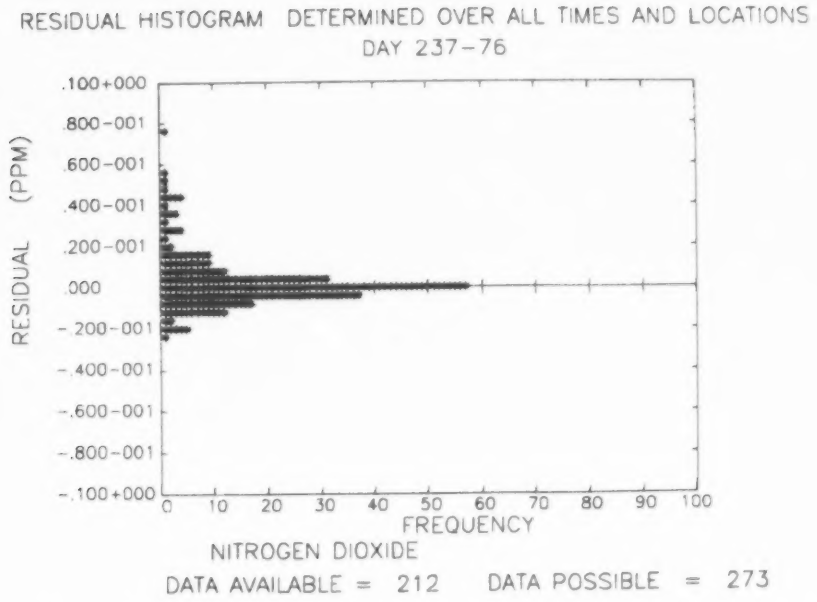

Figure 37a. Residual histogram for NO_2 from the UAM simulation results for Day 237-76.

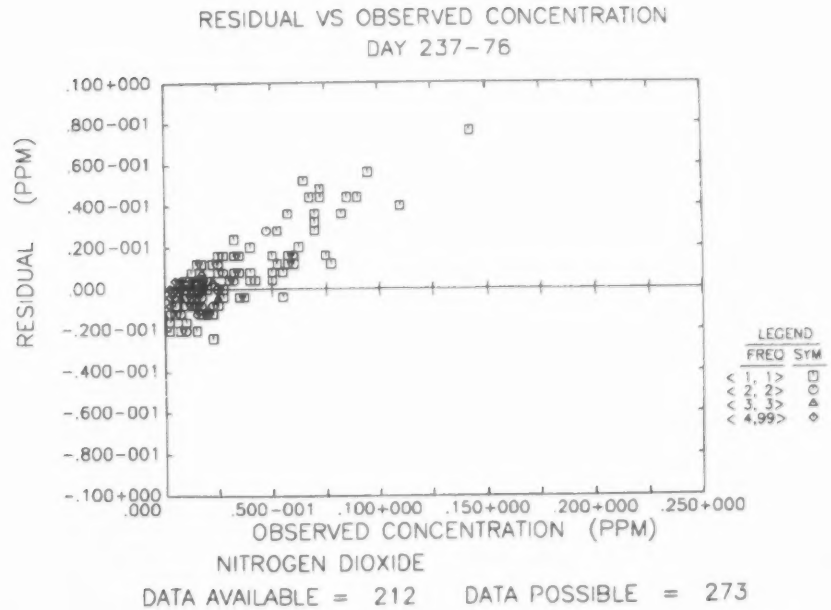

Figure 37b. Residual vs. observed plot for NO_2 from the UAM simulation results for Day 237-76.

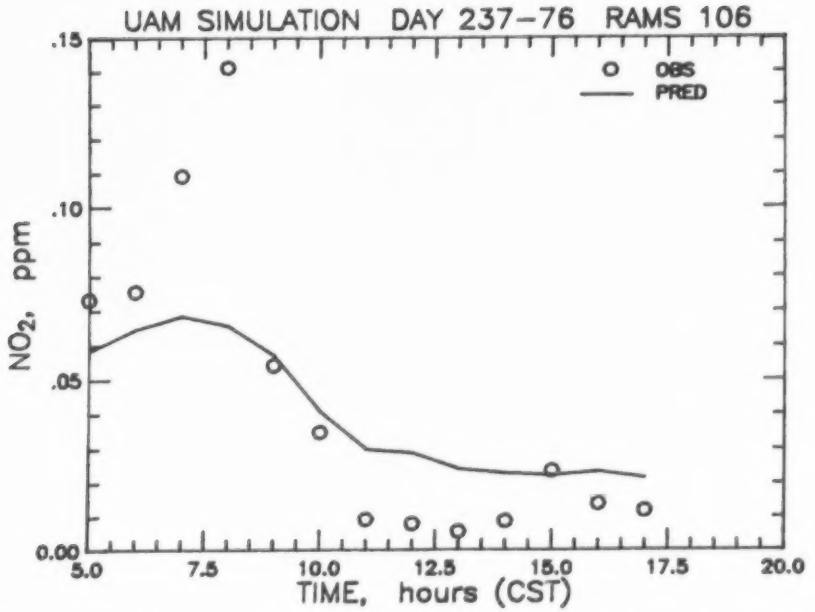

Figure 38. UAM time series of observed and predicted NO_2 concentrations at site 106 on Day 237-76.

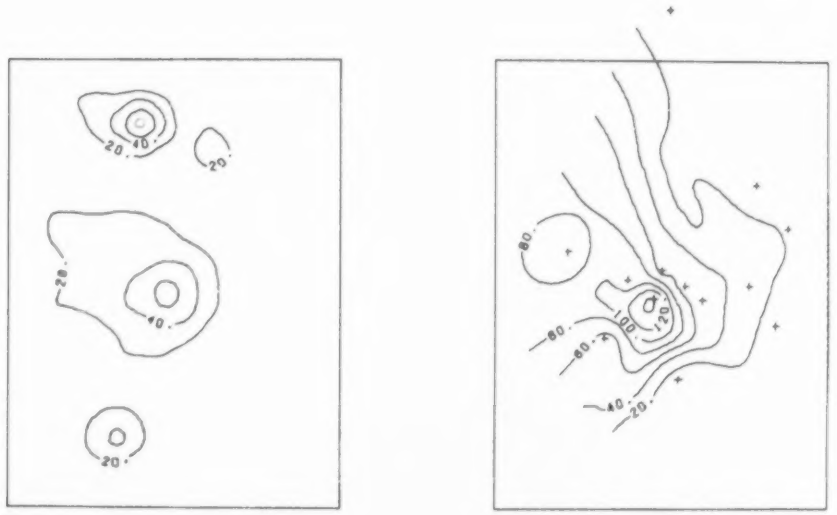
ST. LOUIS AUG. 24,1976 (DAY 237)
PREDICTED CONCENTRATIONS OF NO2 (IN PPB)
HOUR 0800-0900
ST. LOUIS AUG. 24,1976 (DAY 237)
OBSERVED CONCENTRATIONS OF NO2 (IN PPB)
HOUR 0800-0900

(a) (b)

Figure 39. Contours of (a) predicted and (b) observed fields of NO_2 at hour of observed maximum on Day 237-76.

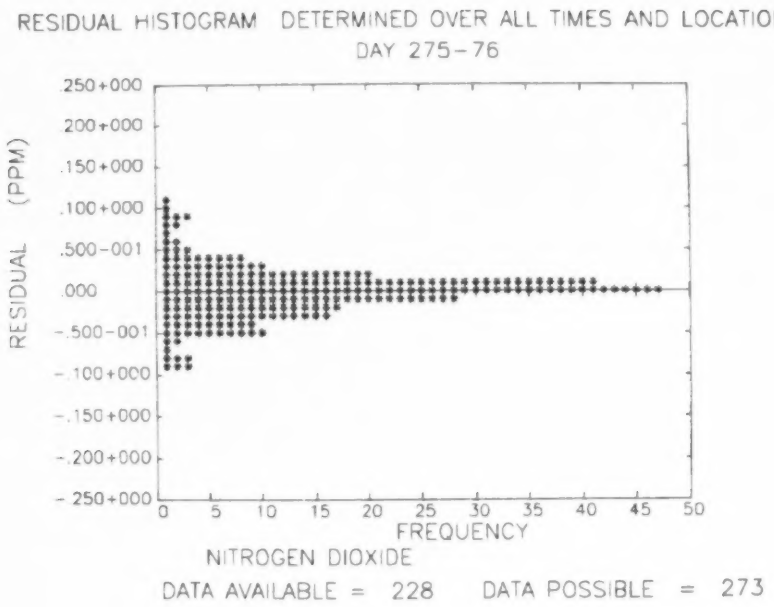

Figure 40a. Residual histogram for NO_2 from the UAM simulation results for Day 275-76.

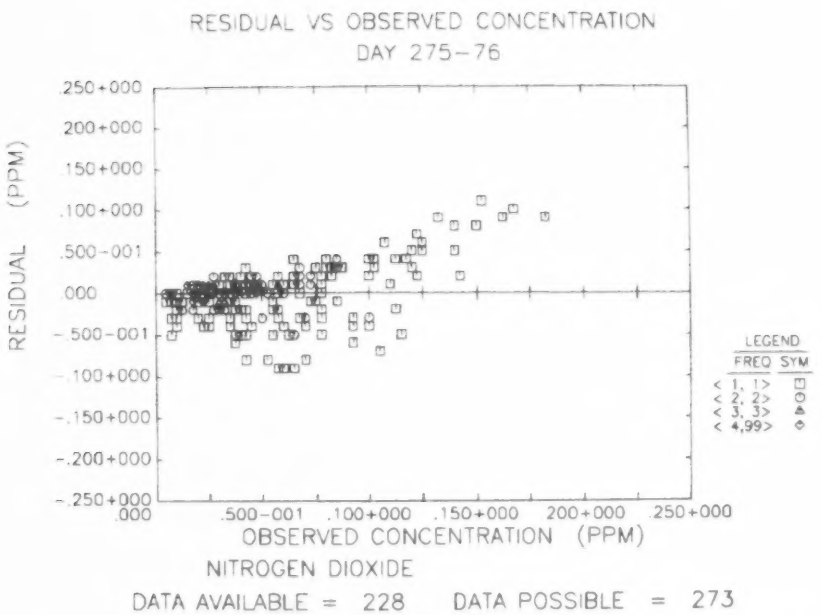

Figure 40b. Residual vs. observed plot for NO_2 from the UAM simulation results for Day 275-76.

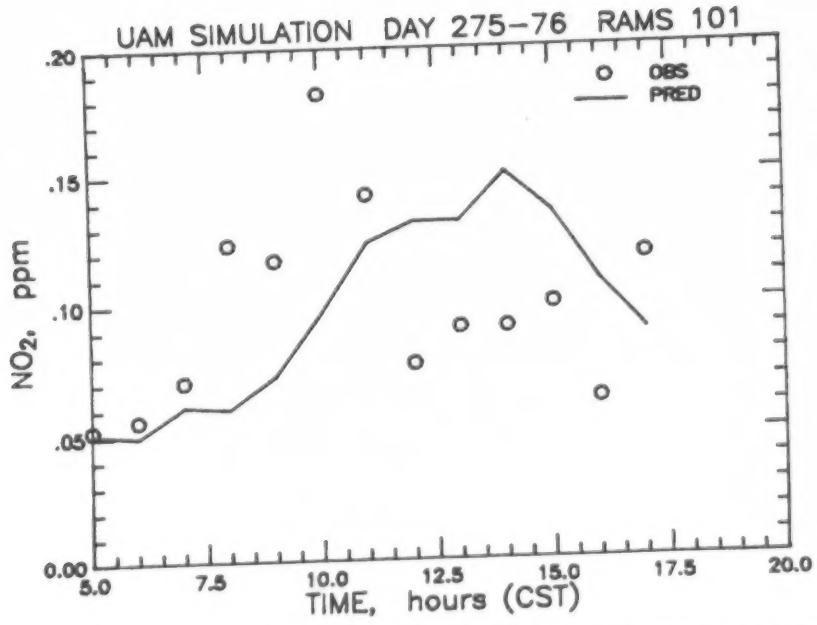

Figure 41. UAM time series of observed and predicted NO_2 concentrations at site 101 on Day 275-76.

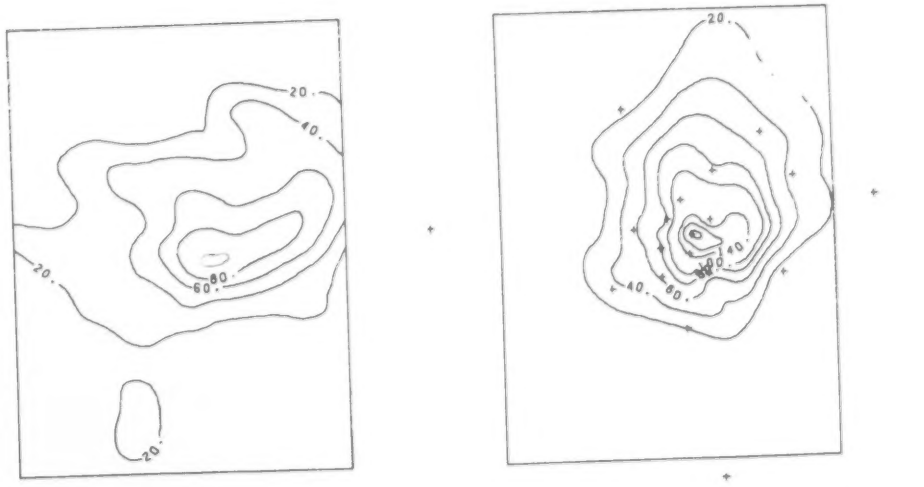

(a) (b)

Figure 42. Contours of (a) predicted and (b) observed fields of NO_2 at hour of observed maximum on Day 275-76.

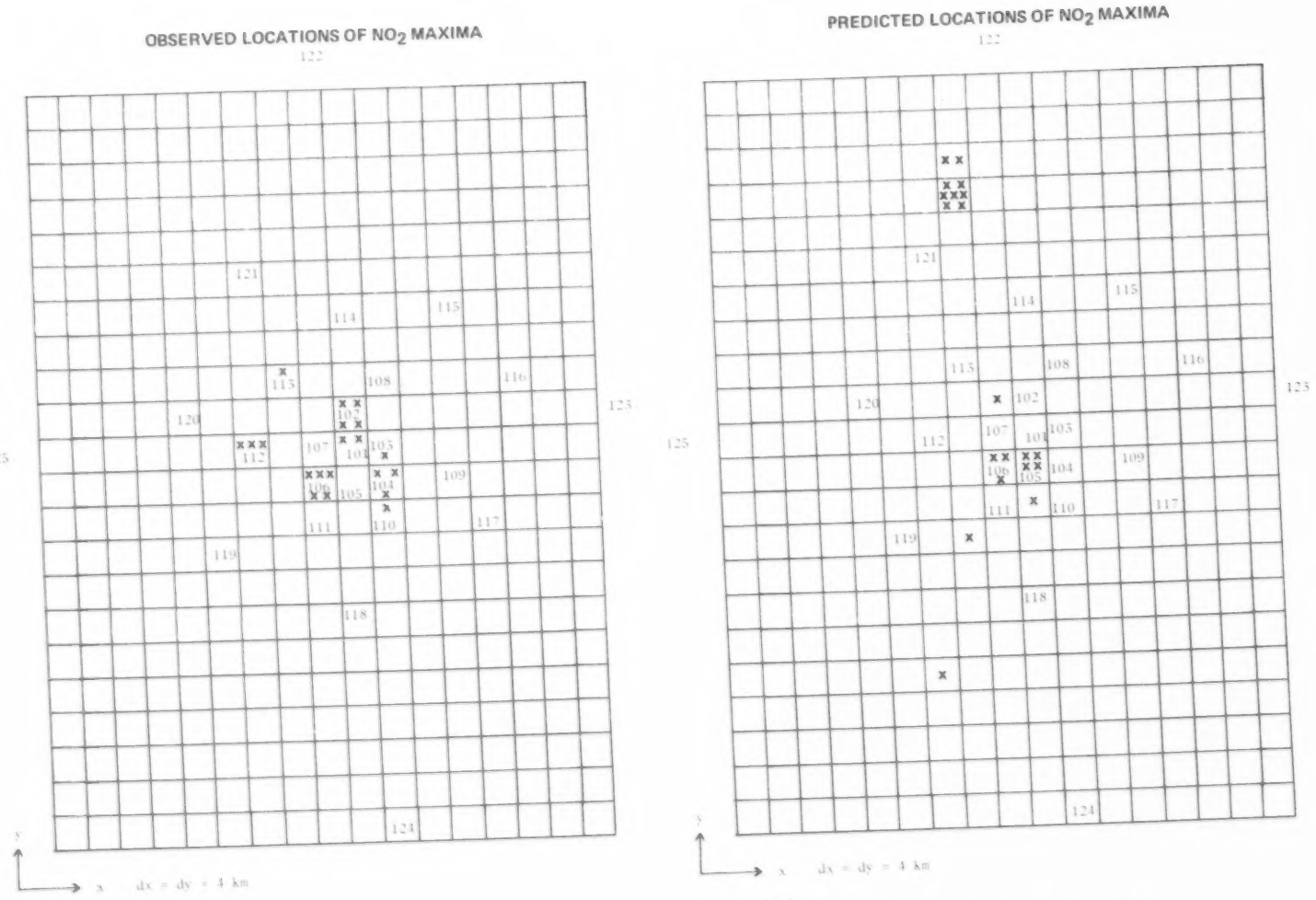

(a) (b)

Figure 43. Locations of (a) observed and (b) predicted daily maximum NO_2 concentrations within the UAM domain over the 20 test days.

REFERENCES

Bencala, K.E. and J.H. Seinfeld, 1979: An air quality model performance assessment package. Atmospheric Environ., 13, 1181-1185.

California Air Resources Board, 1982: Personal Communication.

Evans, R.B., 1979: The contribution of ozone aloft to surface ozone maxima. Ph.D. Dissertation, School of Public Health, Univ. of North Carolina, Chapel Hill, 301 pp.

Lurmann, F., D. Godden, A.C. Lloyd, and R.A. Nordsieck, 1979a: A Lagrangian Photochemical Air Quality Simulation Model. Vol. I-Model Formulation. EPA-600/8-79-015a. U.S. Environmental Protection Agency, Research Triangle Park, NC. 156 pp.

Lurmann, F., D. Godden, A.C. Lloyd, and R.A. Nordsieck, 1979b: A Lagrangian Photochemical Air Quality Simulation Model. Vol. II-User's Manual. EPA-600/8-79-015b. U.S. Environmental Protection Agency, Research Triangle Park, NC. 454 pp.

Lurmann, F., 1980: Modification and Analysis of the Lagrangian Photochemical Air Quality Simulation Model for St. Louis. Environmental Research and Technology, Inc. Document No. P-A095. Westlake Village, CA. 25 pp.

Lurmann, F., 1981: Incorporation of Lateral Diffusion in the Lagrangian Photochemical Air Quality Simulation Model. Environmental Research and Technology, Inc. Document No. P-A748. Westlake Village, CA. 32 pp.

Pooler, F., 1974: Network requirements for the St. Louis RAPS. J. Air Pollut. Control Assoc., 24, pp. 228-231.

Rhoads, R.G., 1982: Monitoring strategies in the United States. Proceedings of the U.S.-Dutch International Symposium-Air Pollution by Nitrogen Oxides. Elsevier, Amsterdam, pp. 183-195.

Schere, K.L. and J.H. Shreffler, 1982: Final Evaluation of Urban-Scale Photochemical Air Quality Simulation Models. EPA-600/3-82-094. U.S. Environmental Protection Agency, Research Triangle Park, NC. 259 pp.

Schiermeier, F.A., 1978: Air monitoring milestones: RAPS field measurements are in. Environ. Sci. Technol., 12, 644-651.

Seigneur, C., T.W. Tesche, P.M. Roth and M.K. Liu, 1983: On the treatment of point source emissions in urban air quality modeling. Atmospheric Environ. (in press)

Shreffler, J.H. and R.B. Evans, 1982: The surface ozone record from the Regional Air Pollution Study, 1975-1976. Atmospheric Environ. 16, pp. 1311-1321.

Shreffler, J.H. and K.L. Schere, 1982: Evaluation of four urban-scale photochemical air quality simulation models. EPA-600/3-82-043. U.S. Environmental Protection Agency, Research Triangle Park, NC. 179 pp.

Shy, C.M., J.P. Creason, M.E. Pearlman, K.E. McClain, F.B. Benson, and M.M. Young, 1970: The Chattanooga school children study: Effects of community exposure to nitrogen dioxide. J. Air Pollut. Control Assoc., 20, pp. 539-545.

APPENDIX A

UAM - TIME SERIES FOR REMAINING TEST DAYS

This appendix contains the NO_2 time series plots for the monitoring station observing the highest hour-average concentration within the boundaries of the UAM domain during the simulation time period. The plots presented here are those that were not specifically discussed within the body of this report. They are from test days 142, 178, 182, 183, 207, 209, 221, 230 and 231 of 1975 and 160, 195, 211, 212, 225 and 226 of 1976.

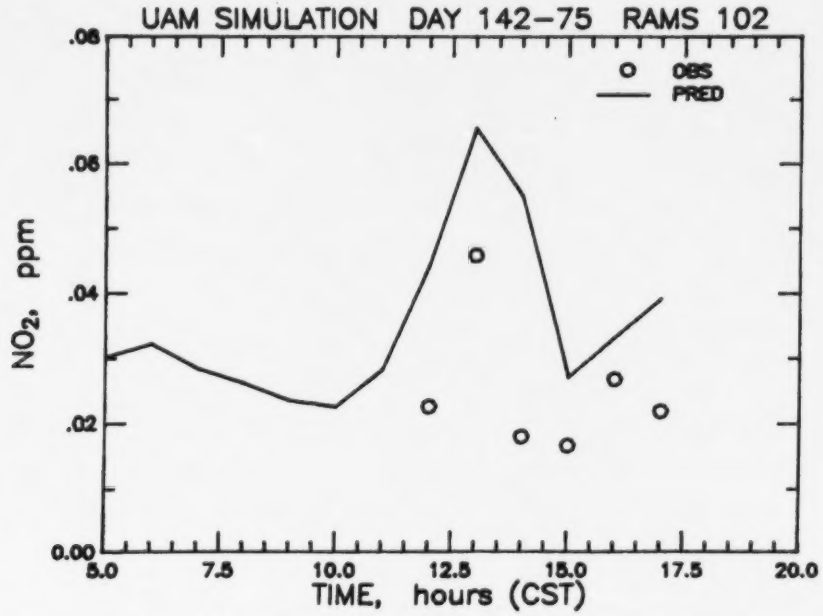

Figure A-1. UAM time series of observed and predicted NO_2 concentrations at site 102 on Day 142-75.

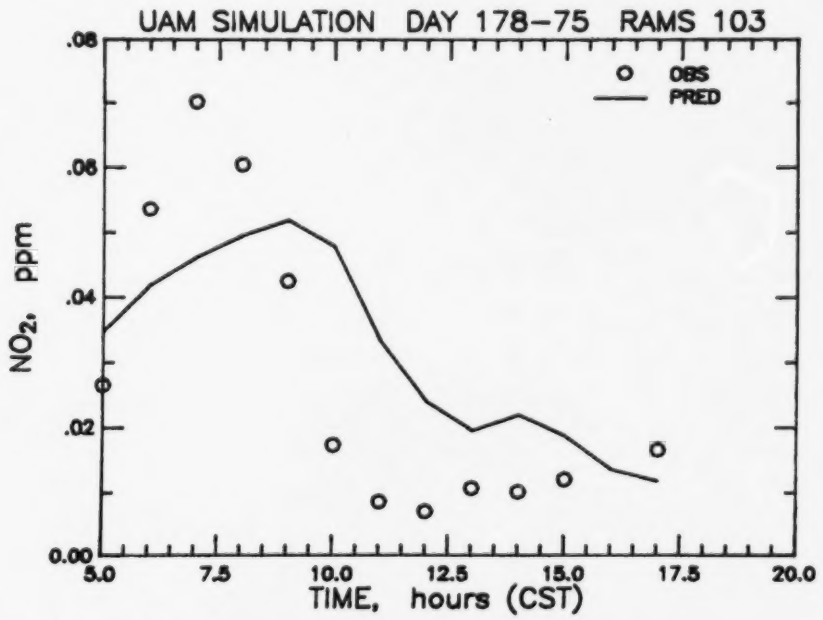

Figure A-2. UAM time series of observed and predicted NO_2 concentrations at site 103 on Day 178-75.

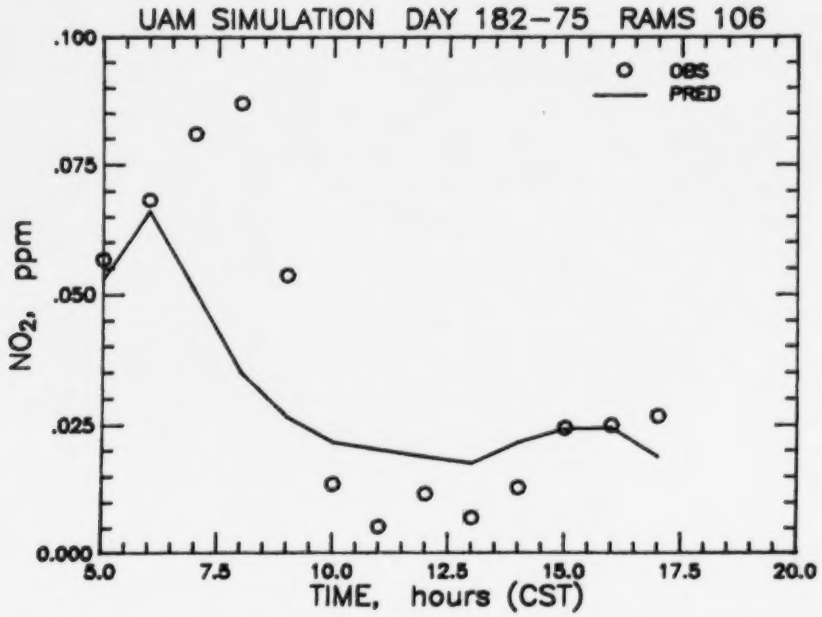

Figure A-3. UAM time series of observed and predicted NO_2 concentrations at site 106 on Day 182-75.

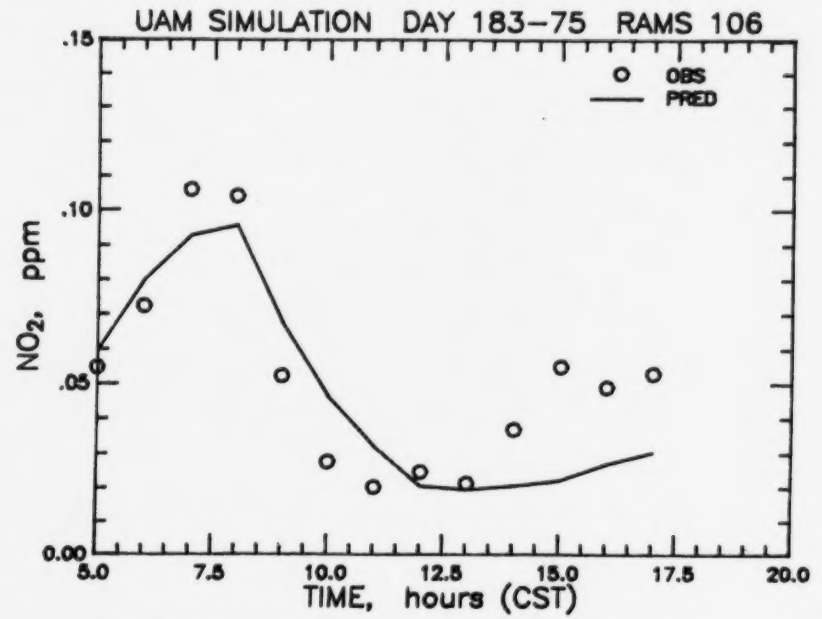

Figure A-4. UAM time series of observed and predicted NO_2 concentrations at site 106 on Day 183-75.

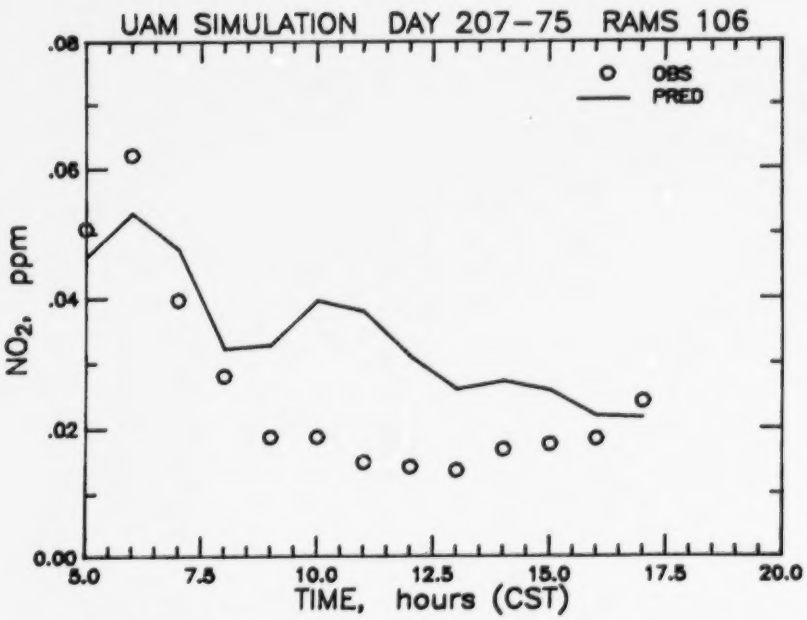

Figure A-5. UAM time series of observed and predicted NO_2 concentrations at site 106 on Day 207-75.

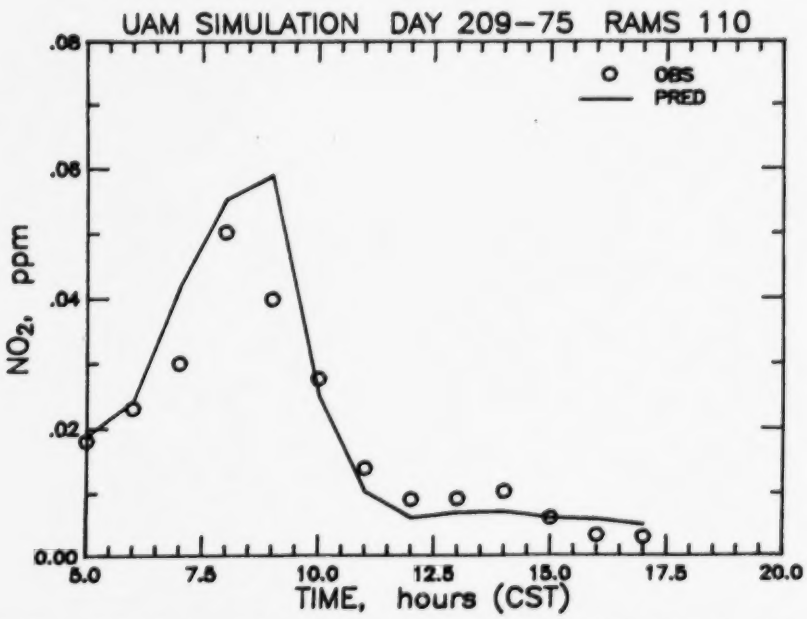

Figure A-6. UAM time series of observed and predicted NO_2 concentrations at site 110 on Day 209-75.

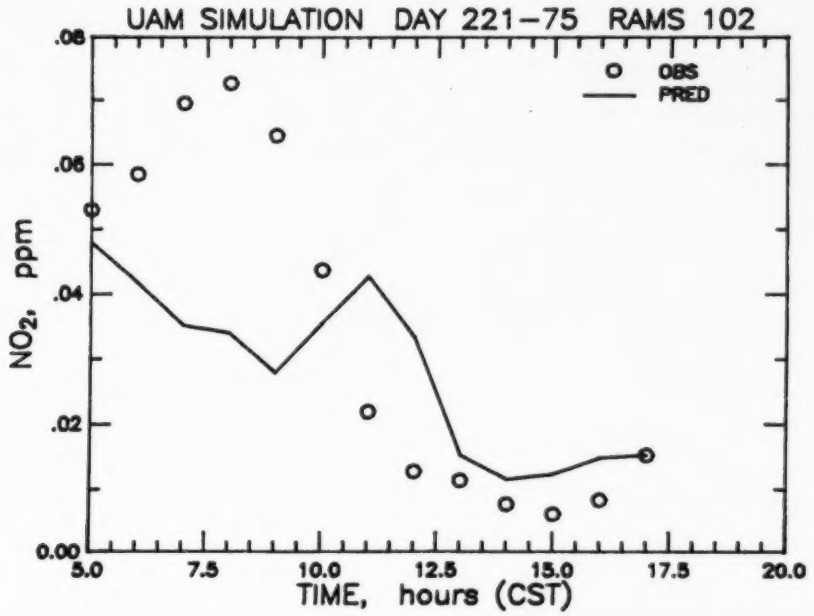

Figure A-7. UAM time series of observed and predicted NO_2 concentrations at site 102 on Day 221-75.

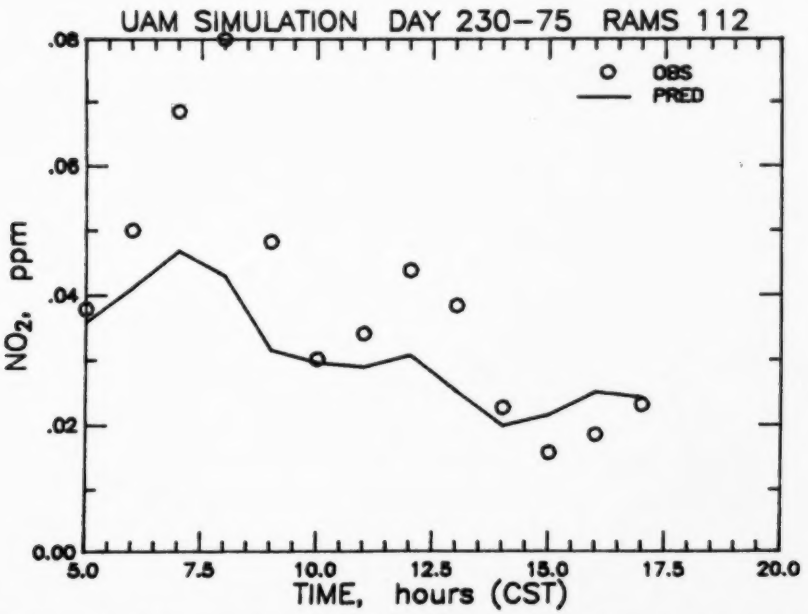

Figure A-8. UAM time series of observed and predicted NO_2 concentrations at site 112 on Day 230-75.

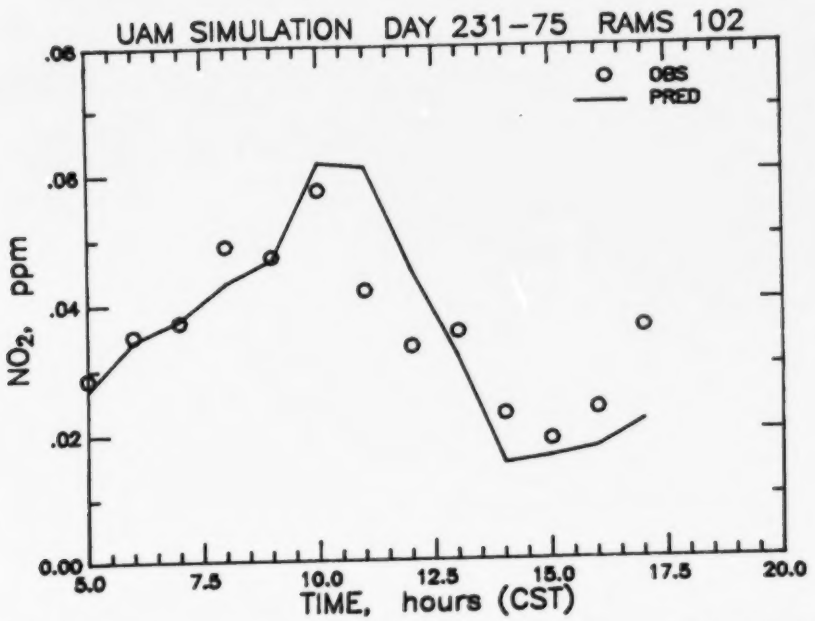

Figure A-9. UAM time series of observed and predicted NO_2 concentrations at site 102 on Day 231-75.

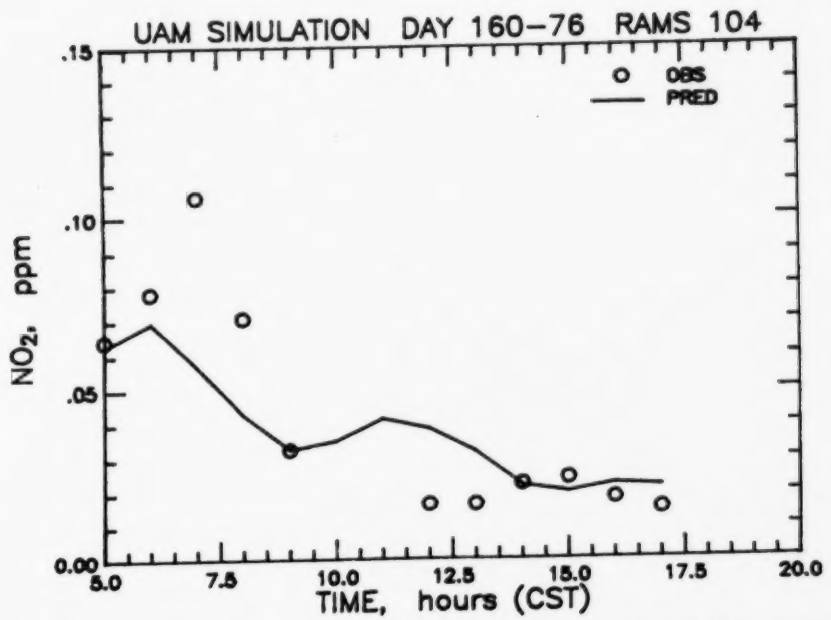

Figure A-10. UAM time series of observed and predicted NO_2 concentrations at site 104 on Day 160-76.

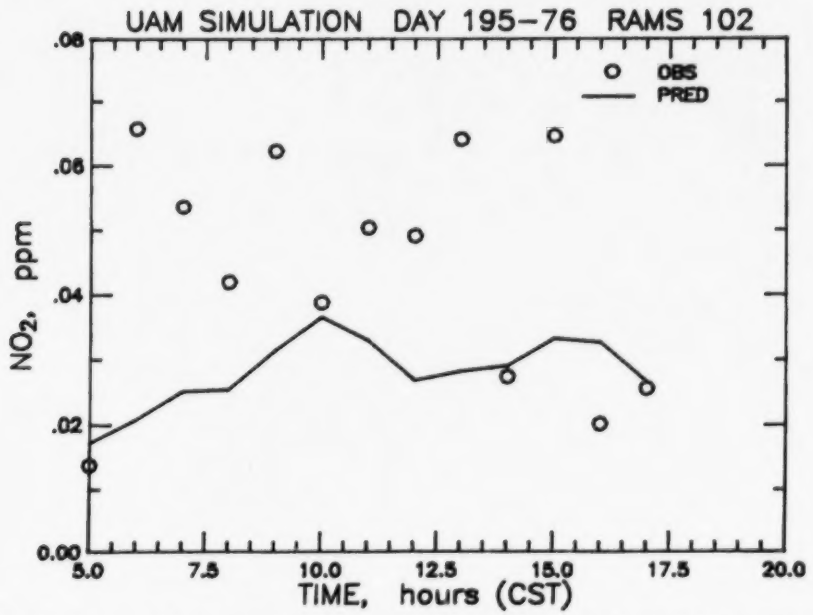

Figure A-11. UAM time series of observed and predicted NO_2 concentrations at site 102 on Day 195-76.

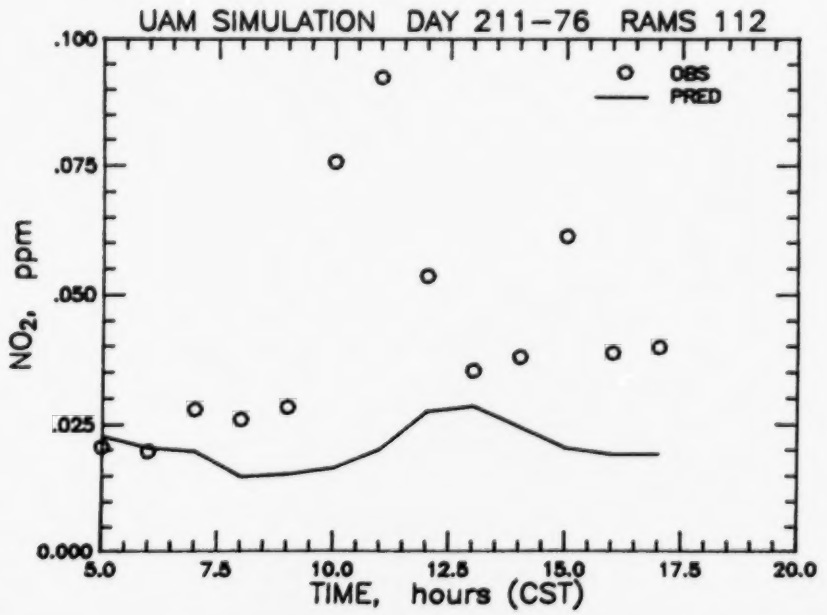

Figure A-12. UAM time series of observed and predicted NO_2 concentrations at site 112 on Day 211-76.

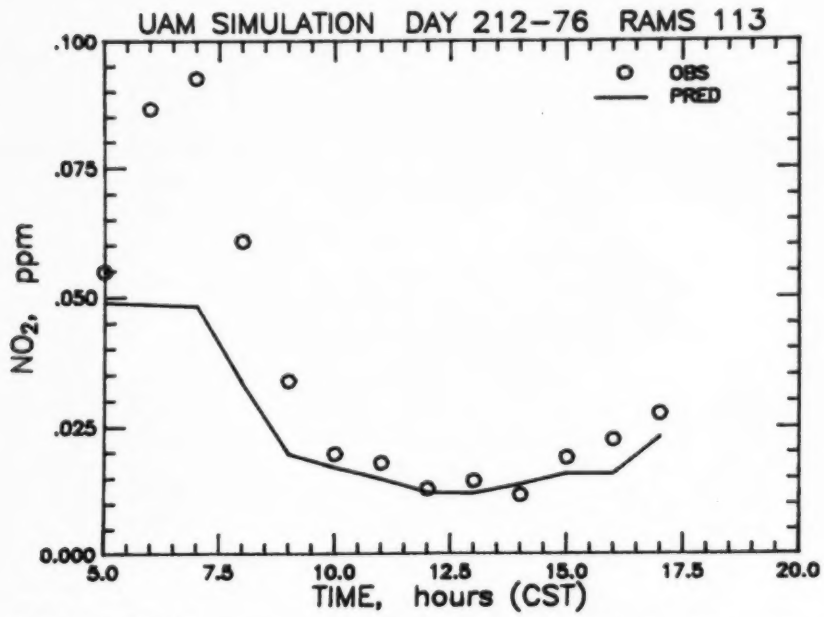

Figure A-13. UAM time series of observed and predicted NO_2 concentrations at site 113 on Day 212-76.

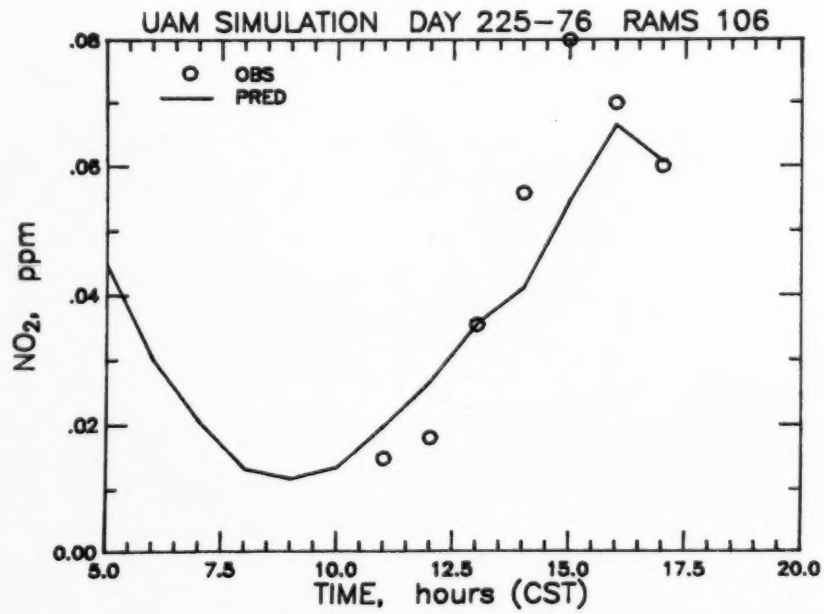

Figure A-14. UAM time series of observed and predicted NO_2 concentrations at site 106 on Day 225-76.

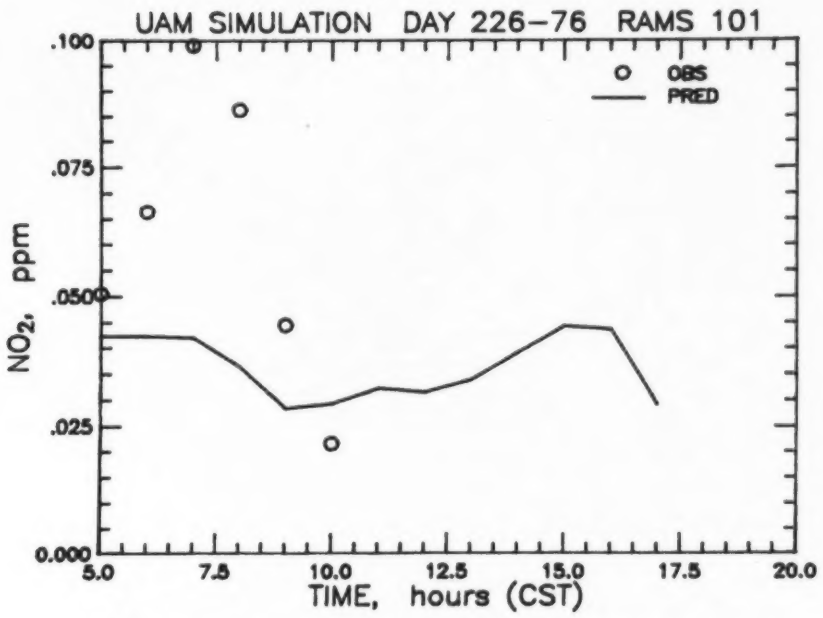

Figure A-15. UAM time series of observed and predicted NO_2 concentrations at site 101 on Day 226-76.

APPENDIX B

UAM - CONTOUR PLOTS FOR REMAINING TEST DAYS

The contour plots of predicted and observed NO_2 concentrations for the hour of the observed concentration maximum are presented here for all test days not specifically discussed within the body of this report.

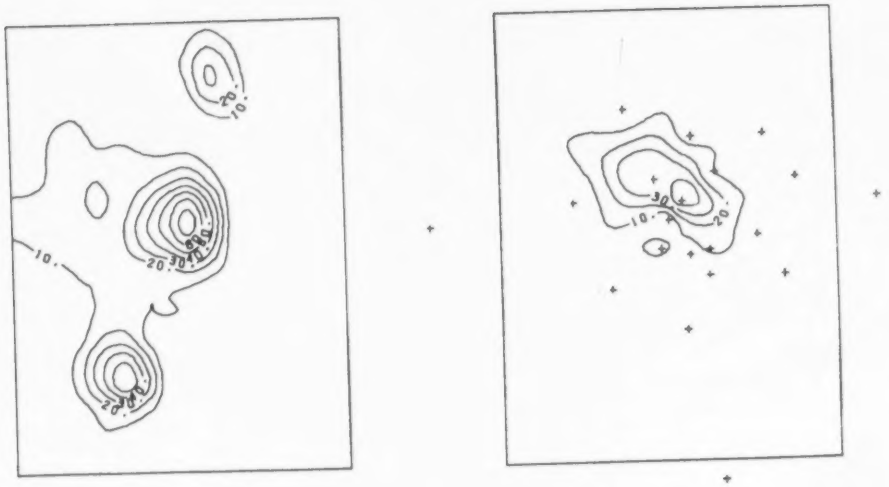
ST. LOUIS MAY 22,1975 (DAY 142)
PREDICTED CONCENTRATIONS OF NO2 (IN PPB)
HOUR 1300-1400
ST. LOUIS MAY 22,1975 (DAY 142)
OBSERVED CONCENTRATIONS OF NO2 (IN PPB)
HOUR 1300-1400

(a) (b)

Figure B-1. Contours of (a) predicted and (b) observed fields of NO_2 at hour of observed maximum on Day 142-75.

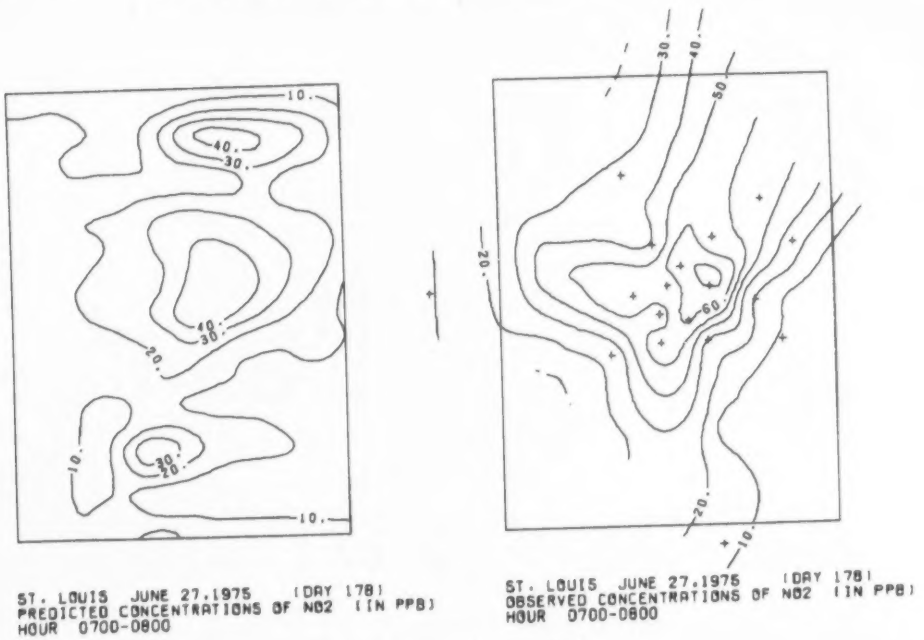
ST. LOUIS JUNE 27,1975 (DAY 178)
PREDICTED CONCENTRATIONS OF NO2 (IN PPB)
HOUR 0700-0800
ST. LOUIS JUNE 27,1975 (DAY 178)
OBSERVED CONCENTRATIONS OF NO2 (IN PPB)
HOUR 0700-0800

(a) (b)

Figure B-2. Contours of (a) predicted and (b) observed fields of NO_2 at hour of observed maximum on Day 178-75.

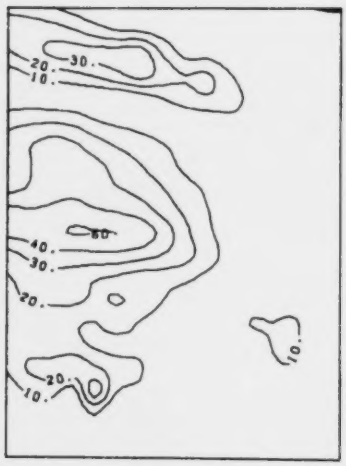

ST. LOUIS JULY 1,1975 (DAY 182)
PREDICTED CONCENTRATIONS OF NO2 (IN PPB)
HOUR 0800-0900

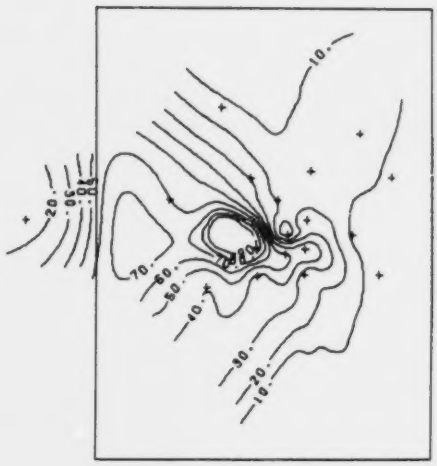

ST. LOUIS JULY 1,1975 (DAY 182)
OBSERVED CONCENTRATIONS OF NO2 (IN PPB)
HOUR 0800-0900

(a) (b)

Figure B-3. Contours of (a) predicted and (b) observed fields of NO_2 at hour of observed maximum on Day 182-75.

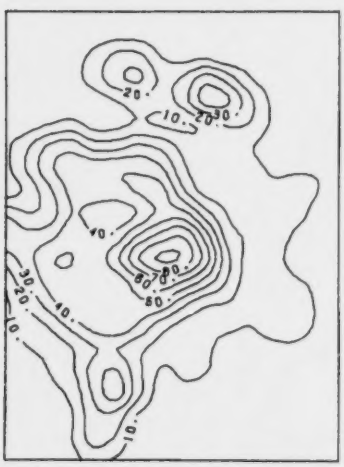

ST. LOUIS JULY 2,1975 (DAY 183)
PREDICTED CONCENTRATIONS OF NO2 (IN PPB)
HOUR 0700-0800

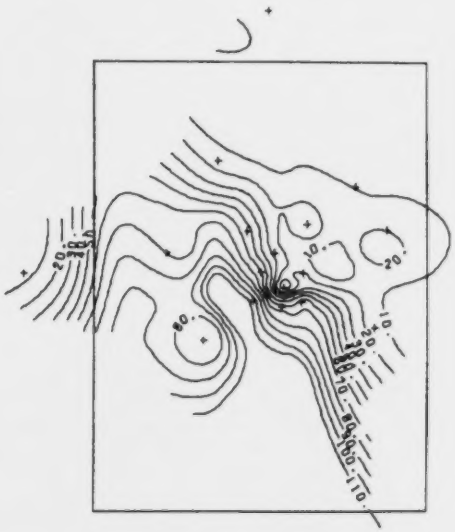

ST. LOUIS JULY 2,1975 (DAY 183)
OBSERVED CONCENTRATIONS OF NO2 (IN PPB)
HOUR 0700-0800

(a) (b)

Figure B-4. Contours of (a) predicted and (b) observed fields of NO_2 at hour of observed maximum on Day 183-75.

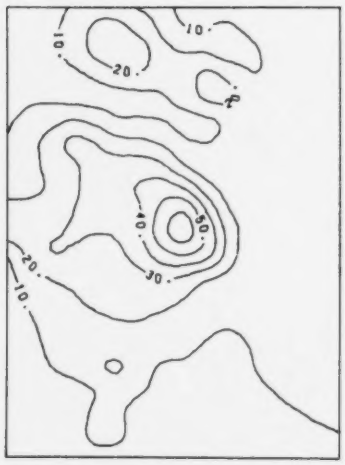

ST. LOUIS JULY 26,1975 (DAY 207)
PREDICTED CONCENTRATIONS OF NO2 (IN PPB)
HOUR 0600-0700

ST. LOUIS JULY 26,1975 (DAY 207)
OBSERVED CONCENTRATIONS OF NO2 (IN PPB)
HOUR 0600-0700

(a) (b)

Figure B-5. Contours of (a) predicted and (b) observed fields of NO_2 at hour of observed maximum on Day 207-75.

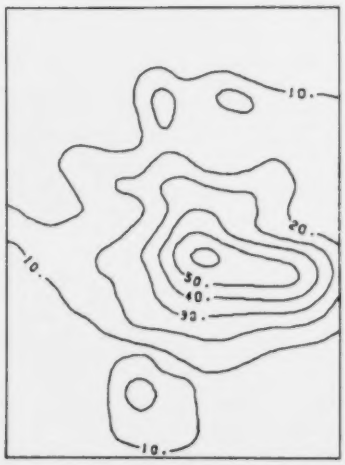

ST. LOUIS JULY 28,1975 (DAY 209)
PREDICTED CONCENTRATIONS OF NO2 (IN PPB)
HOUR 0800-0900

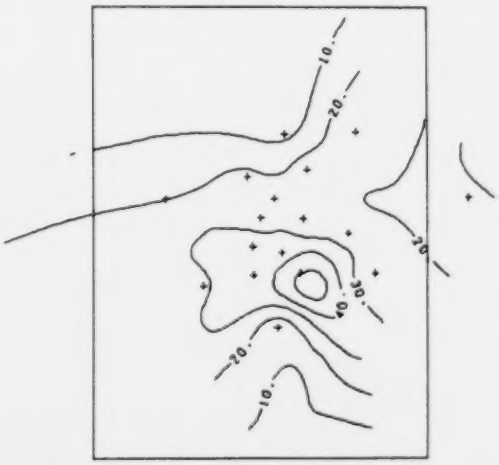

ST. LOUIS JULY 28,1975 (DAY 209)
OBSERVED CONCENTRATIONS OF NO2 (IN PPB)
HOUR 0800-0900

(a) (b)

Figure B-6. Contours of (a) predicted and (b) observed fields of NO_2 at hour of observed maximum on Day 209-75.

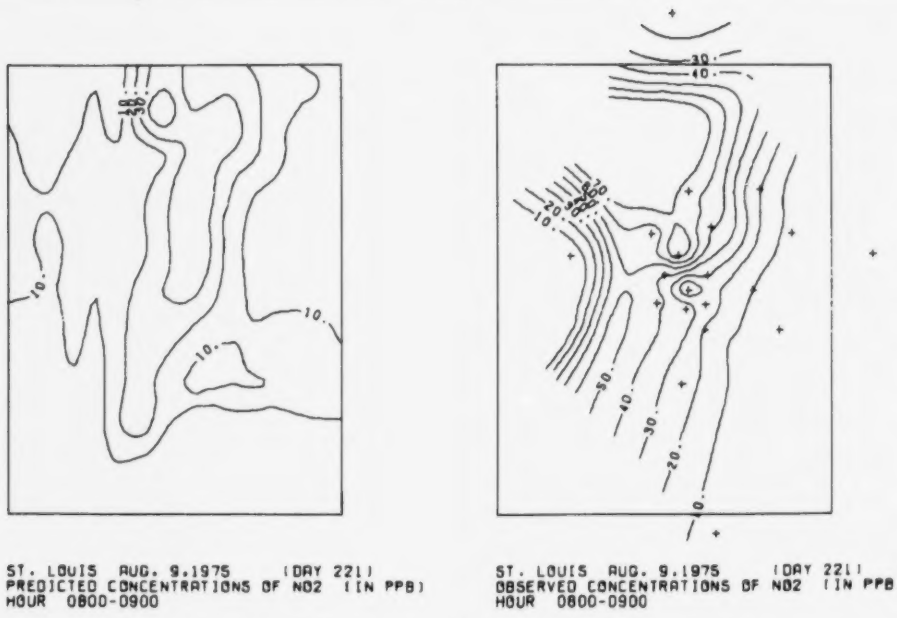
ST. LOUIS AUG. 9,1975 (DAY 221)
PREDICTED CONCENTRATIONS OF NO2 (IN PPB)
HOUR 0800-0900
ST. LOUIS AUG. 9,1975 (DAY 221)
OBSERVED CONCENTRATIONS OF NO2 (IN PPB)
HOUR 0800-0900

(a) (b)

Figure B-7. Contours of (a) predicted and (b) observed fields of NO_2 at hour of observed maximum on Day 221-75.

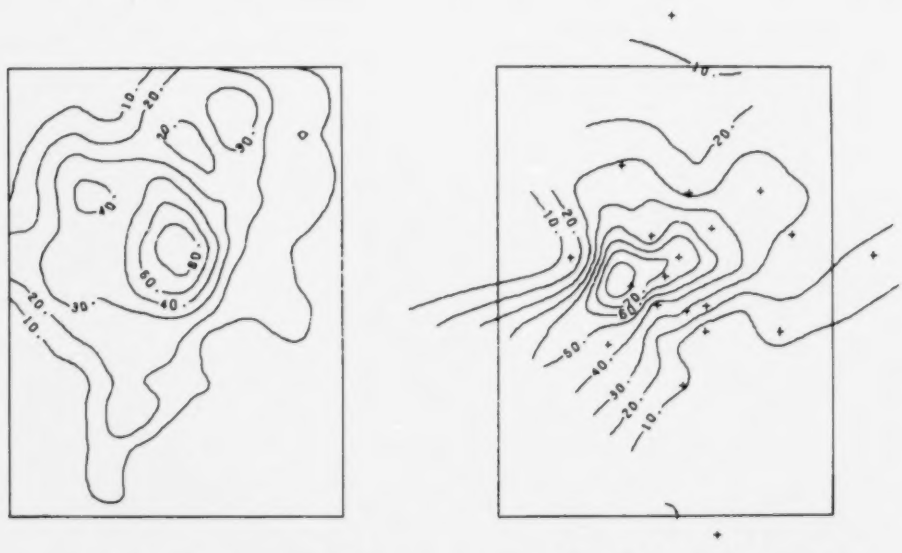
ST. LOUIS AUG. 18,1975 (DAY 230)
PREDICTED CONCENTRATIONS OF NO2 (IN PPB)
HOUR 0800-0900
ST. LOUIS AUG. 18,1975 (DAY 230)
OBSERVED CONCENTRATIONS OF NO2 (IN PPB)
HOUR 0800-0900

(a) (b)

Figure B-8. Contours of (a) predicted and (b) observed fields of NO_2 at hour of observed maximum on Day 230-75.

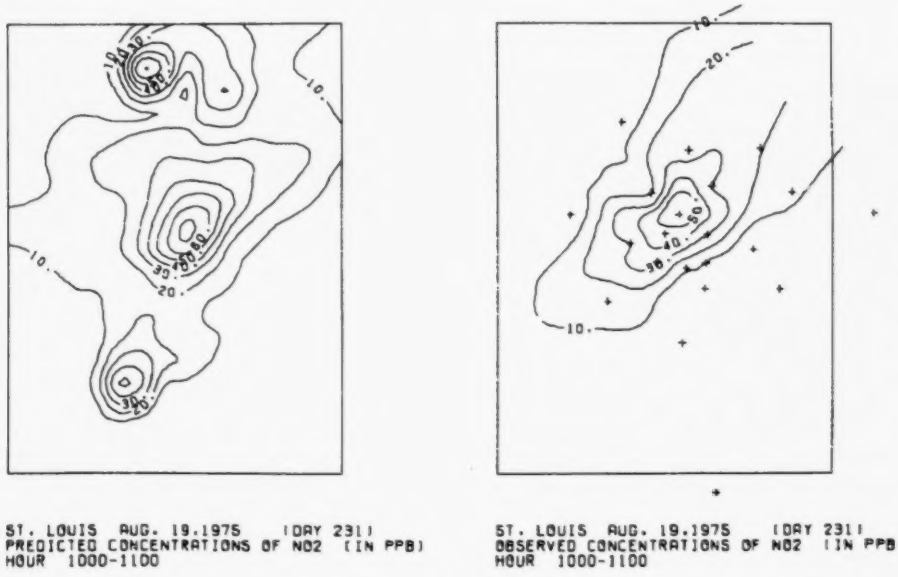
ST. LOUIS AUG. 19,1975 (DAY 231)
PREDICTED CONCENTRATIONS OF NO2 (IN PPB)
HOUR 1000-1100
ST. LOUIS AUG. 19,1975 (DAY 231)
OBSERVED CONCENTRATIONS OF NO2 (IN PPB)
HOUR 1000-1100

(a) (b)

Figure B-9. Contours of (a) predicted and (b) observed fields of NO_2 at hour of observed maximum on Day 231-75.

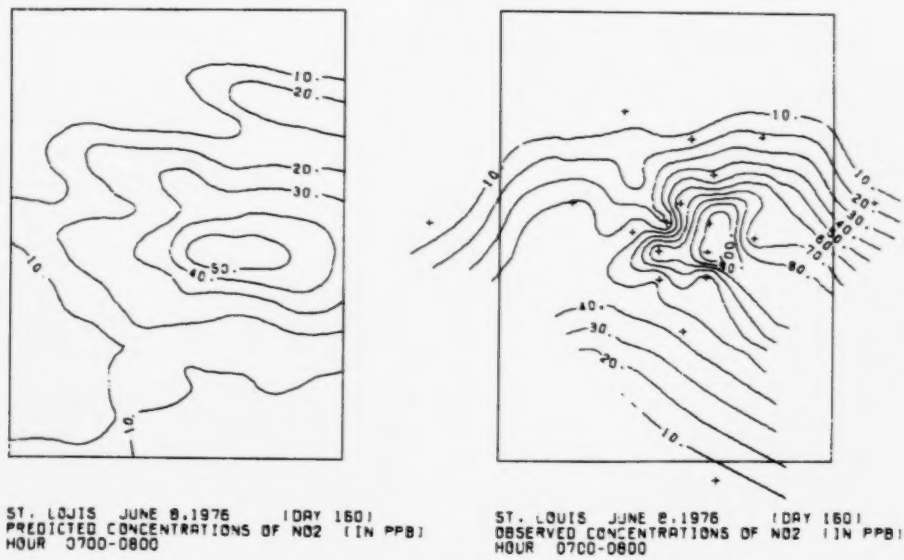
ST. LOUIS JUNE 8,1976 (DAY 160)
PREDICTED CONCENTRATIONS OF NO2 (IN PPB)
HOUR 0700-0800
ST. LOUIS JUNE 8,1976 (DAY 160)
OBSERVED CONCENTRATIONS OF NO2 (IN PPB)
HOUR 0700-0800

(a) (b)

Figure B-10. Contours of (a) predicted and (b) observed fields of NO_2 at hour of observed maximum on Day 160-76.

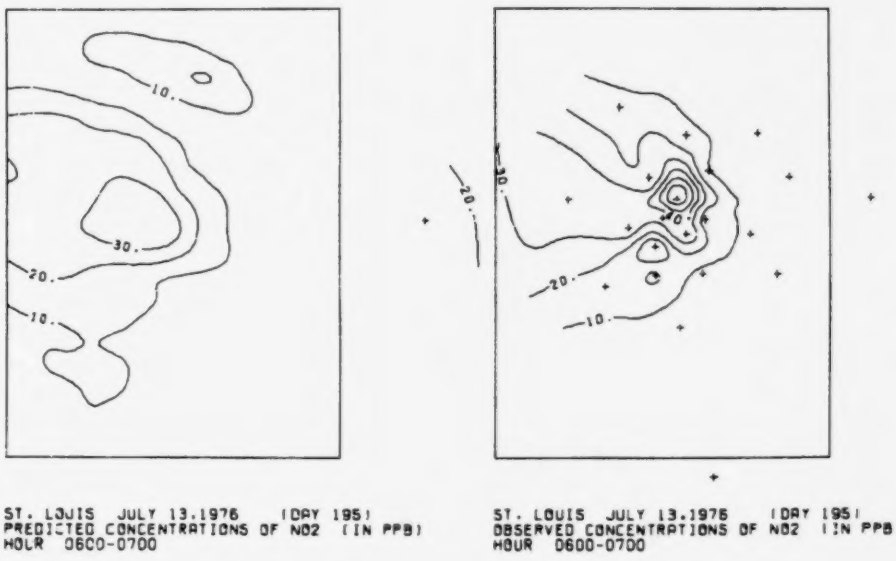

ST. LOUIS JULY 13,1976 (DAY 195)
PREDICTED CONCENTRATIONS OF NO2 (IN PPB)
HOUR 0600-0700

ST. LOUIS JULY 13,1976 (DAY 195)
OBSERVED CONCENTRATIONS OF NO2 (IN PPB)
HOUR 0600-0700

(a) (b)

Figure B-11. Contours of (a) predicted and (b) observed fields of NO_2 at hour of observed maximum on Day 195-76.

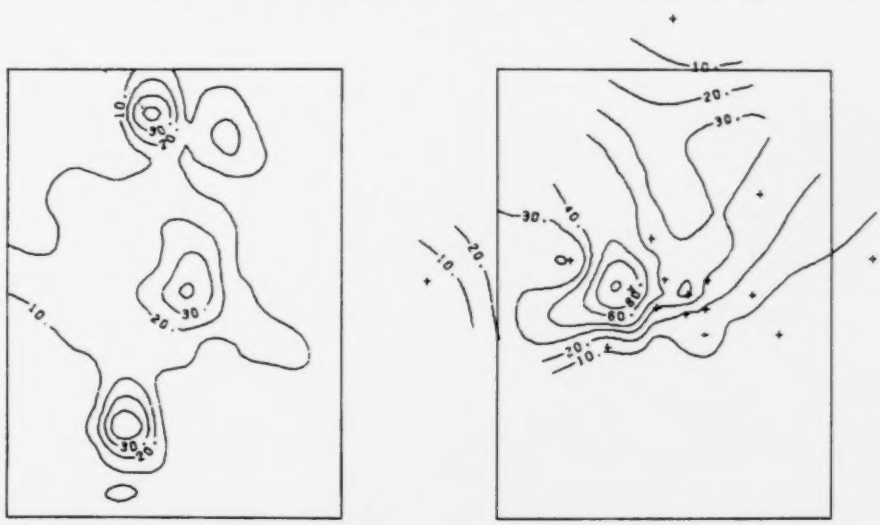

ST. LOUIS JULY 29,1976 (DAY 211)
PREDICTED CONCENTRATIONS OF NO2 (IN PPB)
HOUR 1100-1200

ST. LOUIS JULY 29,1976 (DAY 211)
OBSERVED CONCENTRATIONS OF NO2 (IN PPB)
HOUR 1100-1200

(a) (b)

Figure B-12. Contours of (a) predicted and (b) observed fields of NO_2 at hour of observed maximum on Day 211-76.

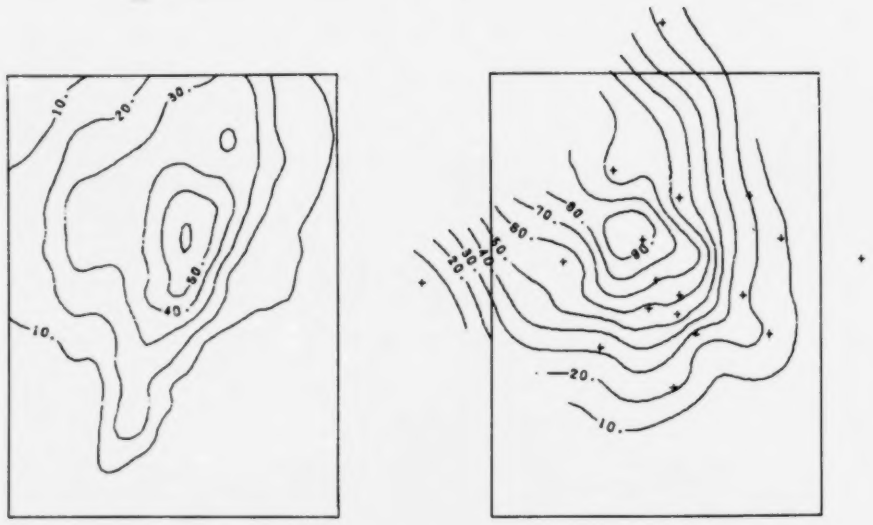
ST. LOUIS JULY 30,1976 (DAY 212)
PREDICTED CONCENTRATIONS OF NO2 (IN PPB)
HOUR 0700-0800
ST. LOUIS JULY 30,1976 (DAY 212)
OBSERVED CONCENTRATIONS OF NO2 (IN PPB)
HOUR 0700-0800

(a) (b)

Figure B-13. Contours of (a) predicted and (b) observed fields of NO_2 at hour of observed maximum on Day 212-76.

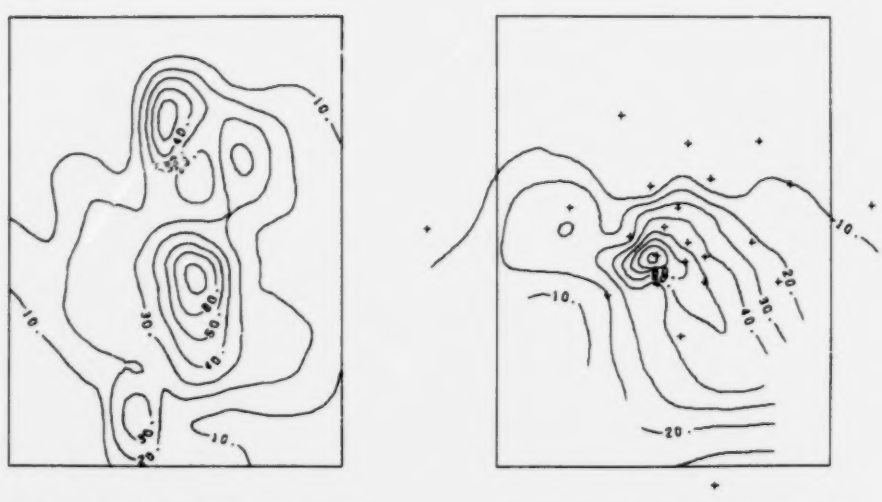
ST. LOUIS AUG. 12,1976 (DAY 225)
PREDICTED CONCENTRATIONS OF NO2 (IN PPB)
HOUR 1500-1600
ST. LOUIS AUG. 12,1976 (DAY 225)
OBSERVED CONCENTRATIONS OF NO2 (IN PPB)
HOUR 1500-1600

(a) (b)

Figure B-14. Contours of (a) predicted and (b) observed fields of NO_2 at hour of observed maximum on Day 225-76.

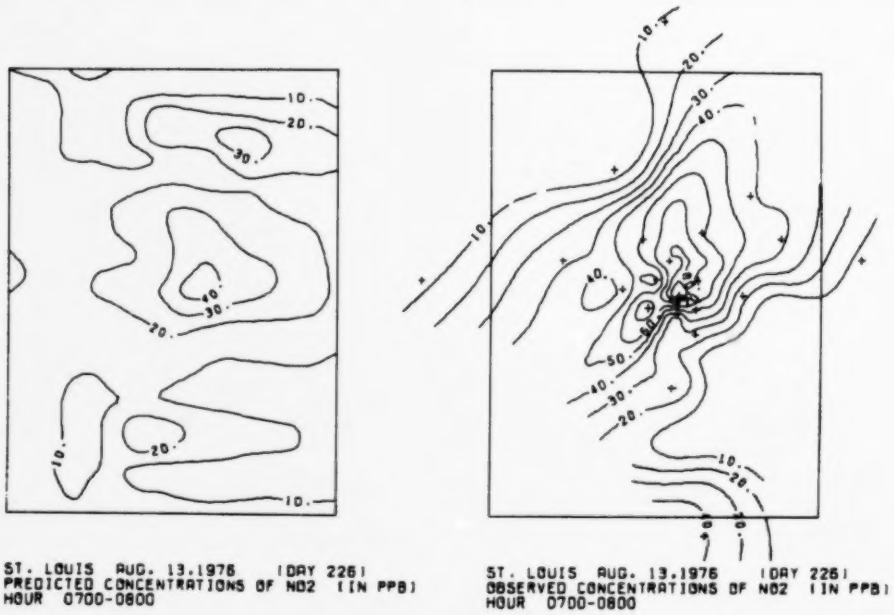
ST. LOUIS AUG. 13,1976 (DAY 226)
PREDICTED CONCENTRATIONS OF NO2 (IN PPB)
HOUR 0700-0800
ST. LOUIS AUG. 13,1976 (DAY 226)
OBSERVED CONCENTRATIONS OF NO2 (IN PPB)
HOUR 0700-0800

(a) (b)

Figure B-15. Contours of (a) predicted and (b) observed fields of NO_2 at hour of observed maximum on Day 226-76.